

Fig. 329. Scanning electron microscope fractograph of generator shaft fracture subsegment "B", Area 2.

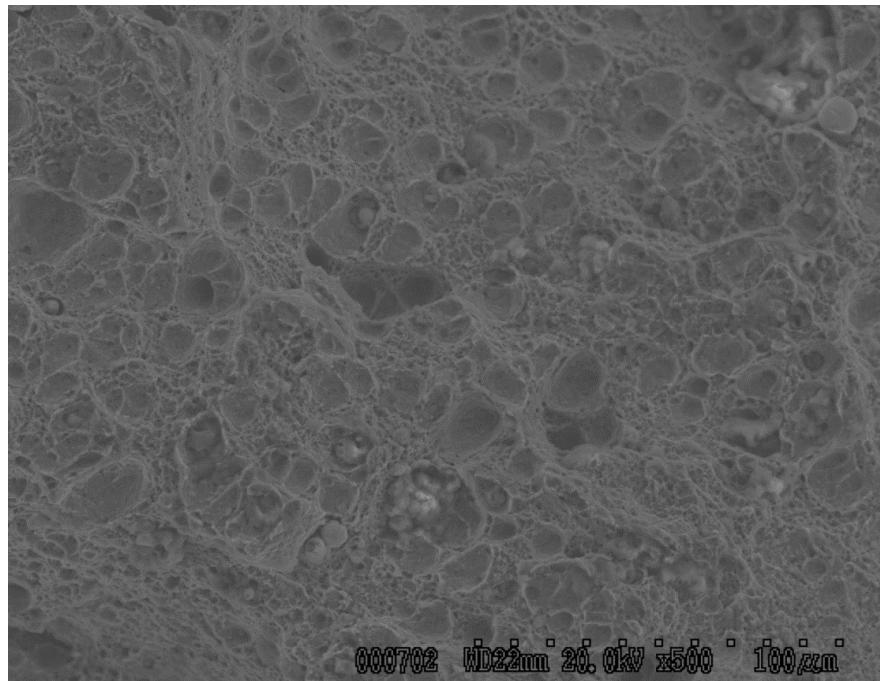


Fig. 330. Scanning electron microscope fractograph of generator shaft fracture subsegment "B", Area 3.



Fig. 331. Close-up photograph of generator shaft forward end fracture half showing two coupons removed for tensile specimens.



Fig. 332. Close-up photograph of generator shaft forward end fracture half showing subsegment removed for hardness testing.

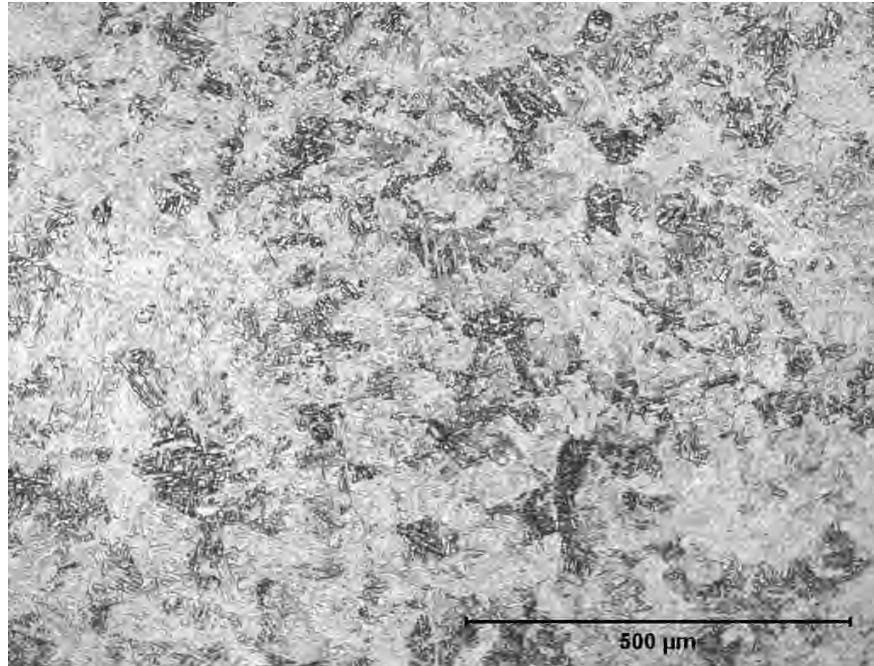


Fig. 333. Photomicrograph of longitudinal section through generator shaft in vicinity of fracture.

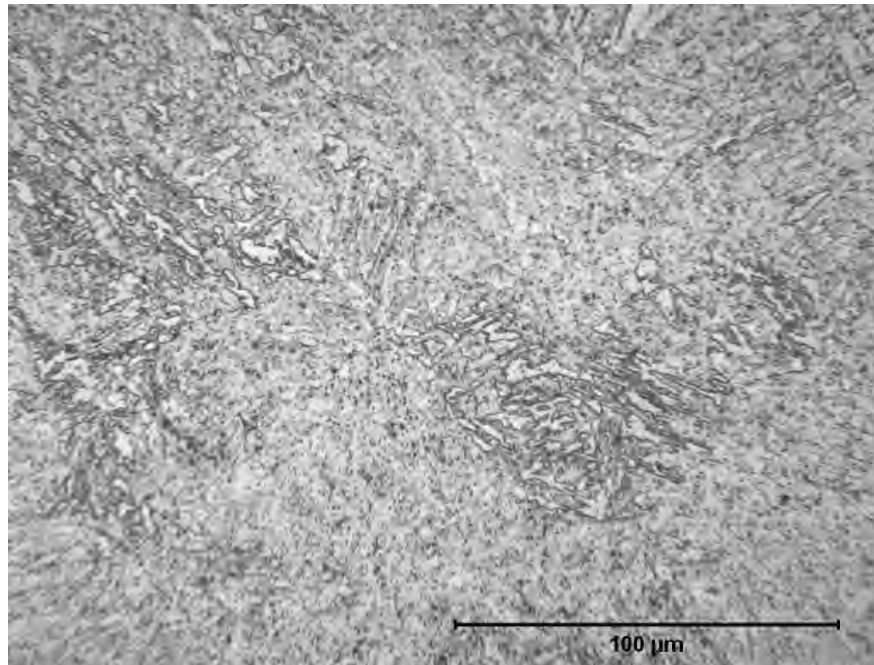


Fig. 334. Photomicrograph of longitudinal section through generator shaft in vicinity of fracture.

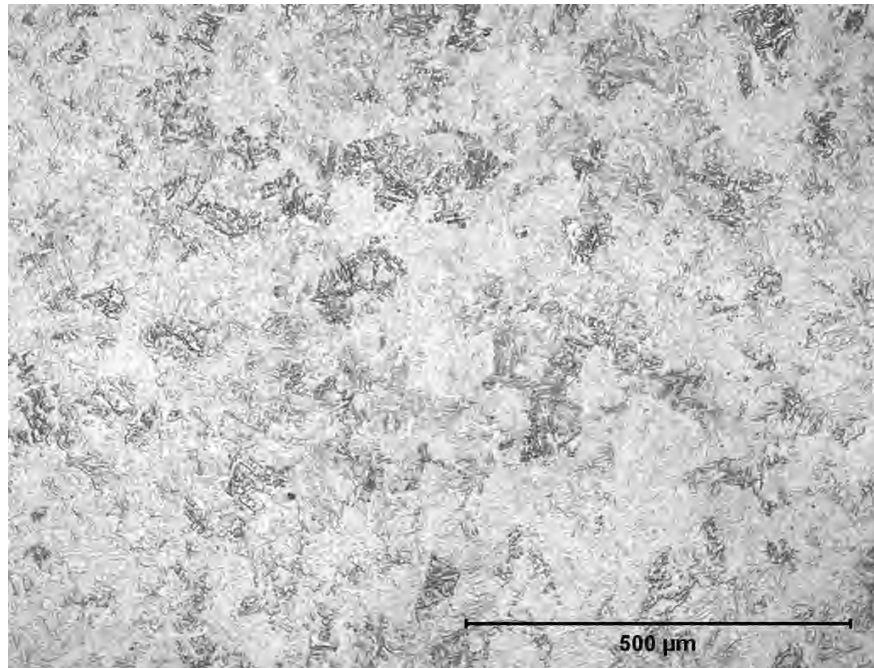


Fig. 335. Photomicrograph of transverse section through generator shaft in vicinity of fracture.

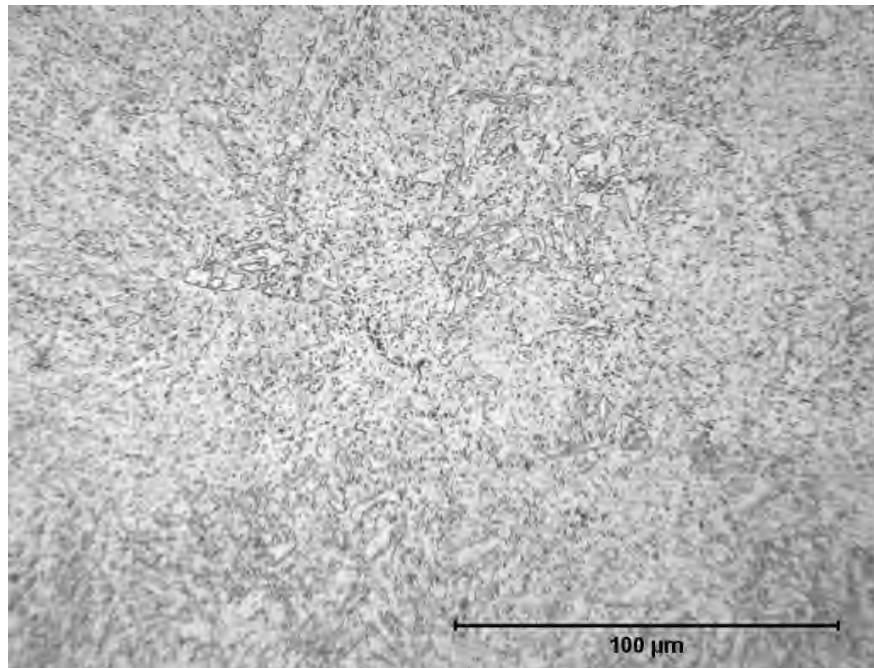


Fig. 336. Photomicrograph of transverse section through generator shaft in vicinity of fracture.



Fig. 337. Sherco Unit 3 exciter shaft that fractured transversely at three locations (arrows) during event of Nov. 19, 2011.



Fig. 338. Photograph of exciter shaft that fractured transversely (arrows) adjacent to the No. 11 bearing.



Fig. 339. Photograph of exciter shaft that fractured transversely (arrows) adjacent to the No. 12 bearing.

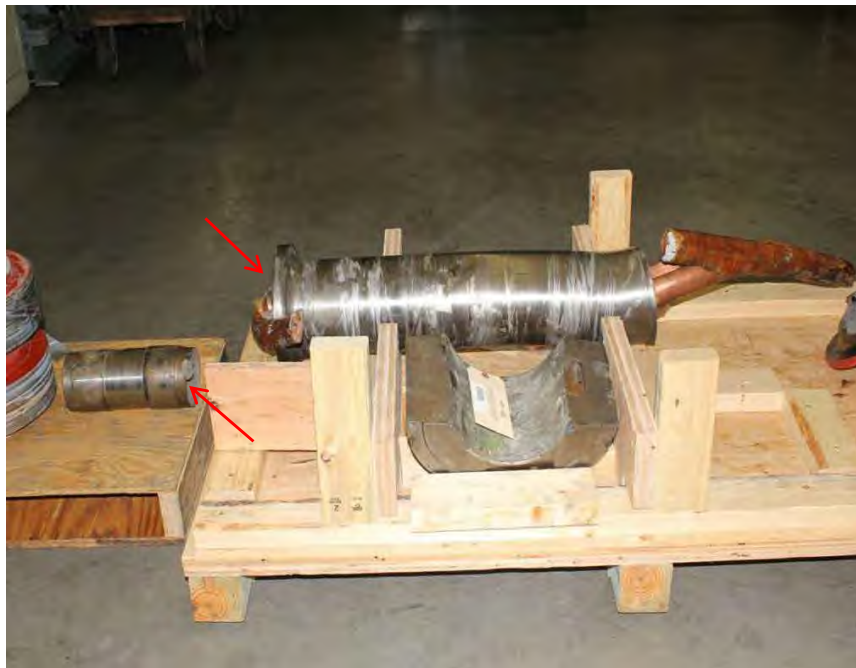


Fig. 340. Photograph of exciter shaft that fractured transversely (arrows) adjacent to the Alterex collector ring.



Fig 341. Close-up of fracture surface of exciter shaft fracture adjacent to the No. 11 bearing.



Fig. 342. Close-up of fracture surface of exciter shaft fracture adjacent to the No. 11 bearing



Fig. 343. Close-up of fracture surface of exciter shaft fracture adjacent to the No. 11 bearing



Fig. 344. Close-up of fracture surface of exciter shaft fracture adjacent to the No. 12 bearing.



Fig. 345. Close-up of fracture surface of exciter shaft fracture adjacent to the No. 12 bearing.



Fig. 346. Close-up of fracture surface of exciter shaft fracture adjacent to the No. 12 bearing.



Fig. 347. Close-up of fracture surface of exciter shaft fracture adjacent to the No. 12 bearing.



Fig. 348. Close-up of fracture surface of exciter shaft fracture adjacent to the No. 12 bearing.



Fig. 349. Close-up of fracture surface of exciter shaft fracture adjacent to the Alterex collector ring.



Fig. 350. Close-up of fracture surface of exciter shaft fracture adjacent to the Alterex collector ring.



Fig. 351. Close-up of fracture surface of exciter shaft fracture adjacent to the Alterex collector ring.



Fig 352. Photograph of exciter shaft fracture adjacent to the No. 11 bearing showing subsegment removed for scanning electron microscope examination.

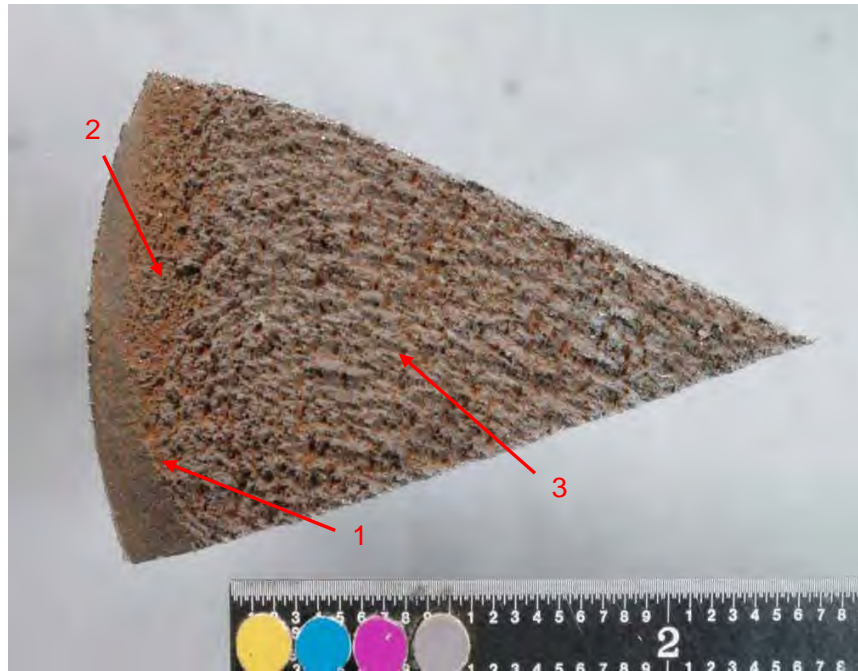


Fig 353. Photograph of exciter shaft fracture adjacent to the No. 11 bearing showing areas examined by scanning electron microscope.

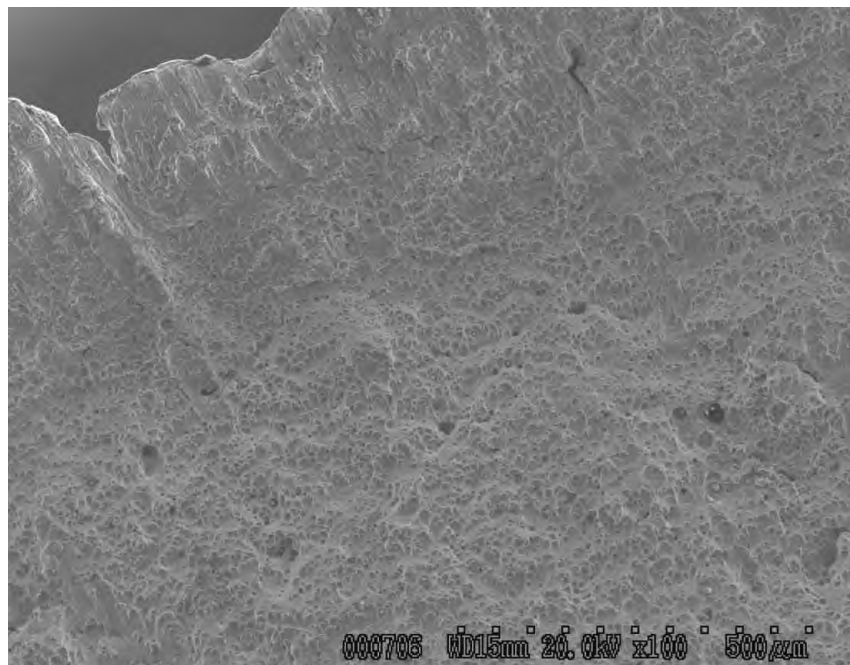


Fig. 354. Scanning electron microscope fractograph of exciter shaft fracture adjacent to the No. 11 bearing at area "1" shown in Fig. 353.

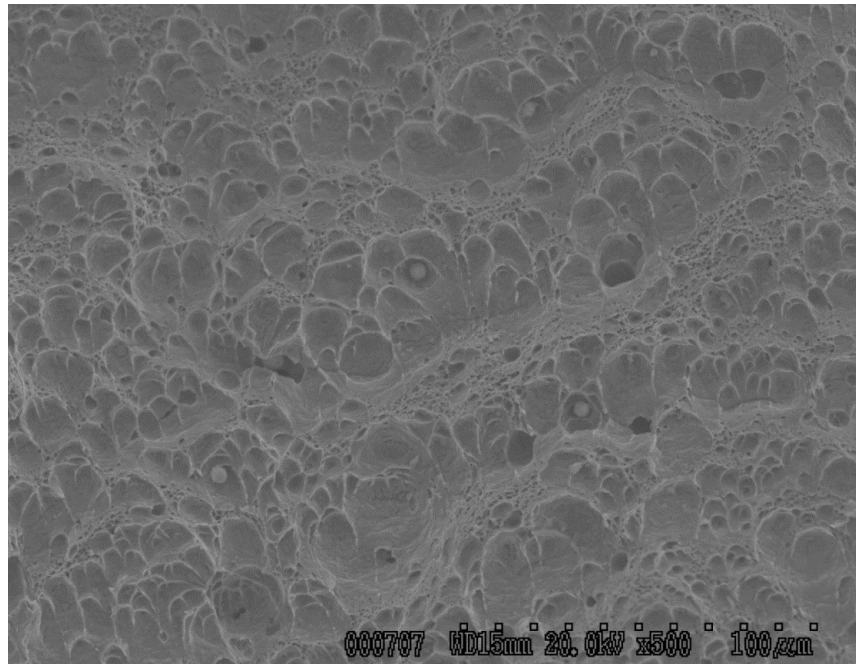


Fig. 355. Scanning electron microscope fractograph of exciter shaft fracture adjacent to the No. 11 bearing at area "1" shown in Fig. 353.

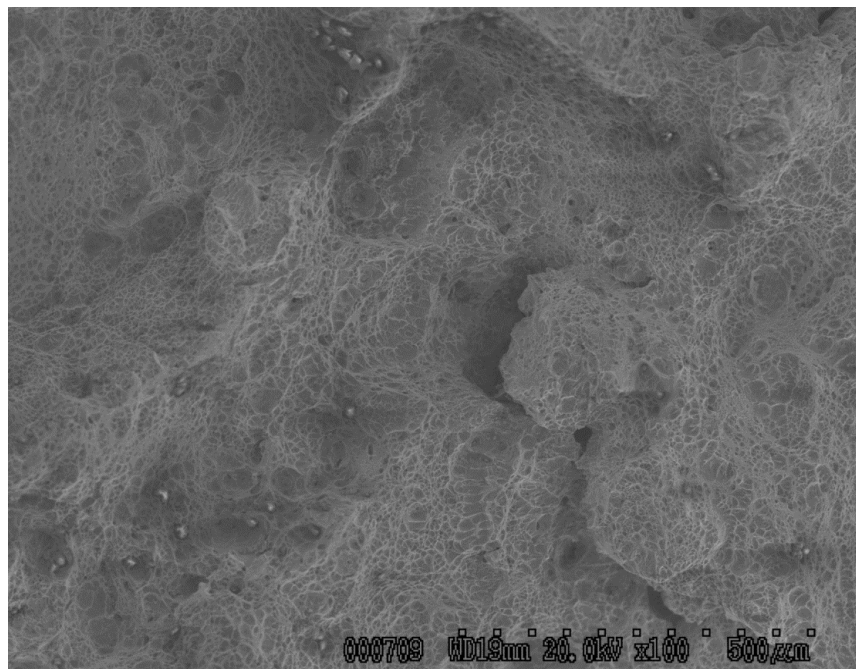


Fig. 356. Scanning electron microscope fractograph of exciter shaft fracture adjacent to the No. 11 bearing at area "2" shown in Fig. 353.

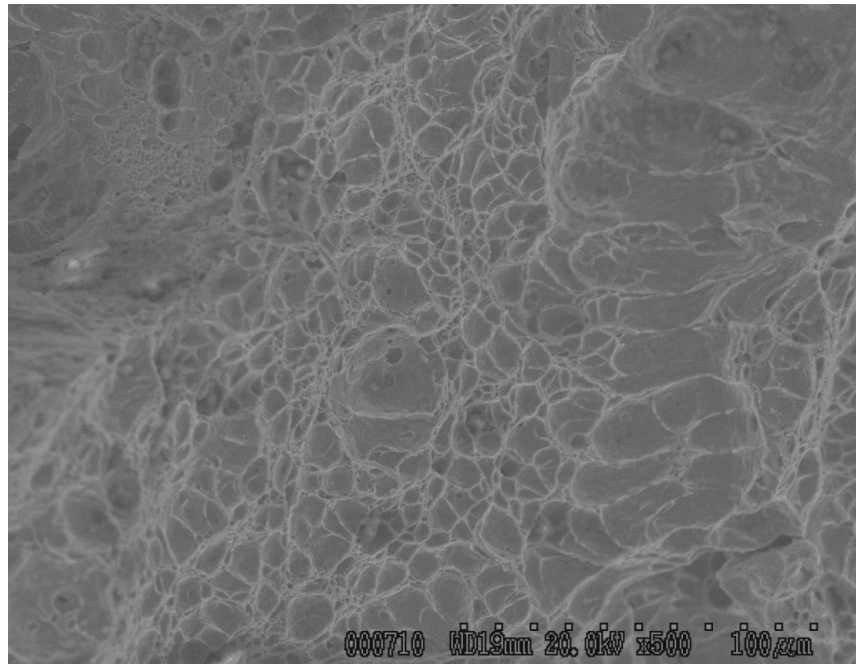


Fig. 357. Scanning electron microscope fractograph of exciter shaft fracture adjacent to the No. 11 bearing at area "2" shown in Fig. 353.

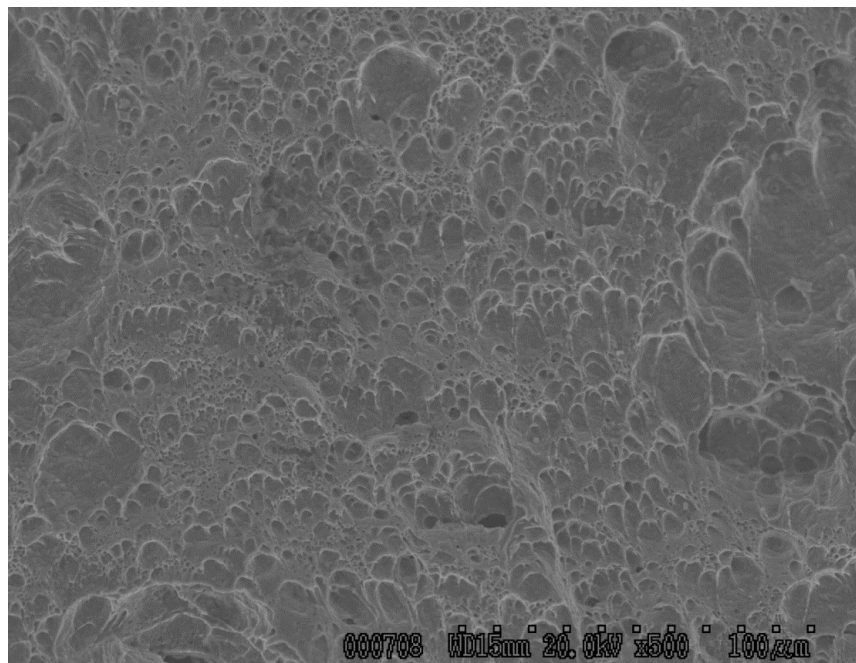


Fig. 358. Scanning electron microscope fractograph of exciter shaft fracture adjacent to the No. 11 bearing at area "3" shown in Fig. 353.



Fig. 359. Photograph of exciter shaft fracture adjacent to the No. 12 bearing showing subsegment removed for scanning electron microscope examination.



Fig. 360. Photograph of exciter shaft fracture adjacent to the No. 12 bearing showing areas examined by scanning electron microscope.

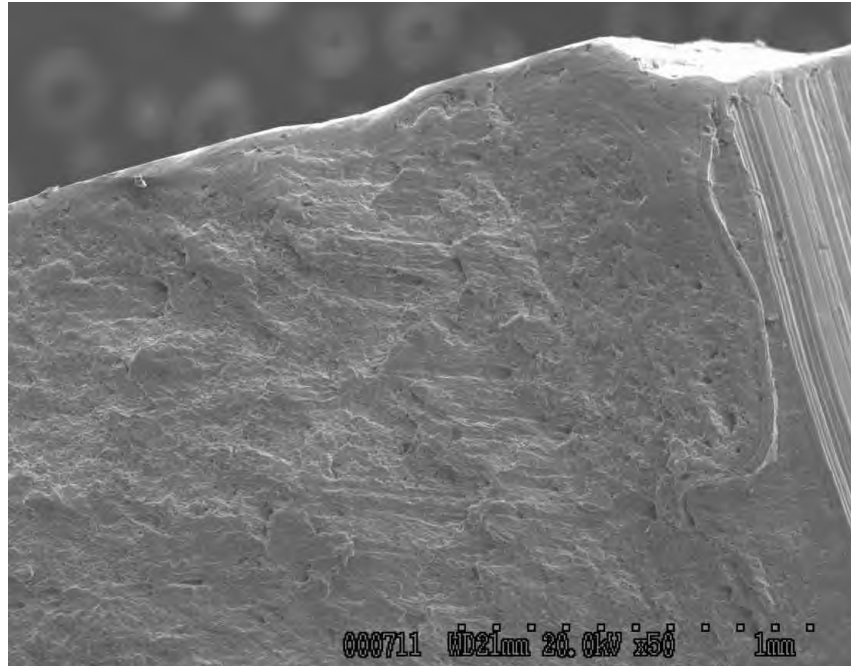


Fig. 361. Scanning electron microscope fractograph of exciter shaft fracture adjacent to the No. 12 bearing at area "1" shown in Fig. 360.

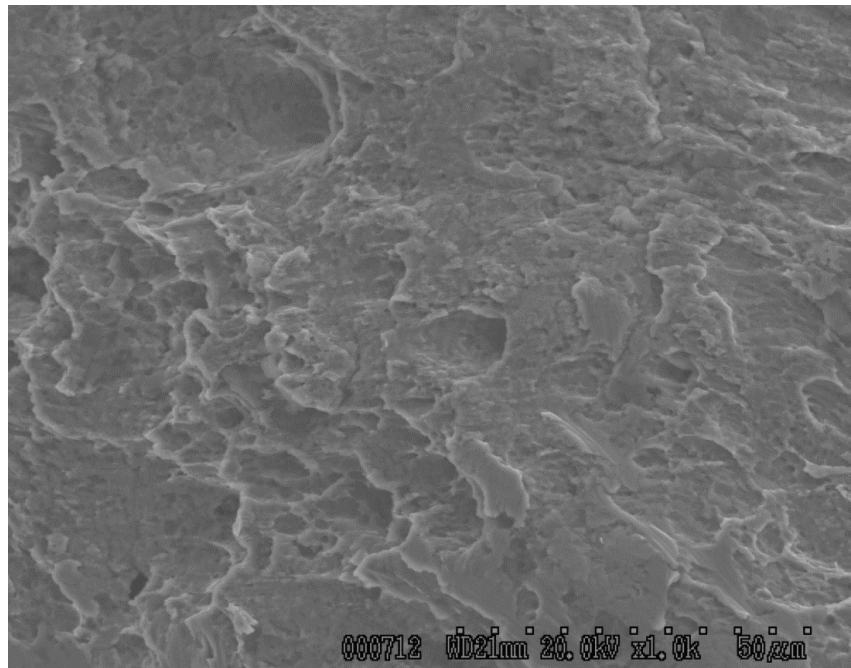


Fig. 362. Scanning electron microscope fractograph of exciter shaft fracture adjacent to the No. 12 bearing at area "1" shown in Fig. 360.

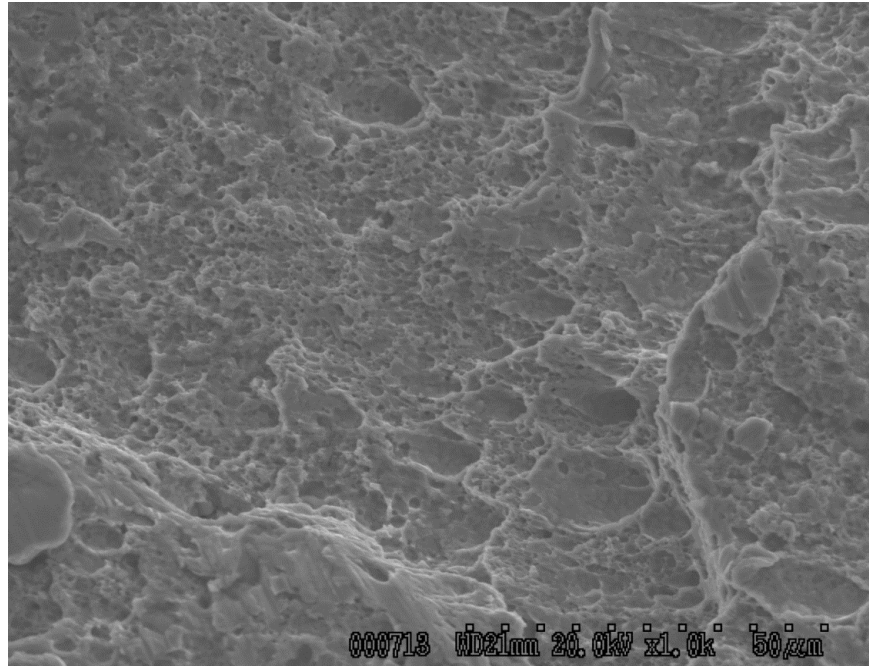


Fig. 363. Scanning electron microscope fractograph of exciter shaft fracture adjacent to the No. 12 bearing at area "1" shown in Fig. 360.

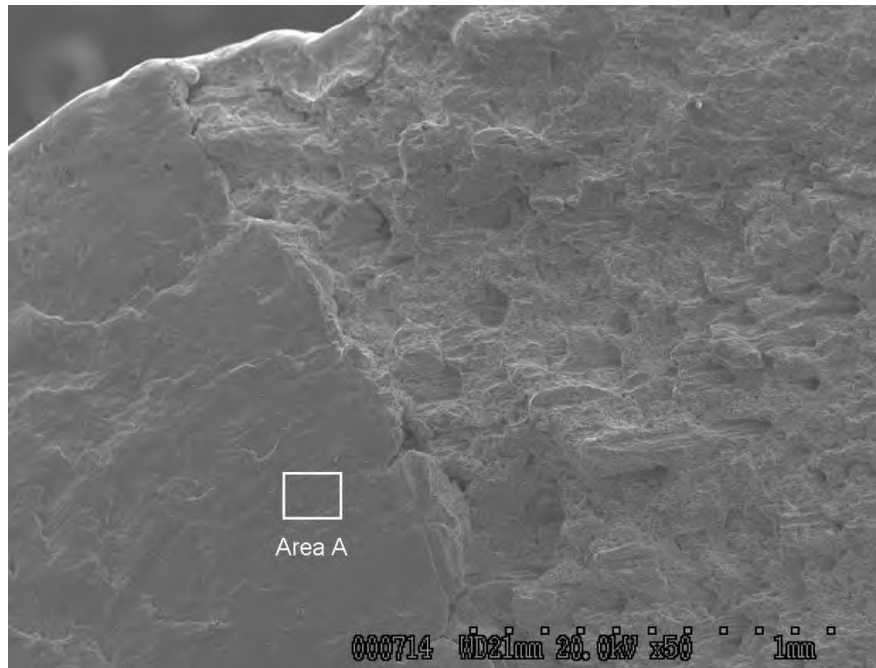


Fig. 364. Scanning electron microscope fractograph of exciter shaft fracture adjacent to the No. 12 bearing at area "2" shown in Fig. 360.

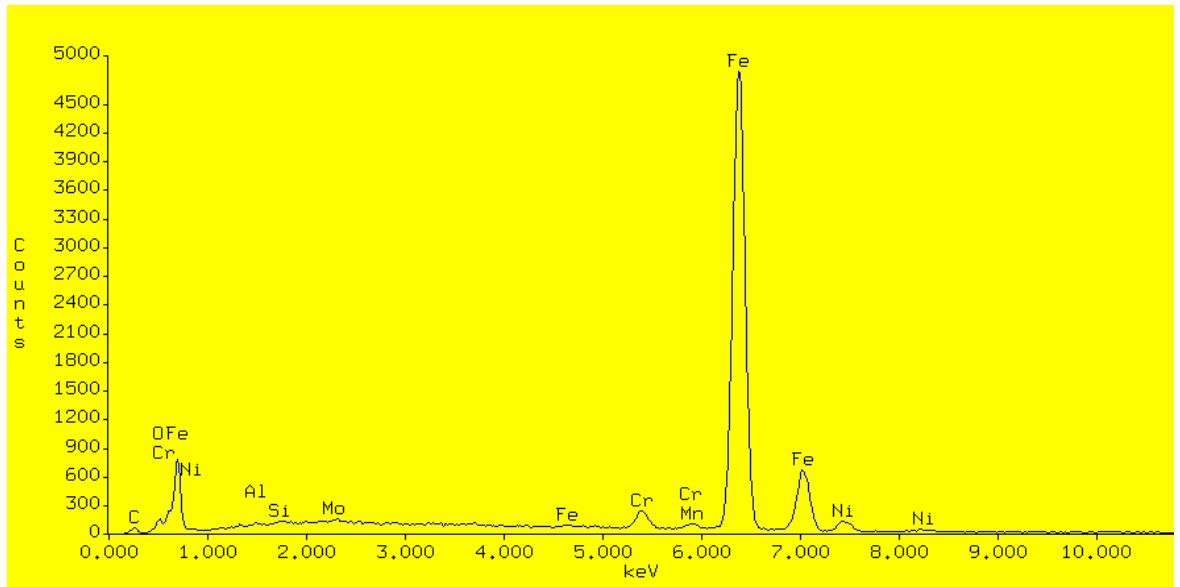


Fig. 365. Energy Dispersive Spectrograph of surface of exciter shaft fracture adjacent to the No. 12 bearing at area "A" shown in Fig. 364.

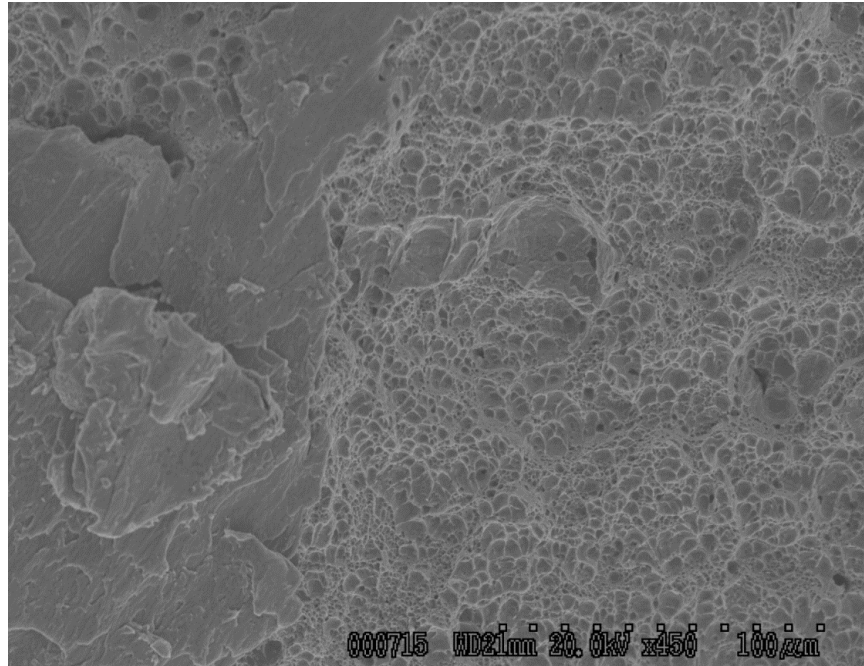


Fig. 366. Scanning electron microscope fractograph of exciter shaft fracture adjacent to the No. 12 bearing at area "3" shown in Fig. 360.

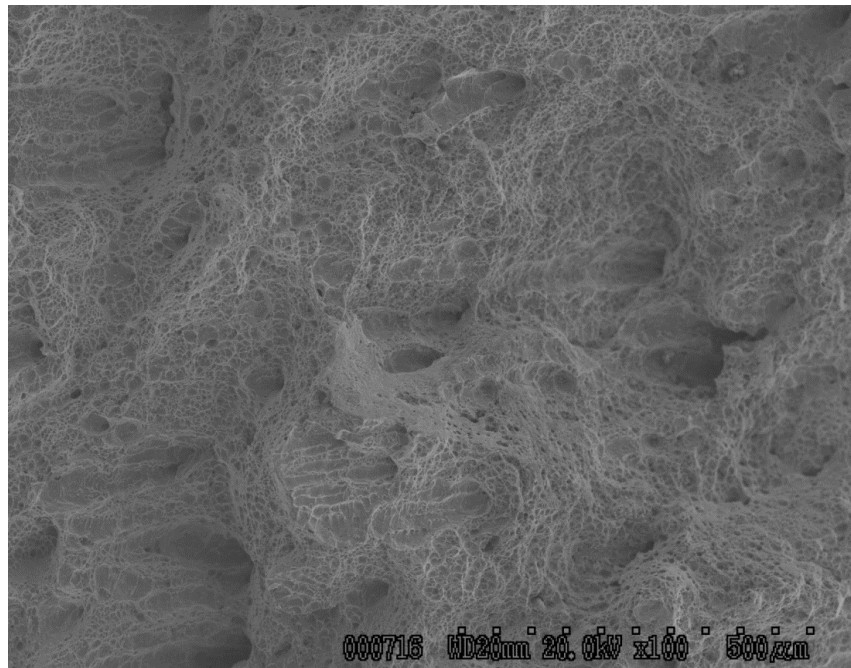


Fig. 367. Scanning electron microscope fractograph of exciter shaft fracture adjacent to the No. 12 bearing at area "4" shown in Fig. 360.



Fig. 368. Photograph of exciter shaft fracture adjacent to the Alterex collector ring showing subsegment removed for scanning electron microscope examination.



Fig. 369. Photograph of exciter shaft fracture adjacent to the Alterex collector ring showing areas examined by scanning electron microscope.

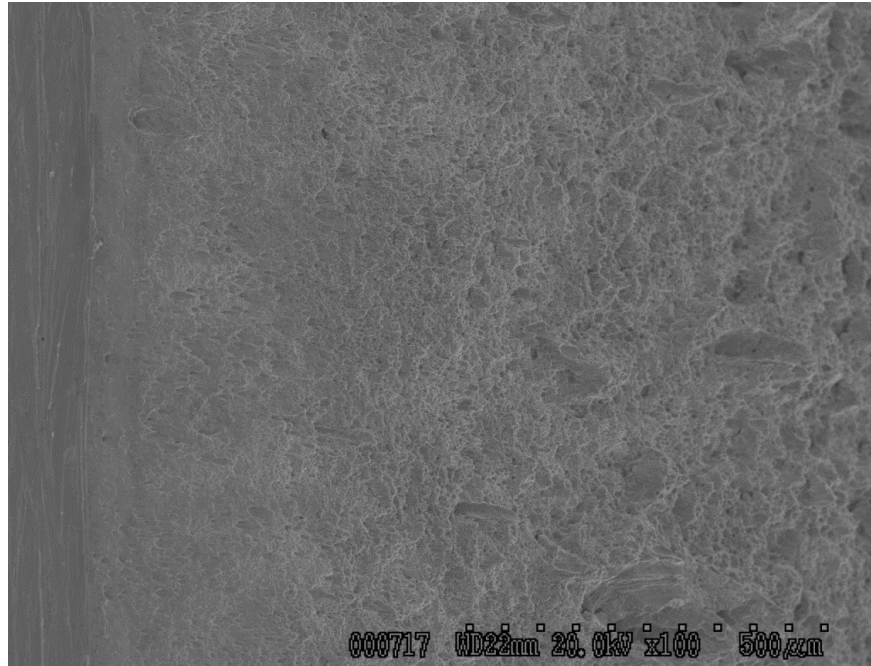


Fig. 370. Scanning electron microscope fractograph of exciter shaft fracture adjacent to the Alterex collector ring at area "1" shown in Fig. 369.

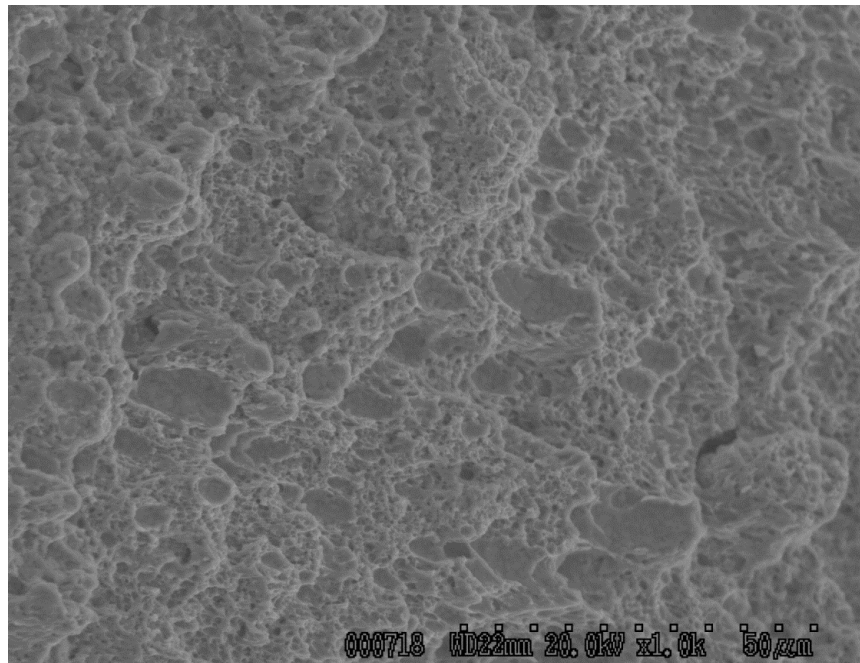


Fig. 371. Scanning electron microscope fractograph of exciter shaft fracture adjacent to the Alterex collector ring at area "1" shown in Fig. 369.

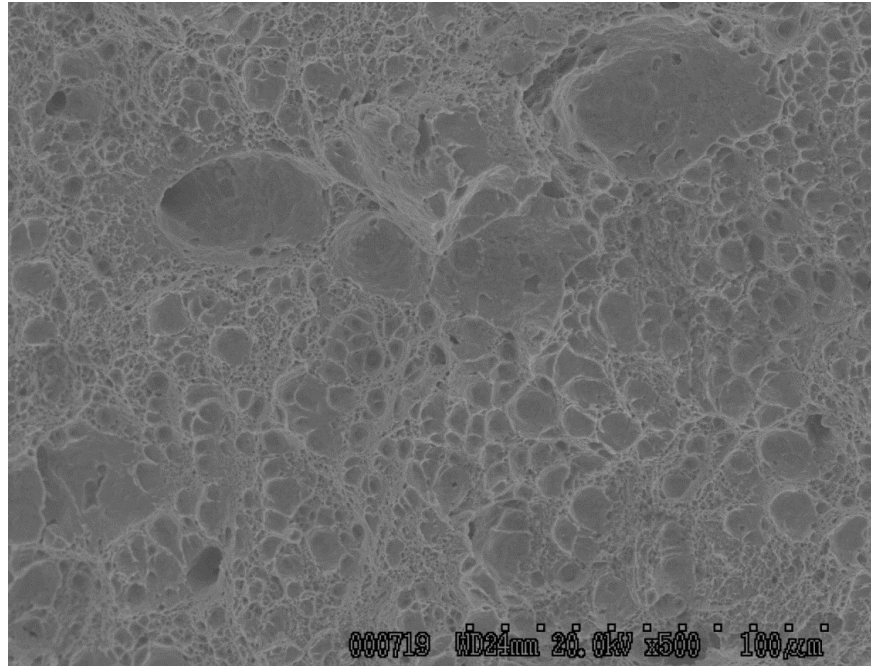


Fig. 372. Scanning electron microscope fractograph of exciter shaft fracture adjacent to the Alterex collector ring at area "2" shown in Fig. 369.

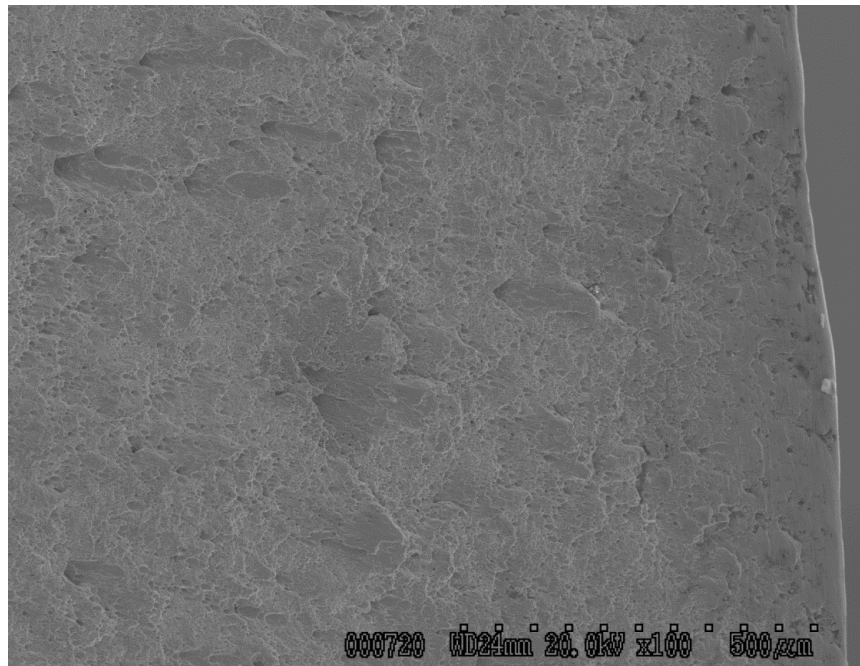


Fig. 373. Scanning electron microscope fractograph of exciter shaft fracture adjacent to the Alterex collector ring at area "3" shown in Fig. 369.

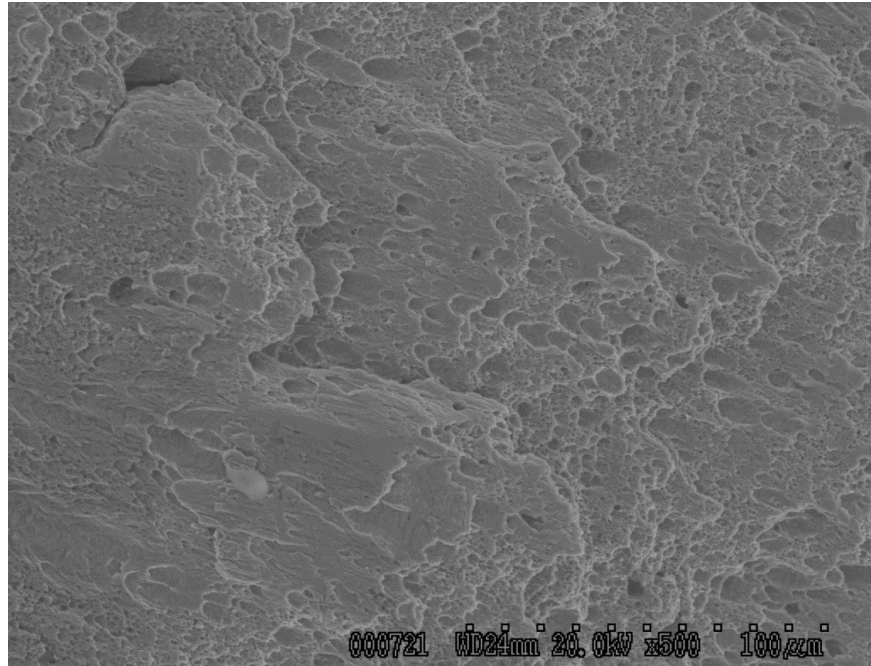


Fig. 374. Scanning electron microscope fractograph of exciter shaft fracture adjacent to the Alterex collector ring at area "3" shown in Fig. 369.

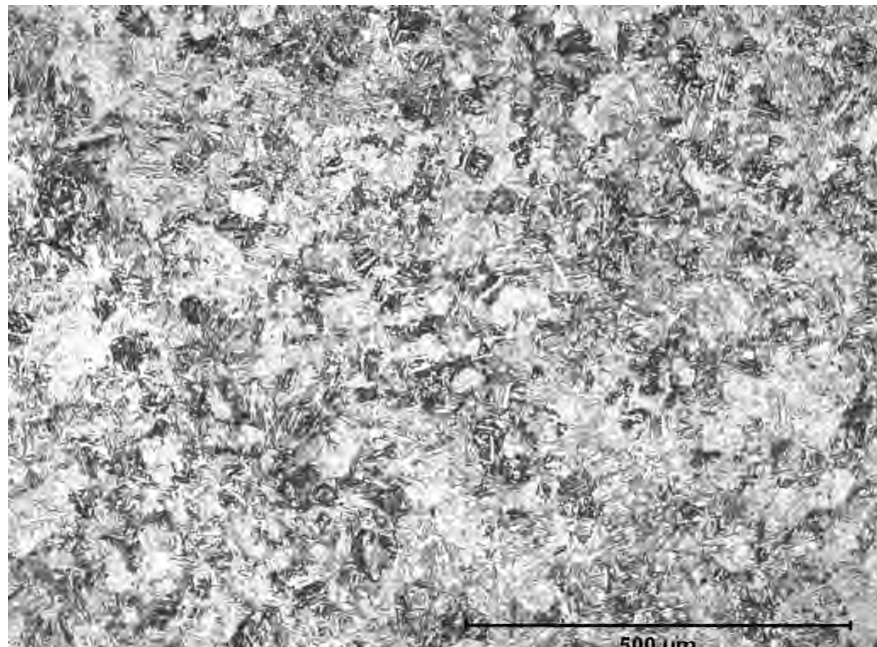


Fig. 375. Photomicrograph of longitudinal section through exciter shaft.

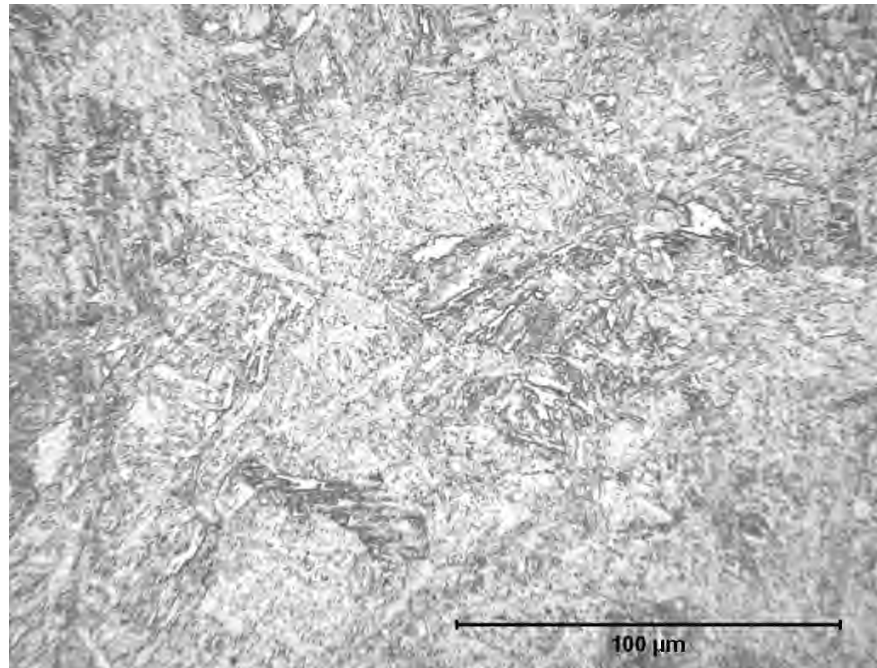


Fig. 376. Photomicrograph of longitudinal section through exciter shaft.

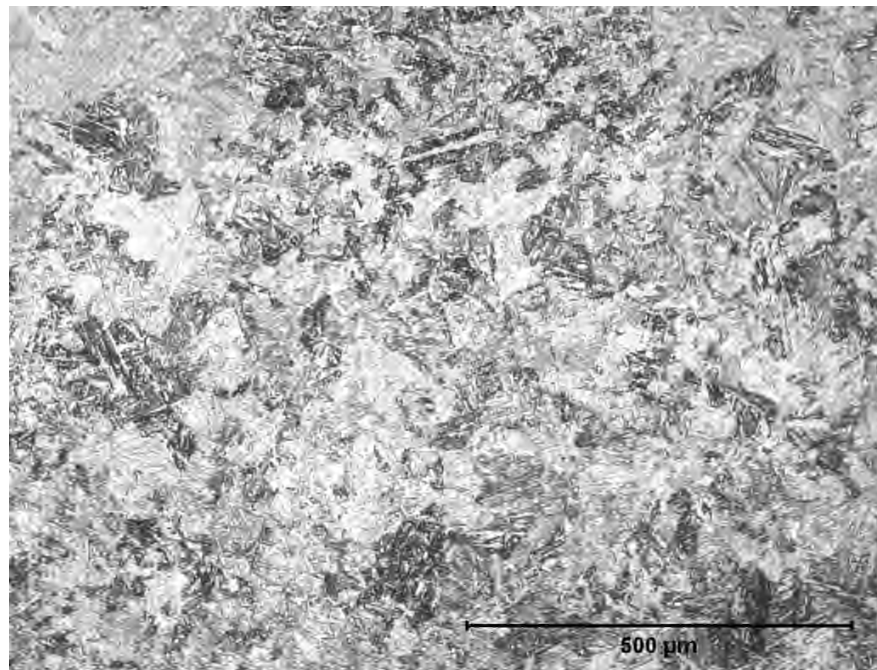


Fig 377. Photomicrograph of transverse section through exciter shaft.

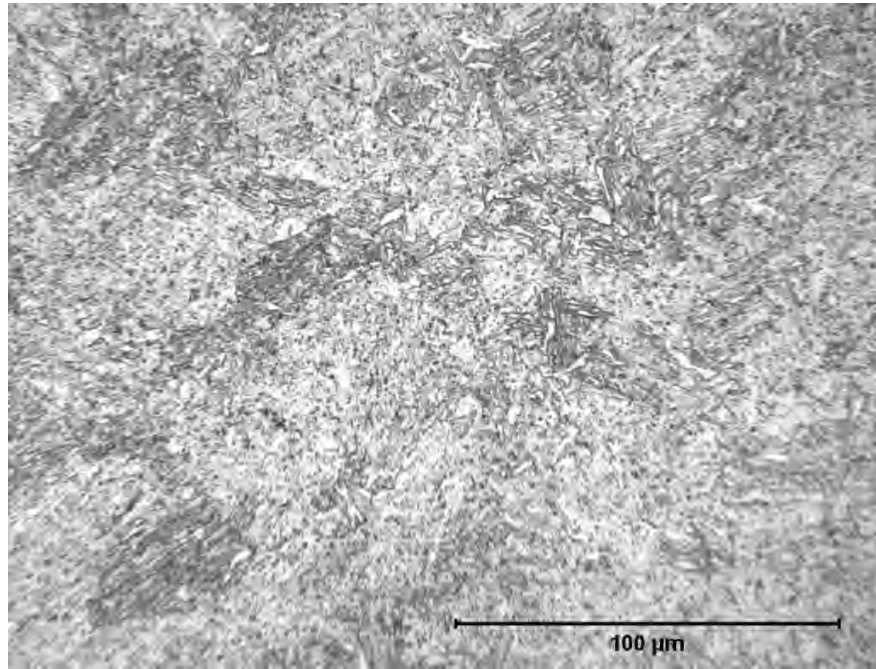


Fig. 378. Photomicrograph of transverse section through exciter shaft.



Fig. 379. Photograph of turbine end L-1 disk rim from LP turbine "A". The disk rim had been sectioned and removed at GE Repair Facility in Chicago, Illinois.



Fig. 380. Photograph of generator end L-1 disk rim from LP turbine "A". The disk rim had been sectioned and removed at GE Repair Facility in Chicago, Illinois.



Fig. 381. Photograph of turbine end L-1 disk rim from LP turbine "A". The disk rim had been sectioned and removed at GE Repair Facility in Chicago, Illinois.



Fig. 382. Close-up photograph of turbine end L-1 finger pinned blade attachment from LP turbine "A" showing location of cracks (arrows). Pc "A2", side 2.

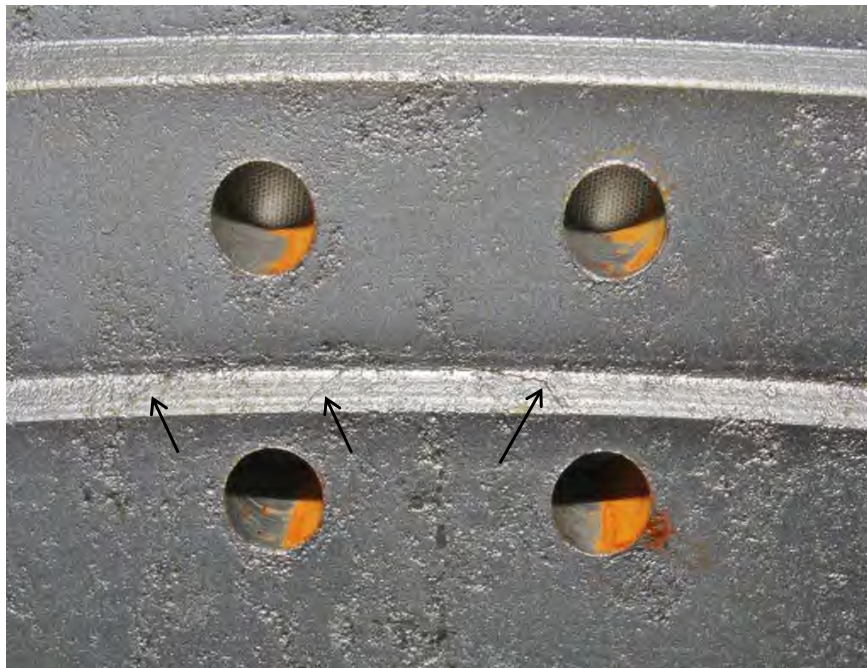


Fig. 383. Close-up photograph of turbine end L-1 finger pinned blade attachment from LP turbine "A" showing location of cracks (arrows).Pc "A2", side 2.



Fig. 384. Close-up photograph of turbine end L-1 finger pinned blade attachment from LP turbine "A" showing location of cracks (arrows).Pc "A3", side 1.



Fig. 385. Close-up photograph of turbine end L-1 finger pinned blade attachment from LP turbine "A" showing location of cracks (arrows).Pc "A3", side 2.

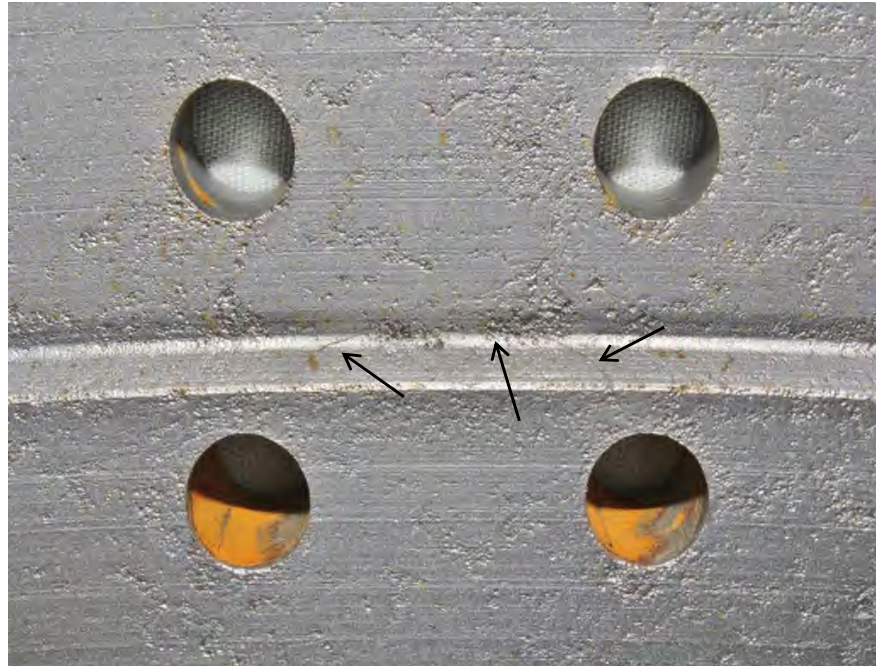


Fig 386. Close-up photograph of generator end L-1 finger pinned blade attachment from LP turbine "A" showing location of cracks (arrows). Pc "A2", side 1.



Fig. 387. Close-up photograph of generator end L-1 finger pinned blade attachment from LP turbine "A" showing location of cracks (arrows). Pc "A2", side 2.



Fig. 388. Close-up photograph of generator end L-1 finger pinned blade attachment from LP turbine "A" showing location of cracks (arrows).Pc "A3", side 1.



Fig. 389. Close-up photograph of generator end L-1 finger pinned blade attachment from LP turbine "A" showing location of cracks (arrows).Pc "A5", side 1.



Fig. 390. Close-up photograph of generator end L-1 finger pinned blade attachment from LP turbine "B" showing location of cracks (arrows).Pc "A2", side 1.



Fig. 391. Close-up photograph of generator end L-1 finger pinned blade attachment from LP turbine "B" showing location of cracks (arrows). Pc "A2", side 2.

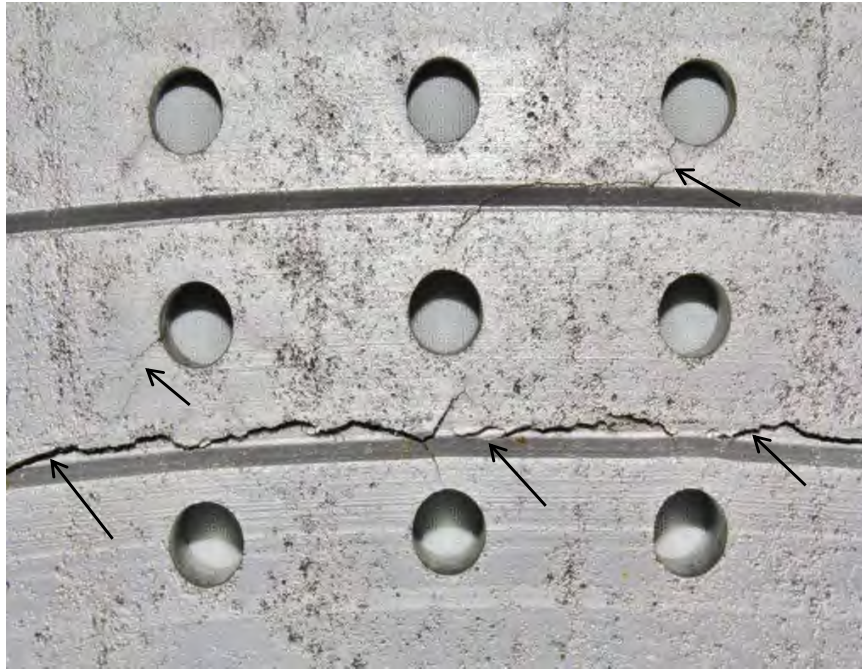


Fig. 392. Close-up photograph of generator end L-1 finger pinned blade attachment from LP turbine "B" showing location of cracks (arrows). Pc "A3", side 1.



Fig. 393. Close-up photograph of generator end L-1 finger pinned blade attachment from LP turbine "B" showing location of cracks (arrows). Pc "A3", side 2.



Fig. 394. Close-up photograph of generator end L-1 finger pinned blade attachment from LP turbine "B" showing location of cracks (arrows). Pc "A4", side 1.



Fig 395. Close-up photograph of generator end L-1 finger pinned blade attachment from LP turbine "B" showing location of cracks (arrows). Pc "A4", side 2.



Fig. 396. Close-up photograph of generator end L-1 finger pinned blade attachment from LP turbine "B" showing location of cracks (arrows).Pc "A5", side 1.

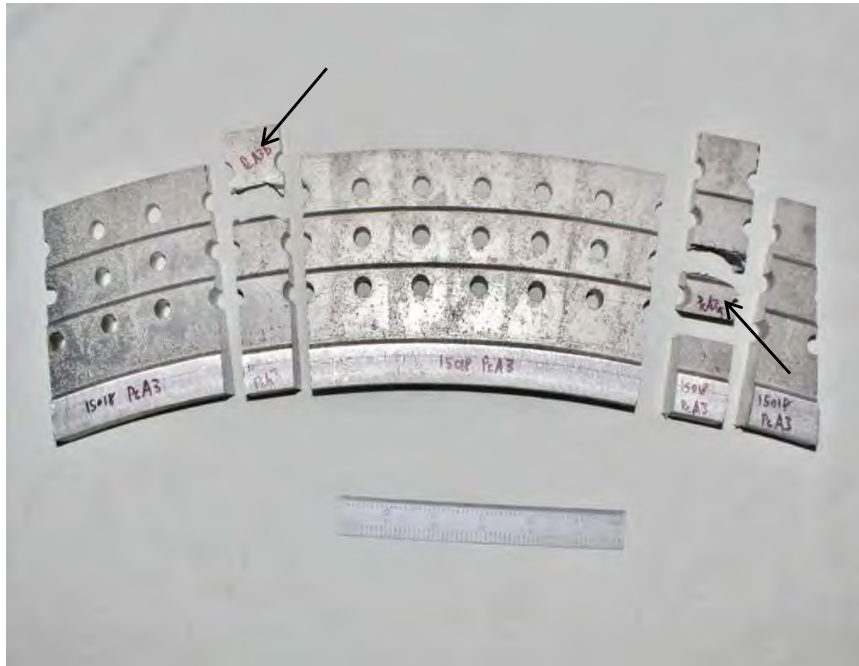


Fig. 397. Turbine end finger pinned blade attachment, Pc A3, from LP turbine "A" showing sectioning of cracks (arrows) for further examination.



Fig. 398. Close-up photograph of subsegment A3a from LP turbine "A" containing a circumferential crack shown in Fig. 397.



Fig. 399. Close-up photograph of subsegment A3b from LP turbine "A" containing a circumferential crack shown in Fig. 397.



Fig. 400. Close-up photograph of crack surface from subsegment A3a shown in Fig. 398. Arrows show areas examined by scanning electron microscopy.



Fig. 401 Close-up photograph of crack surface from subsegment A3a shown in Fig. 398.



Fig. 402. Close-up photograph of crack surface from subsegment A3b shown in Fig. 399.



Fig. 403. Generator end finger pinned blade attachment, Pc A4, from LP turbine "A" showing sectioning of cracks (arrows) for further examination.



Fig. 404. Close-up photograph of subsegment A4a from LP turbine "A" containing a circumferential crack shown in Fig 403.



Fig. 405. Close-up photograph of subsegment A4b from LP turbine "A" containing a circumferential crack shown in Fig 403.



Fig. 406. Close-up photograph of crack surface from subsegment A4a shown in Fig. 404.



Fig. 407. Close-up photograph of crack surface from subsegment A4a shown in Fig. 404.



Fig. 408. Close-up photograph of crack surface from subsegment A4b shown in Fig. 405.



Fig. 409. Generator end finger pinned blade attachment, Pc A4, from LP turbine "B" showing sectioning of cracks (arrows) for further examination.

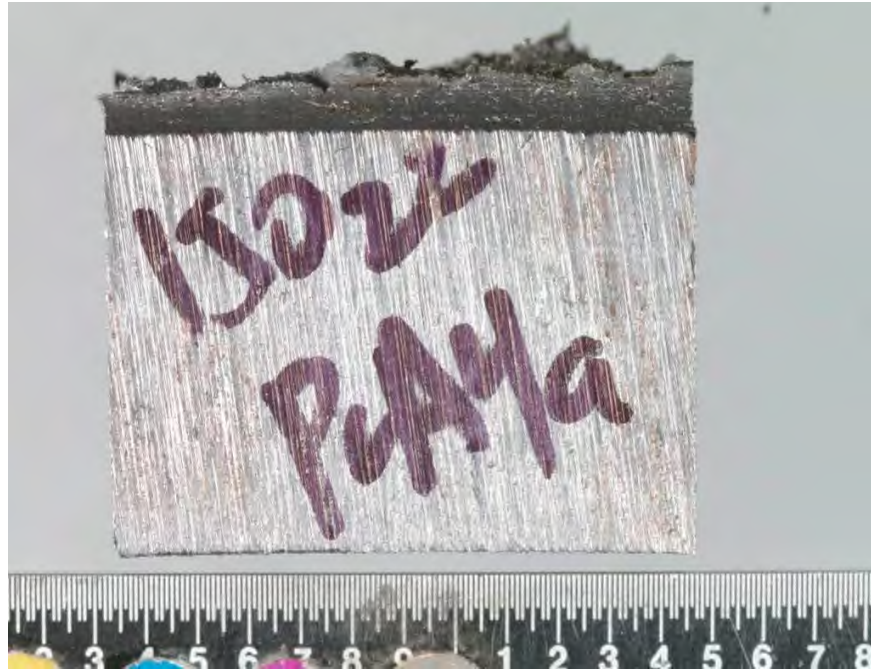


Fig. 410. Close-up photograph of subsegment A4a from LP turbine "B" containing circumferential crack shown in Fig 409.



Fig. 411. Close-up photograph of subsegment A4b from LP turbine "B" containing a circumferential/radial crack shown in Fig 409.

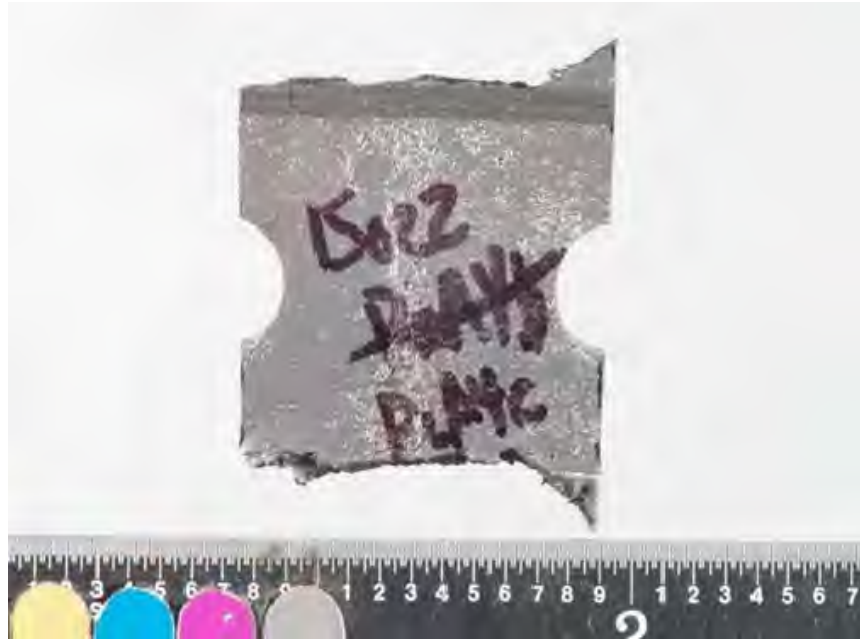


Fig. 412. Close-up photograph of subsegment A4c from LP turbine "B" containing a circumferential crack shown in Fig 409.



Fig. 413. Close-up photograph of subsegment A4d from LP turbine "B" containing a circumferential crack shown in Fig 409.



Fig. 414. Close-up photograph of crack surface from subsegment A4a shown in Fig. 410.



Fig. 415. Close-up photograph of crack surface from subsegment A4b shown in Fig. 411.



Fig. 416. Close-up photograph of crack surface from subsegment A4c shown in Fig. 412.



Fig. 417. Close-up photograph of crack surface from subsegment A4d shown in Fig. 413.

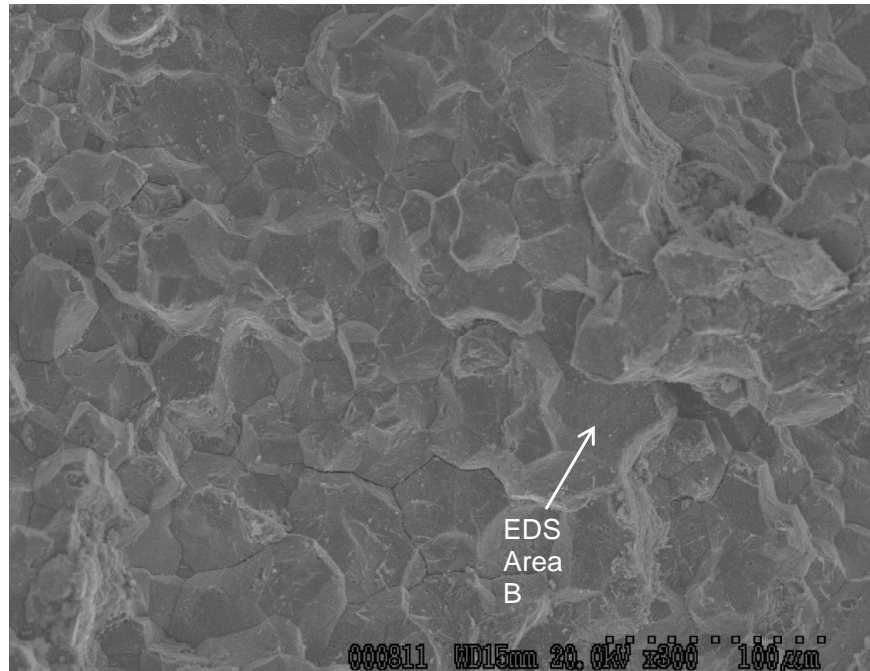


Fig. 418. Scanning electron microscope fractograph of fracture through crack "A3a" shown in Fig. 400 at area 1.

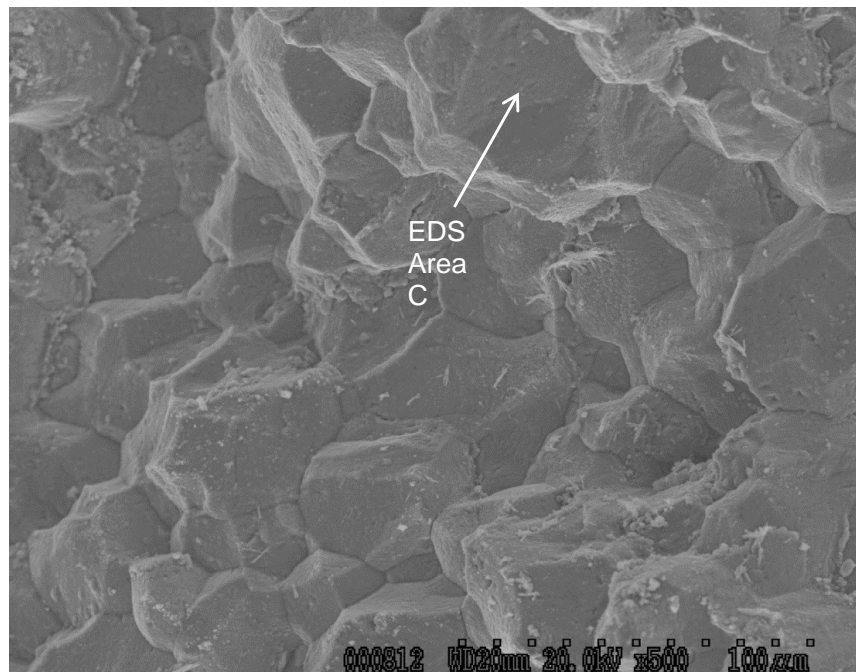


Fig. 419. Scanning electron microscope fractograph of fracture through crack "A3a" shown in Fig. 400 at area 2.

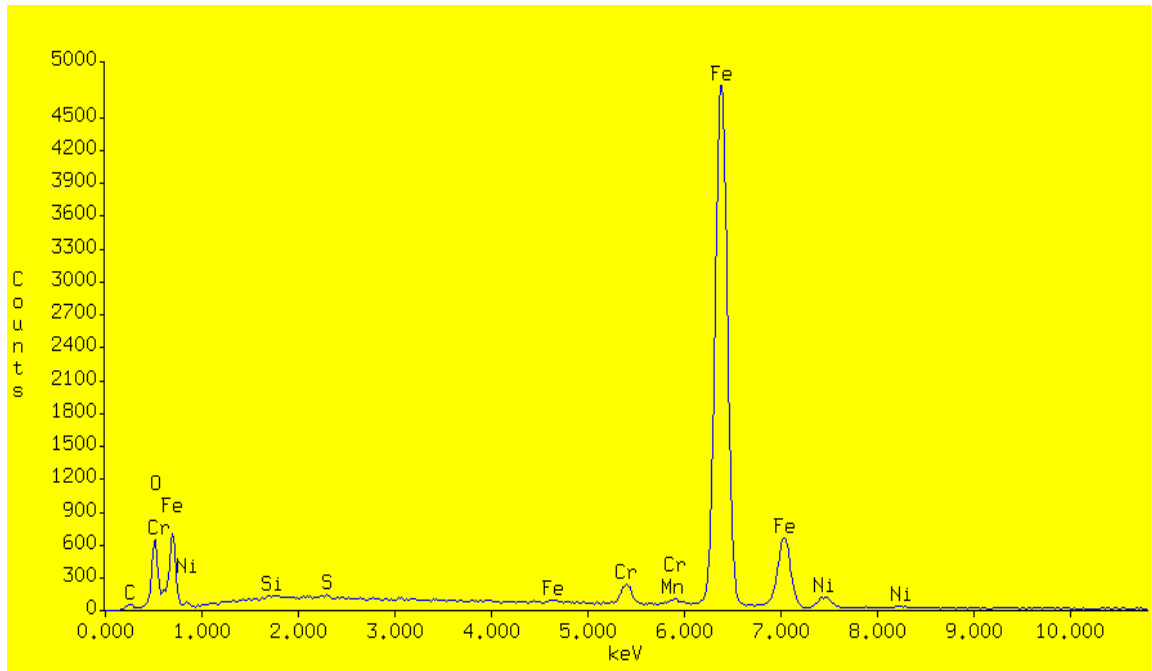


Fig. 420. Energy Dispersive Spectrograph of crack surface "A3a" shown in Fig. 418 at EDS area B.

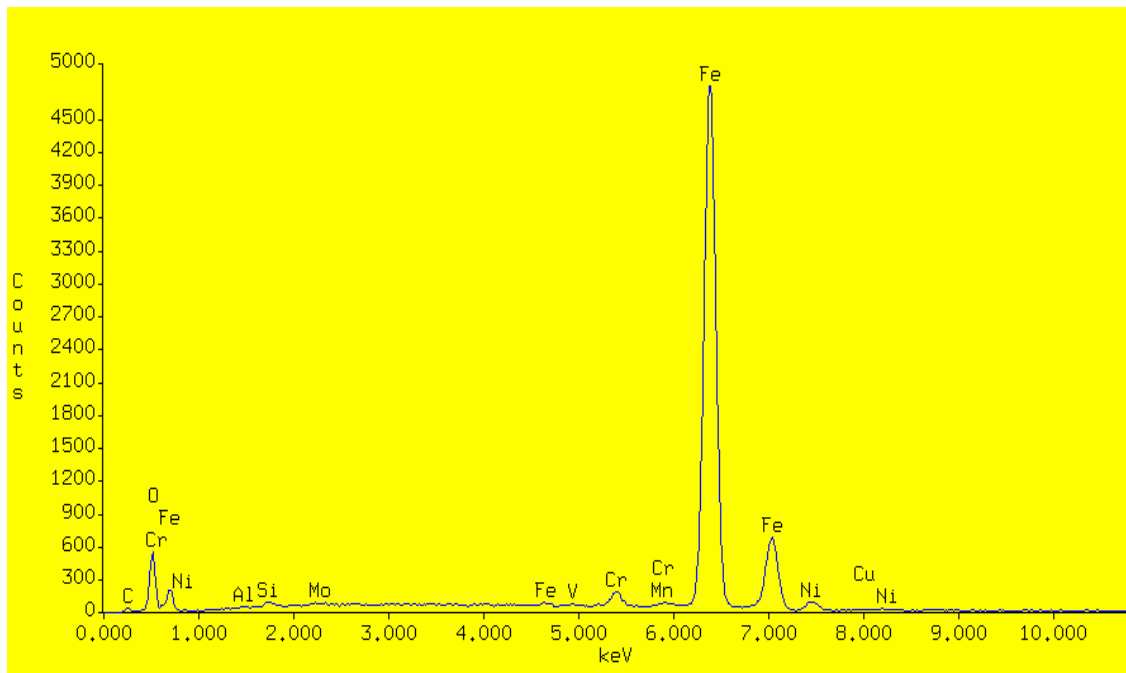


Fig. 421. Energy Dispersive Spectrograph of crack surface "A3a" shown in Fig. 419 at EDS area C.

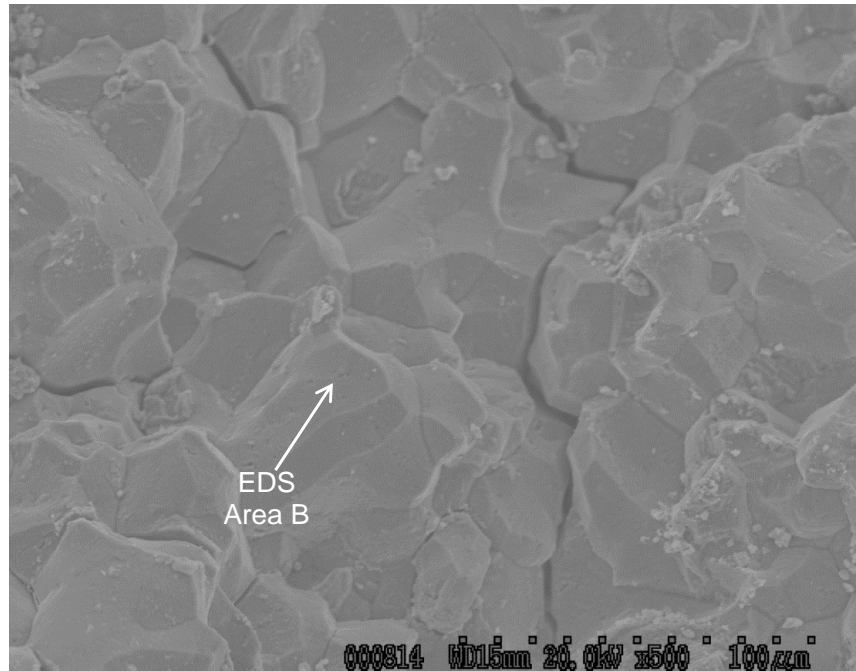


Fig. 422. Scanning electron microscope fractograph of fracture through crack "A4a" at area 1 shown in Fig. 406.

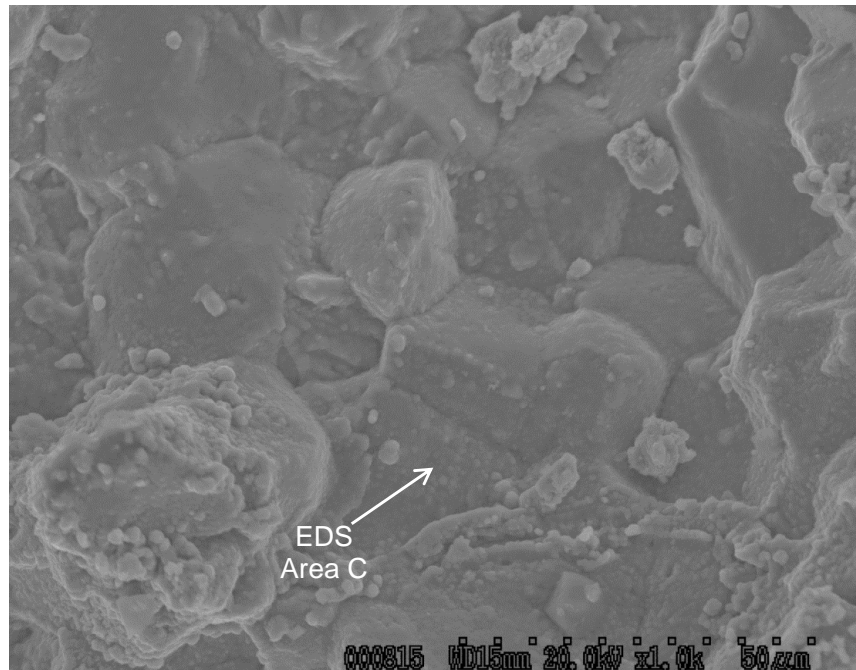


Fig. 423. Scanning electron microscope fractograph of fracture through crack "A4a" at area 2 shown in Fig. 406.

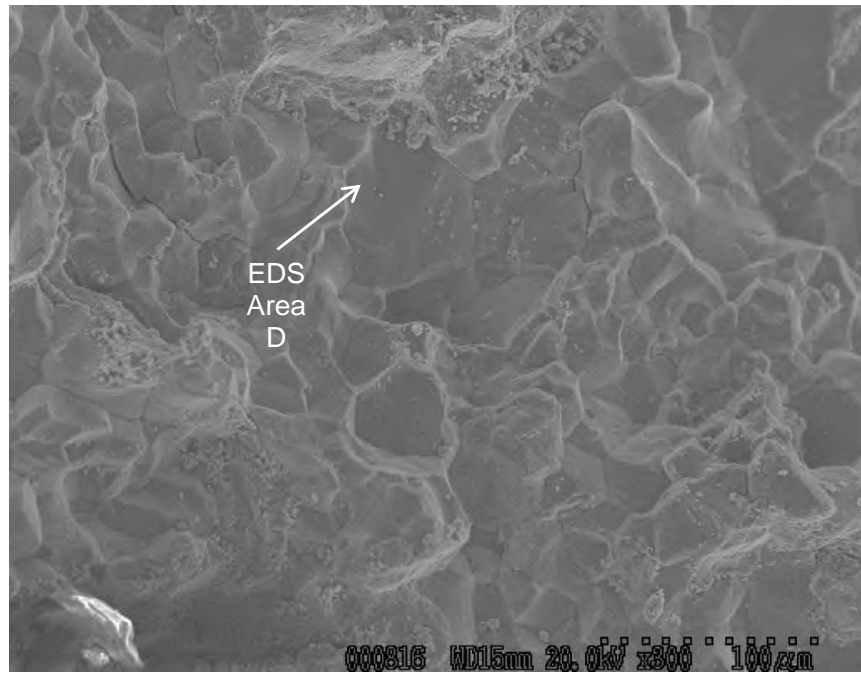


Fig. 424. Scanning electron microscope fractrograph of fracture through crack "A4a" at area 3 shown in Fig. 406.

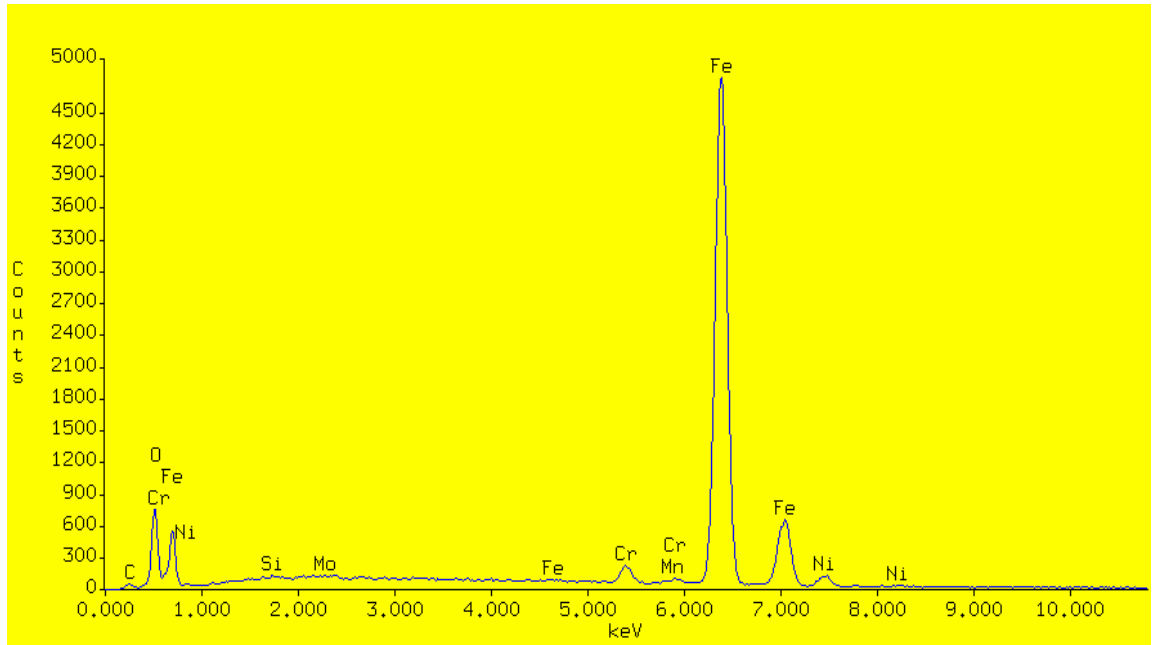


Fig. 425. Energy Dispersive Spectrograph of crack surface "A4a" shown in Fig. 423 at EDS area B.

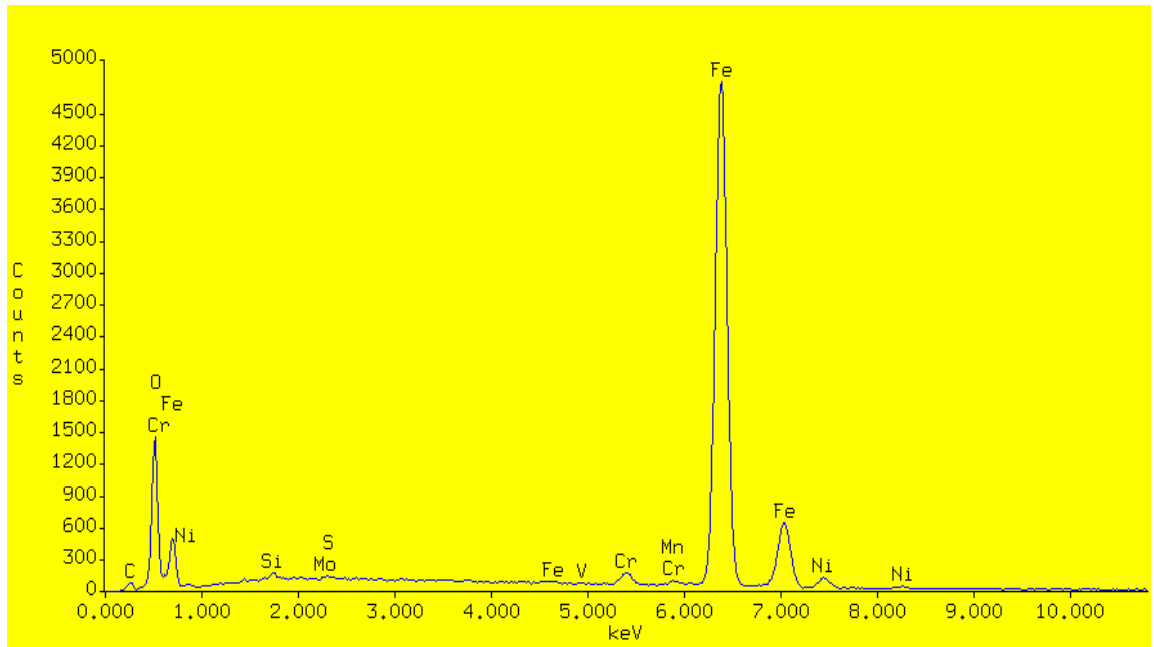


Fig. 426. Energy Dispersive Spectrograph of crack surface "A4a" shown in Fig. 424 at EDS area C.

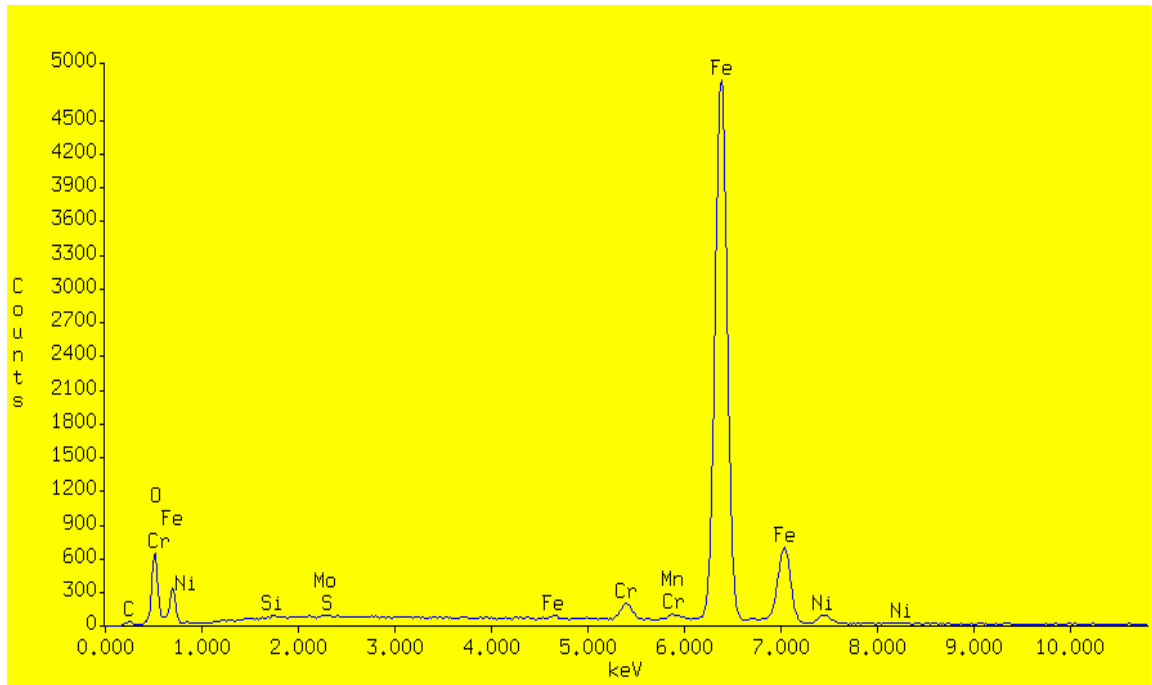


Fig. 427. Energy Dispersive Spectrograph of crack surface "A4a" shown in Fig.re 422 EDS area D.

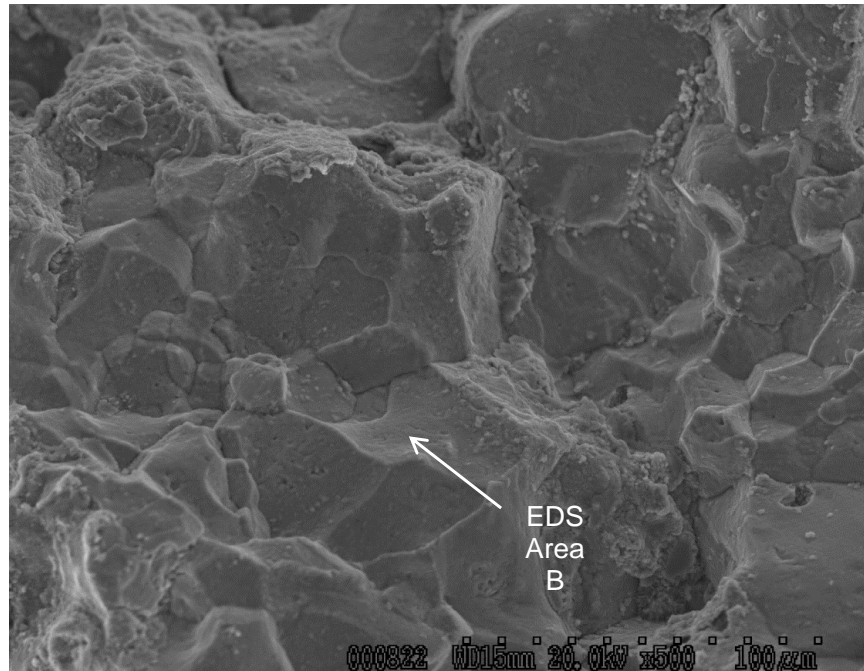


Fig. 428. Scanning electron microscope fractograph of fracture through crack "A4a" shown in Fig. 414 at area 1.

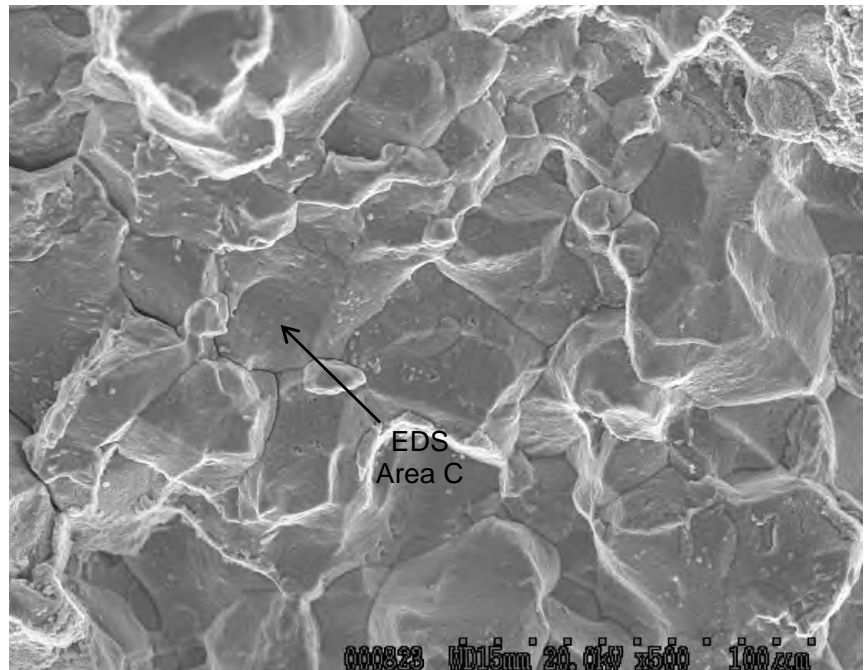


Fig. 429. Scanning electron microscope fractograph of fracture through crack "A4a" shown in Fig. 414 at area 2.

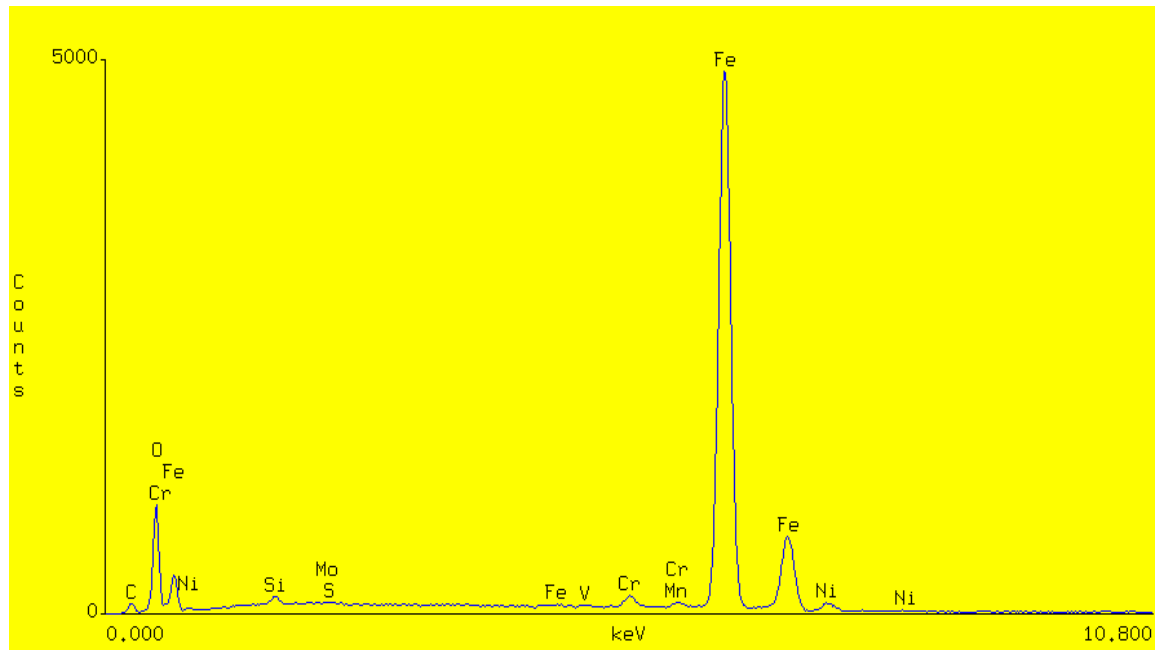


Fig. 430. Energy Dispersive Spectrograph of crack surface "A4a" shown in Fig. 428 at EDS area B.

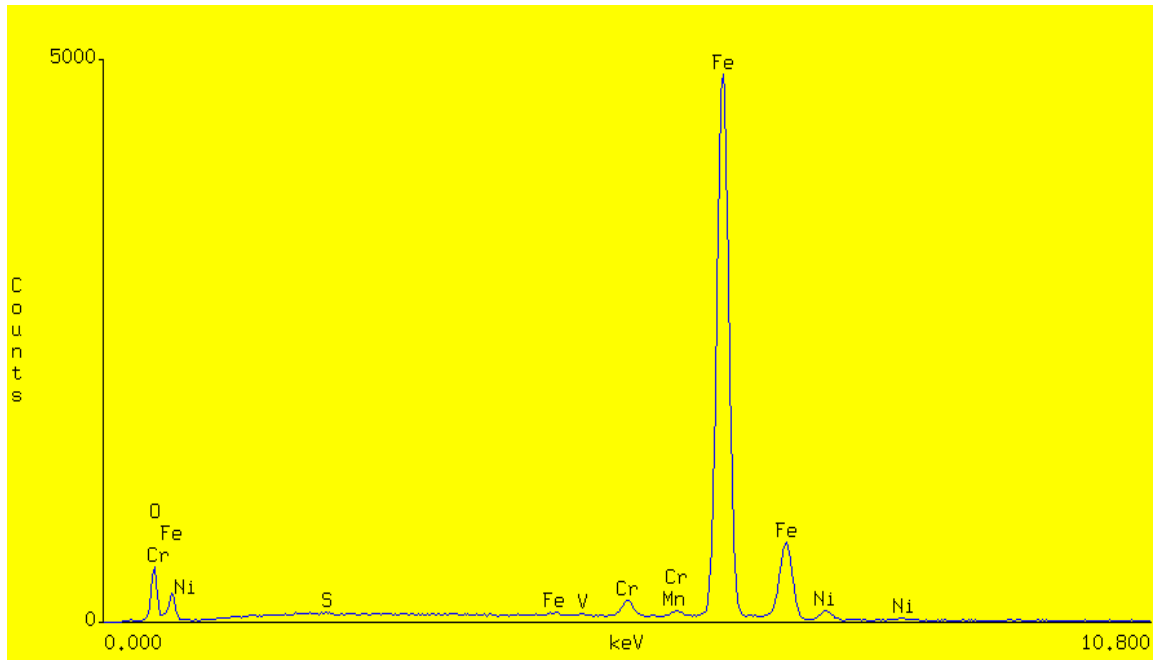


Fig. 431. Energy Dispersive Spectrograph of crack surface "A4a" shown in Fig. 429 at EDS area C.

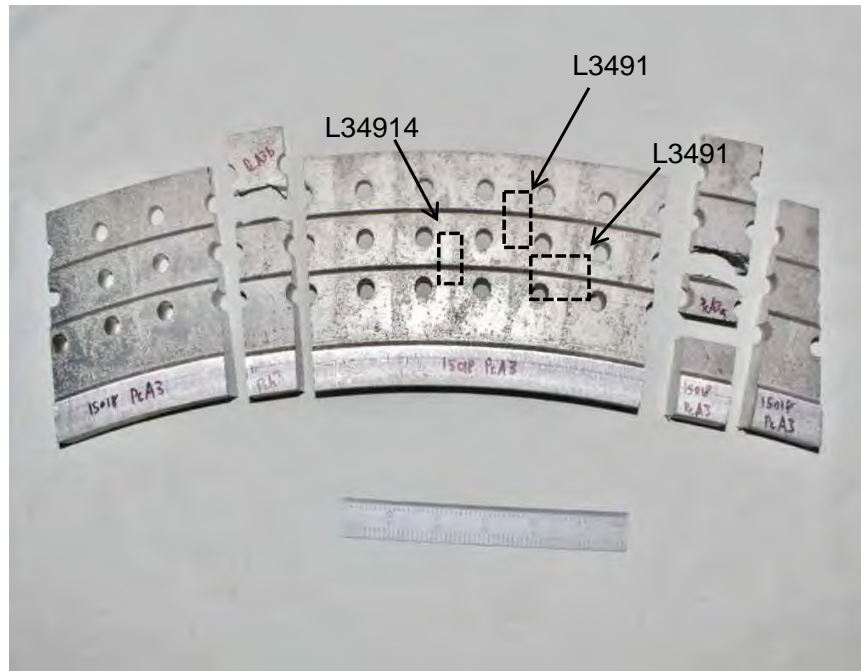


Fig. 432. Turbine end finger pinned blade attachment, Pc A3, from LP turbine "A" showing location of coupons removed for metallography (arrows).

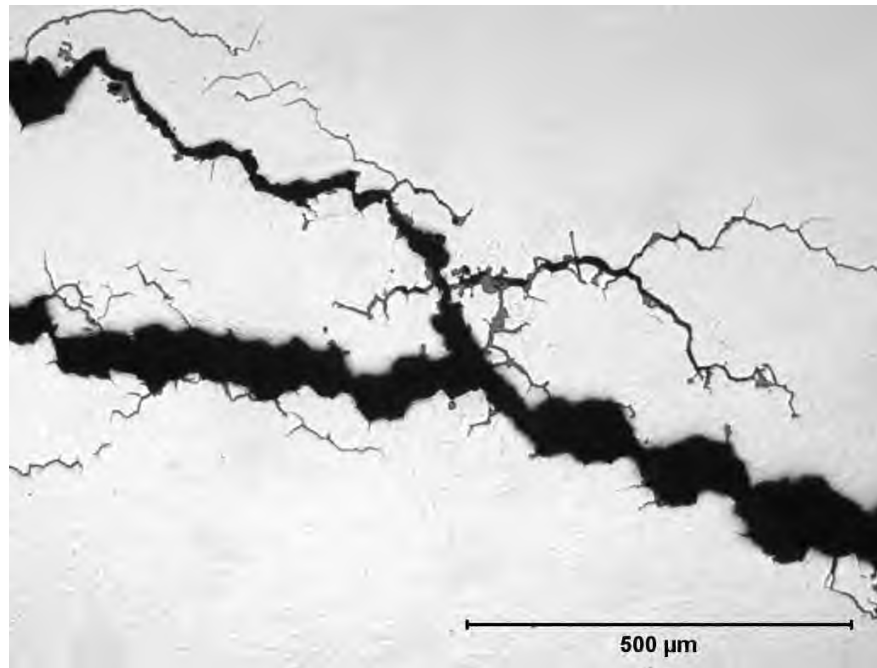


Fig. 433. Photomicrograph of planar section L349146 at location shown in Fig. 432.

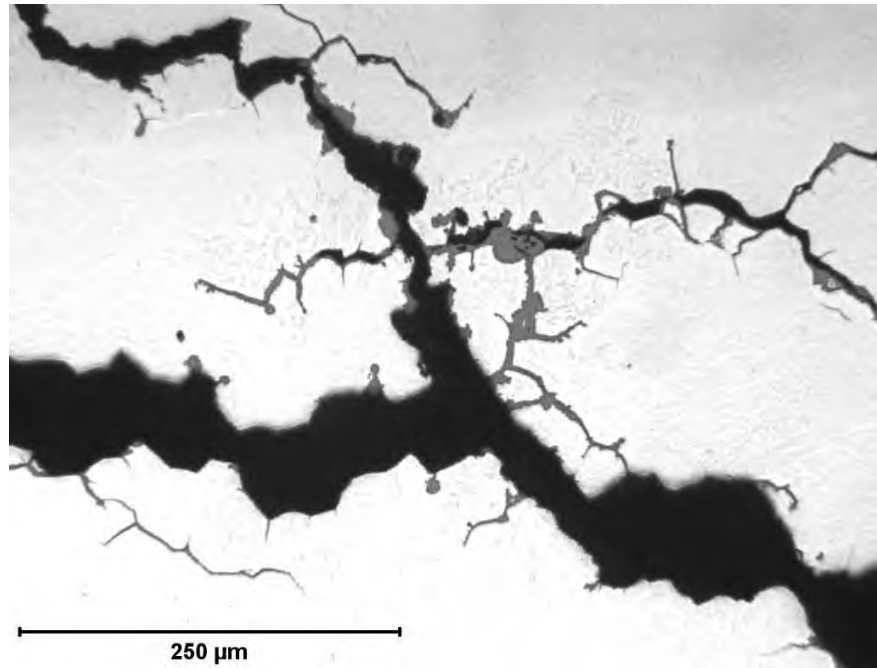


Fig. 434. Photomicrograph of planar section L349146 at location shown in Fig. 432.

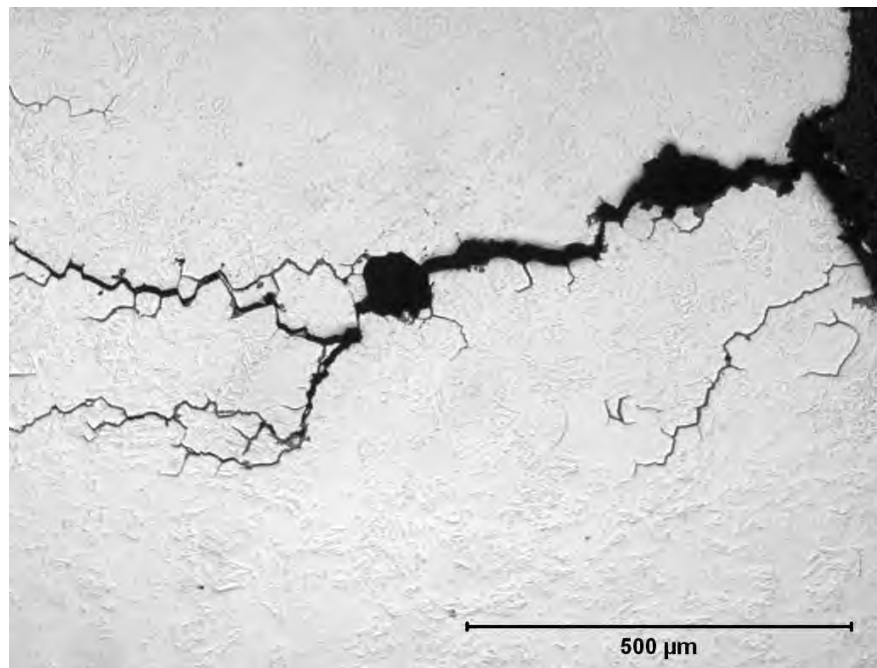


Fig. 435. Photomicrograph of transverse section L349147 at location shown in Fig. 432.

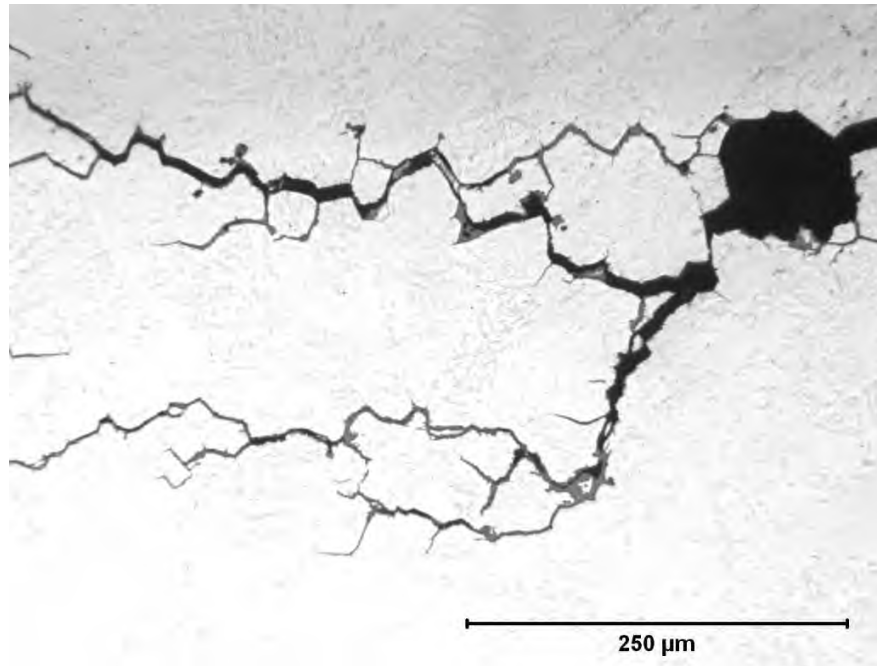


Fig. 436. Photomicrograph of transverse section L349147 at location shown in Fig. 432.

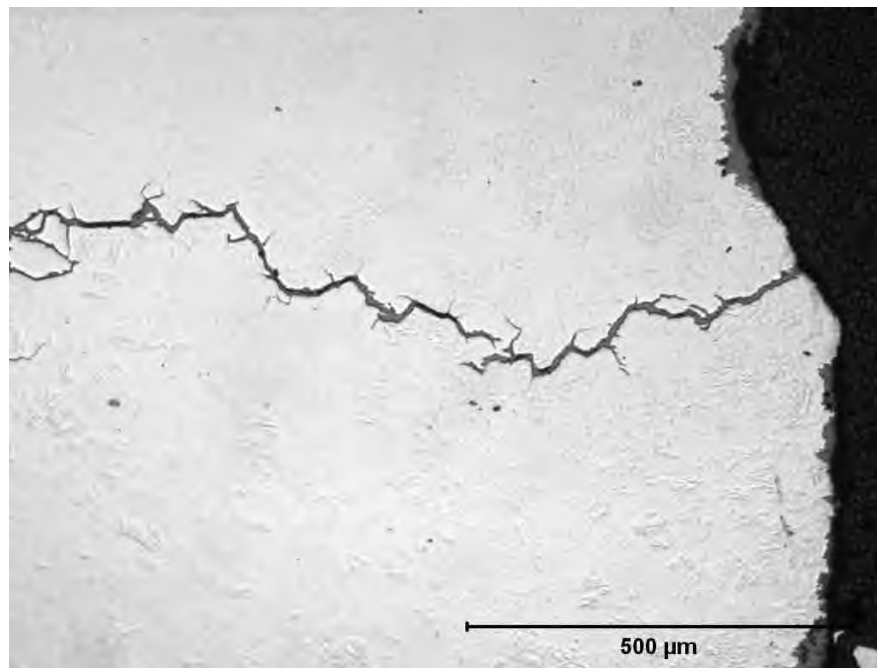


Fig. 437. Photomicrograph of transverse section L349148 at location shown in Fig. 432.

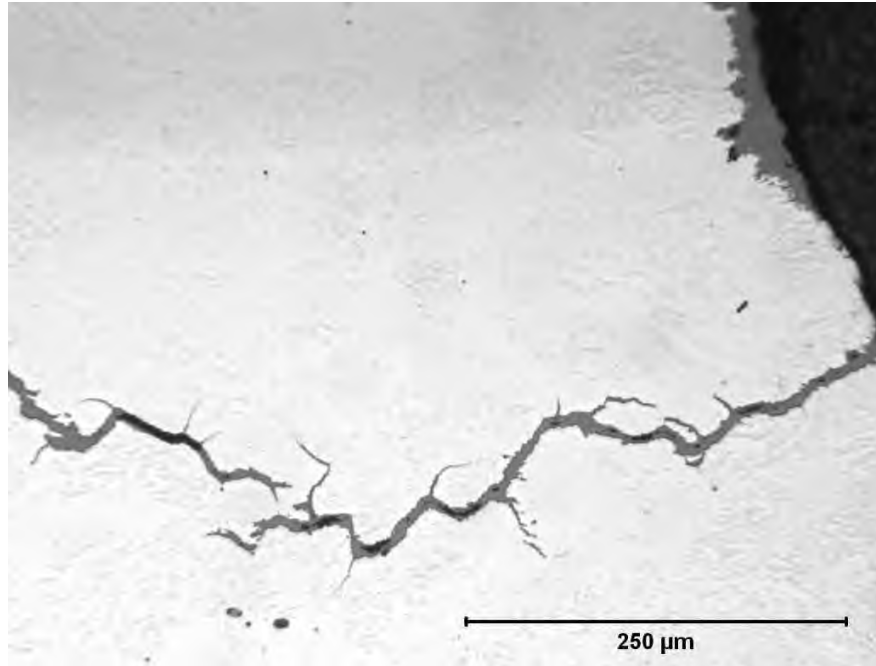


Fig. 438. Photomicrograph of transverse section L349148 at location shown in Fig. 432.

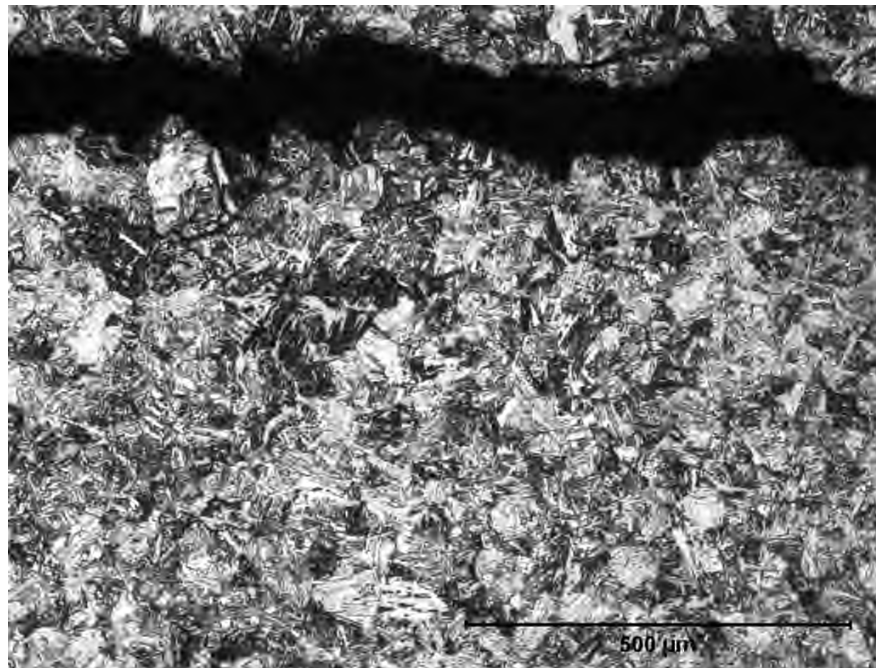


Fig. 439. Photomicrograph of planar section L349146 at location shown in Fig. 432.

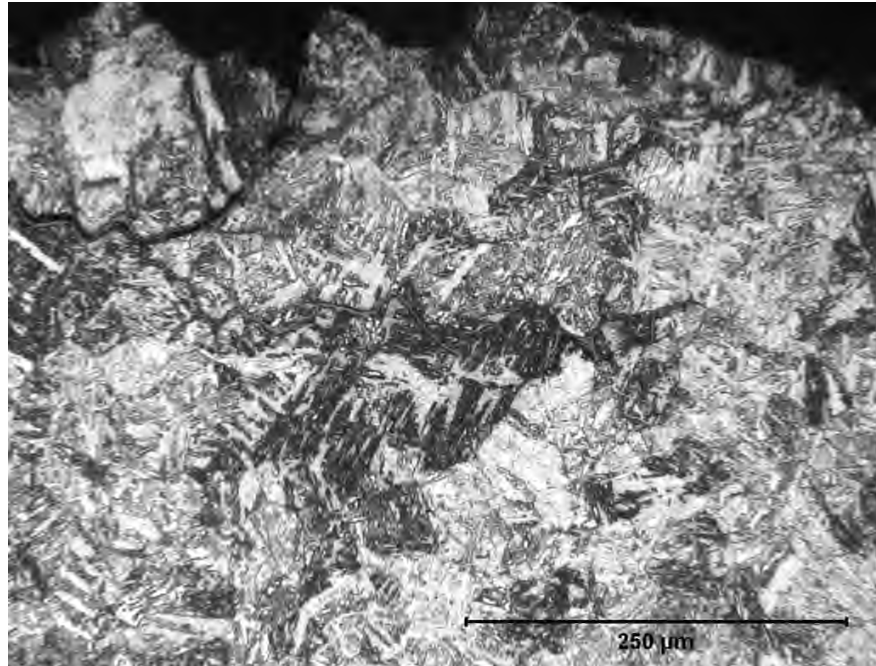


Fig. 440. Photomicrograph of planar section L349146 at location shown in Fig. 432.

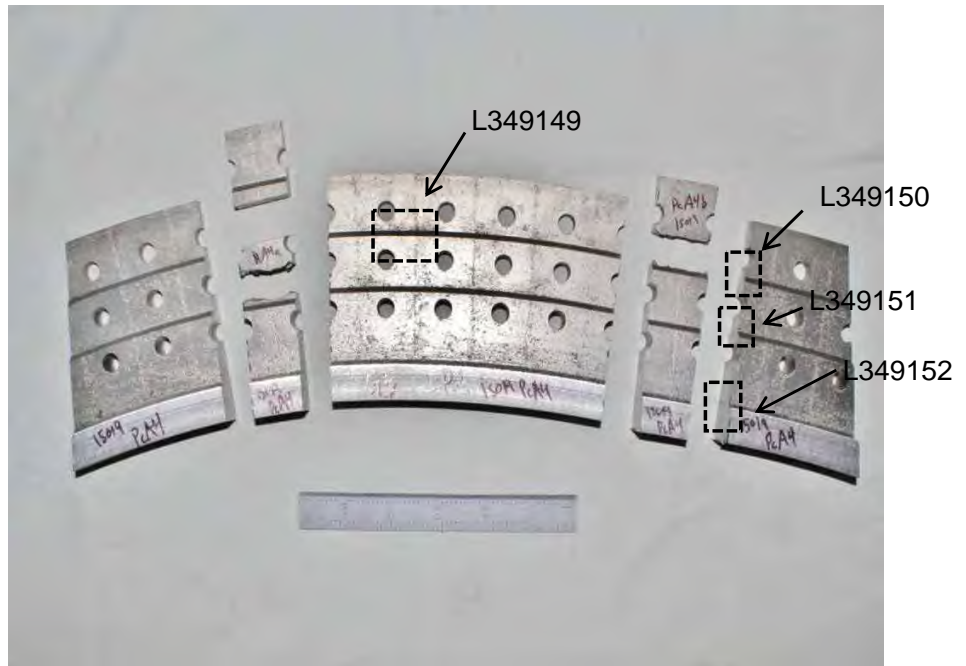


Fig. 441. Generator end finger pinned blade attachment, Pc A4, from LP turbine "A" showing location of coupons removed for metallography (arrows).

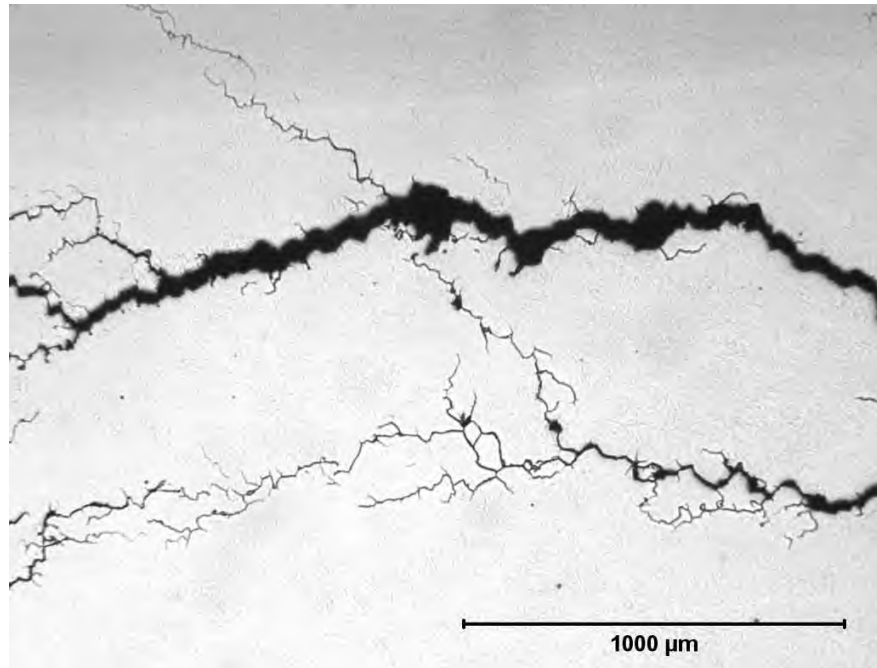


Fig. 442. Photomicrograph of planar section L349149 at location shown in Fig. 441.

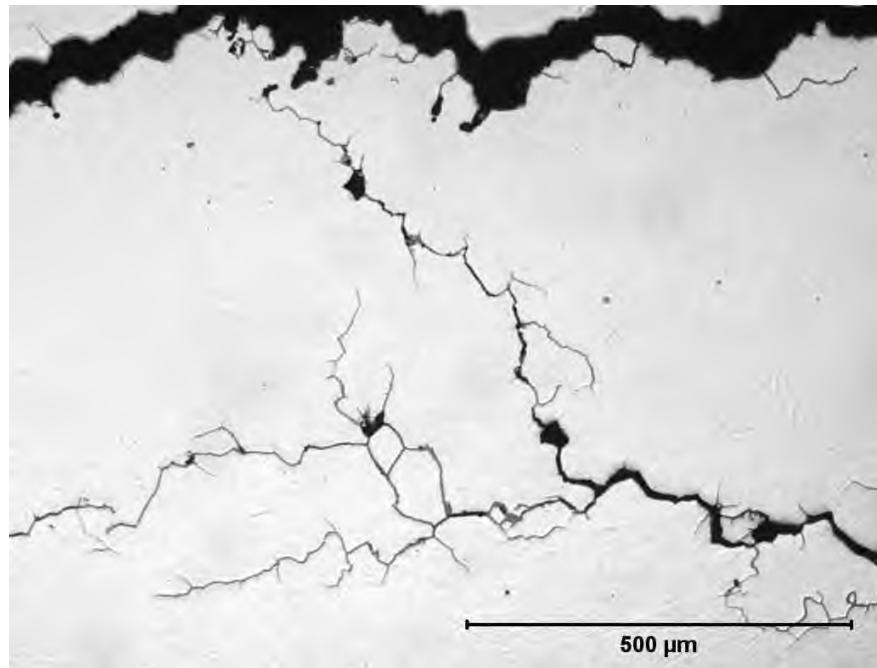


Fig. 443. Photomicrograph of planar section L349149 at location shown in Fig. 441.

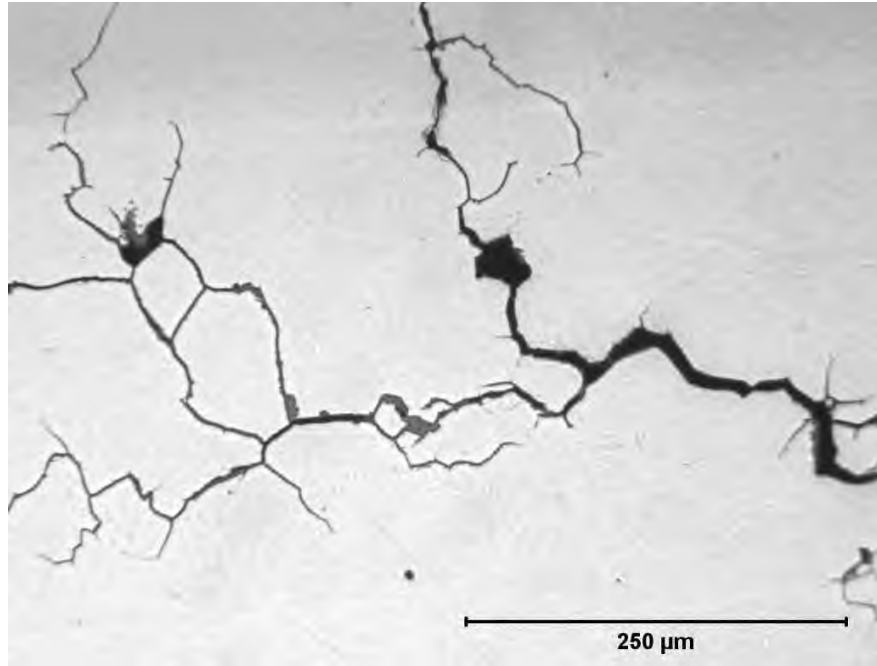


Fig. 444. Photomicrograph of planar section L349149 at location shown in Fig. 441.

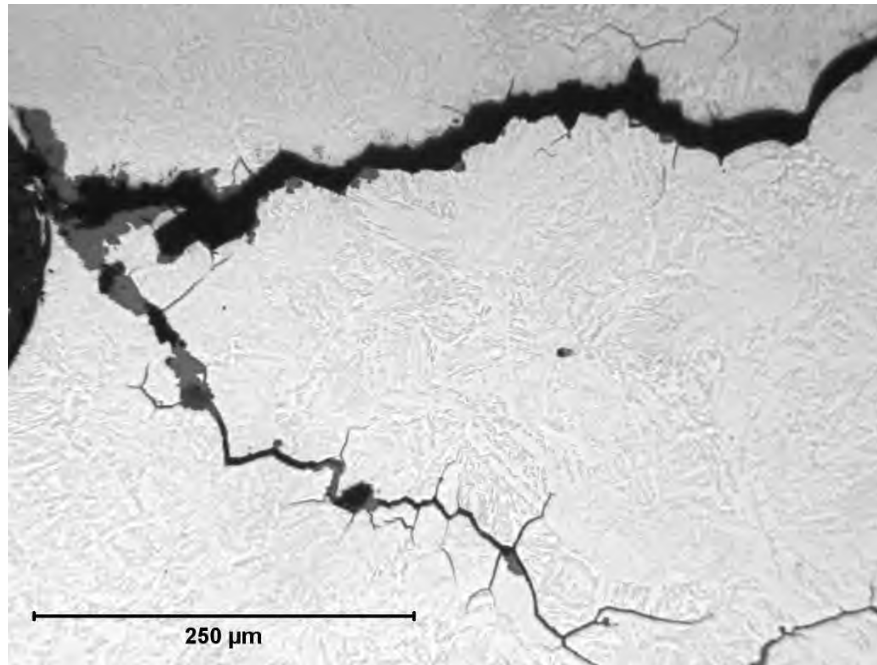


Fig. 445. Photomicrograph of transverse section L349150 at location shown in Fig. 441.

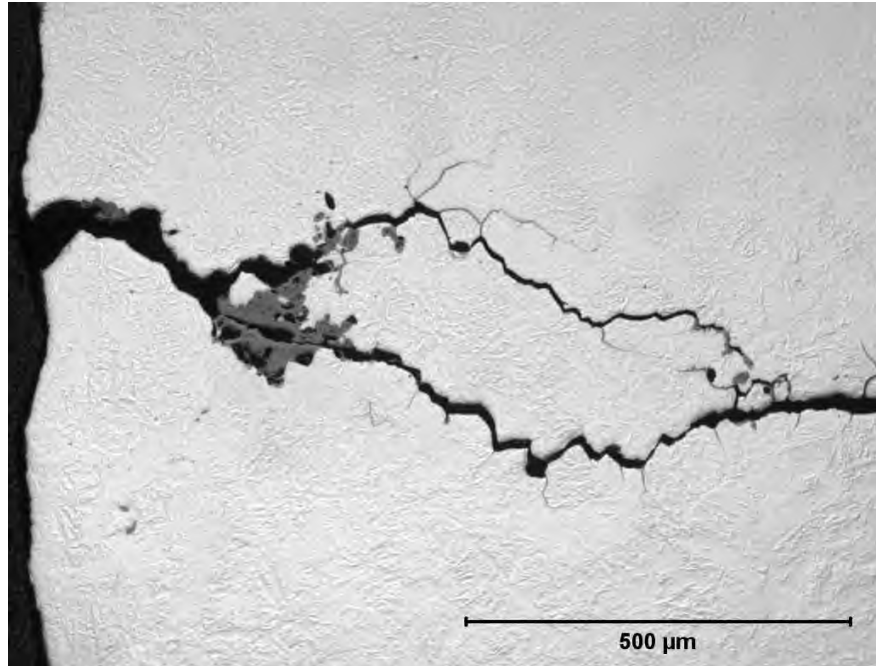


Fig. 446. Photomicrograph of transverse section L349150 at location shown in Fig. 441.

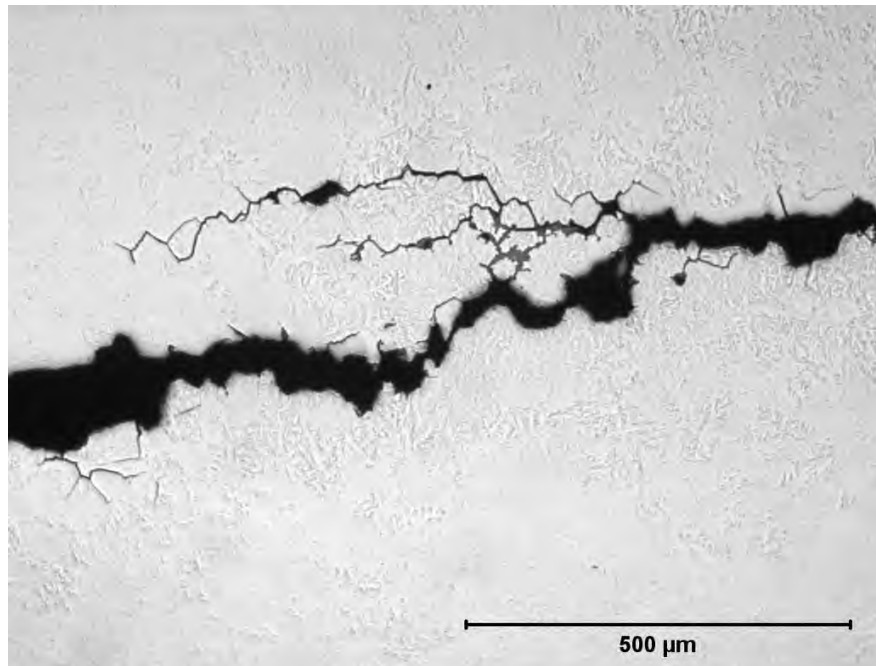


Fig. 447. Photomicrograph of transverse section L349151 at location shown in Fig. 441.

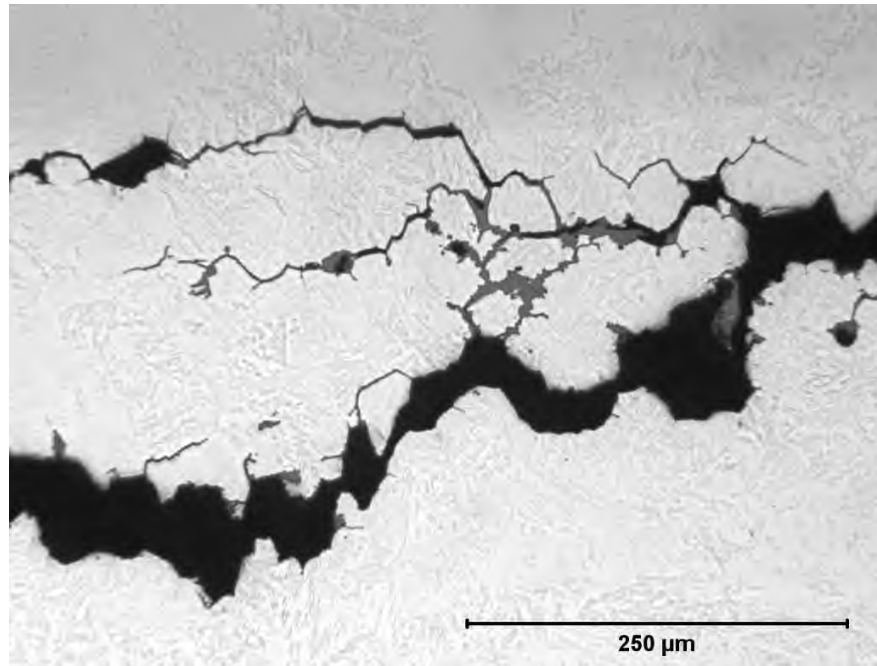


Fig. 448. Photomicrograph of transverse section L349151 at location shown in Fig. 441.

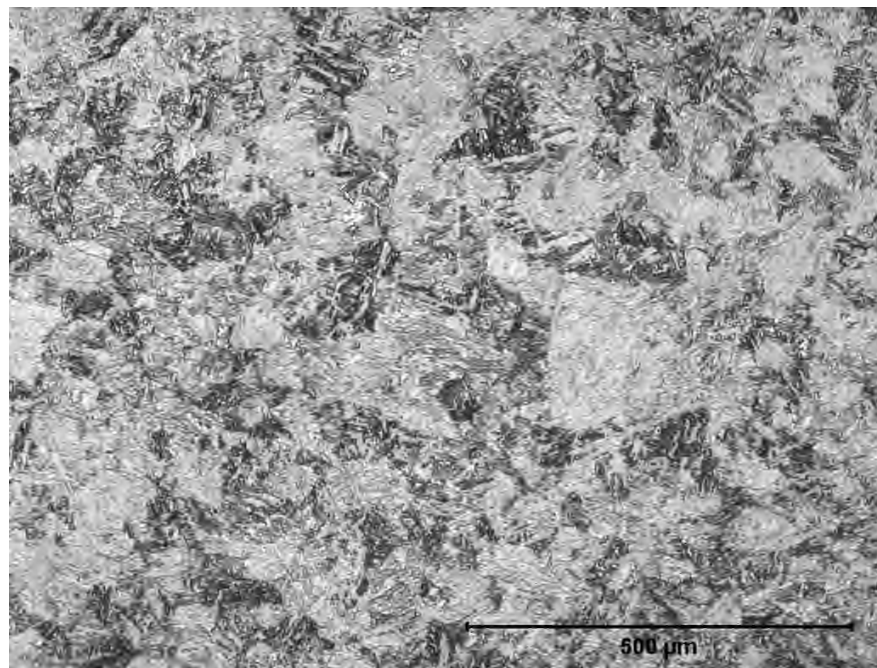


Fig. 449. Photomicrograph of transverse section L349152 at location shown in Fig. 441.

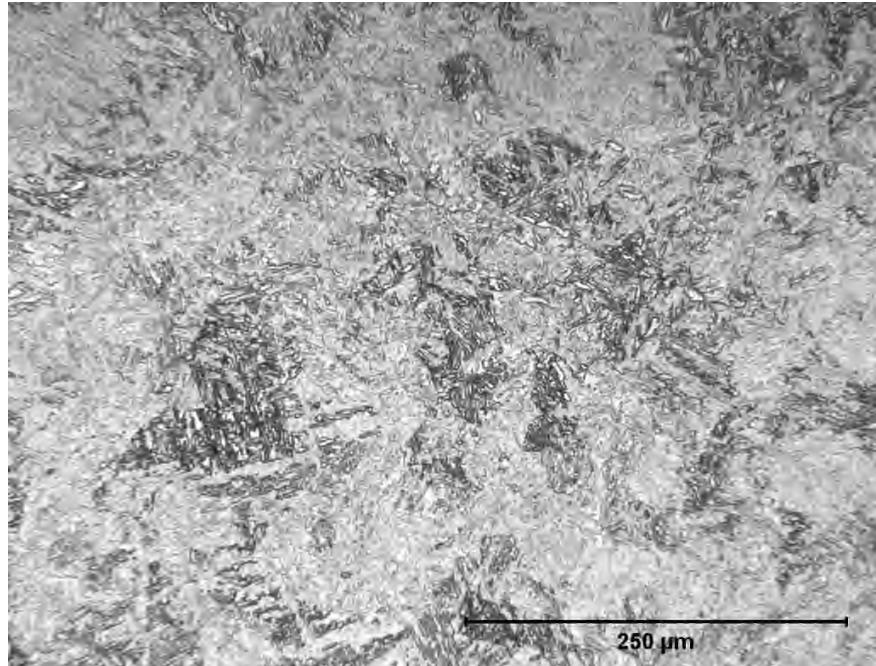


Fig. 450. Photomicrograph of transverse section L349152 at location shown in Fig. 441.

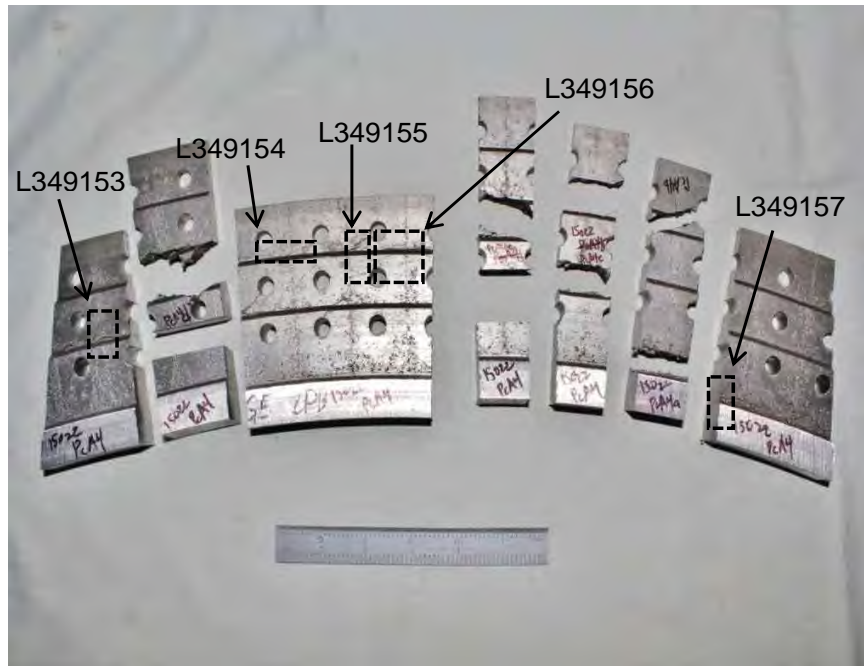


Fig. 451. Generator end finger pinned blade attachment, Pc A4, from LP turbine "B" showing sectioning of cracks (arrows) for further examination.

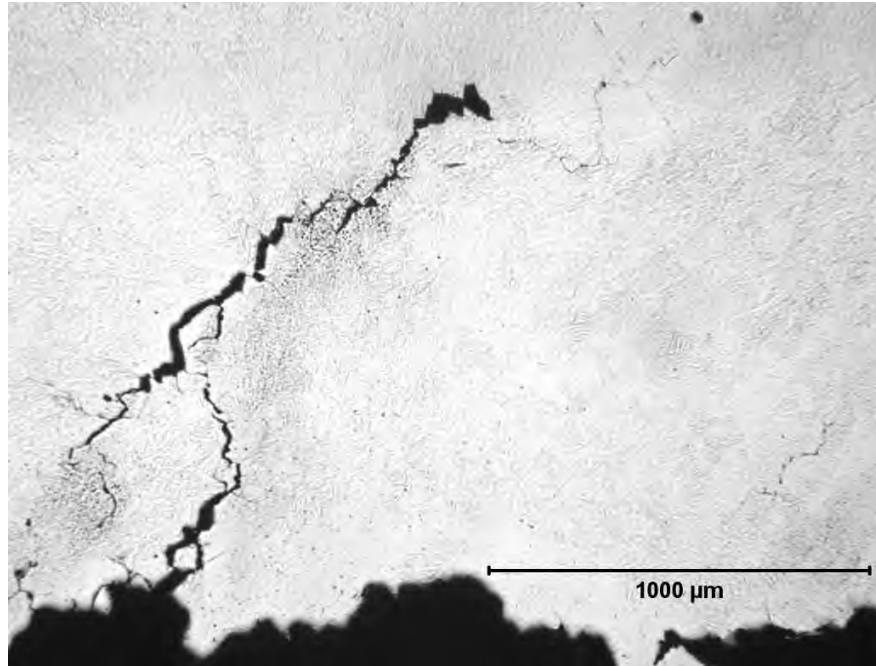


Fig. 452. Photomicrograph of transverse section L349153 at location shown in Fig. 451.

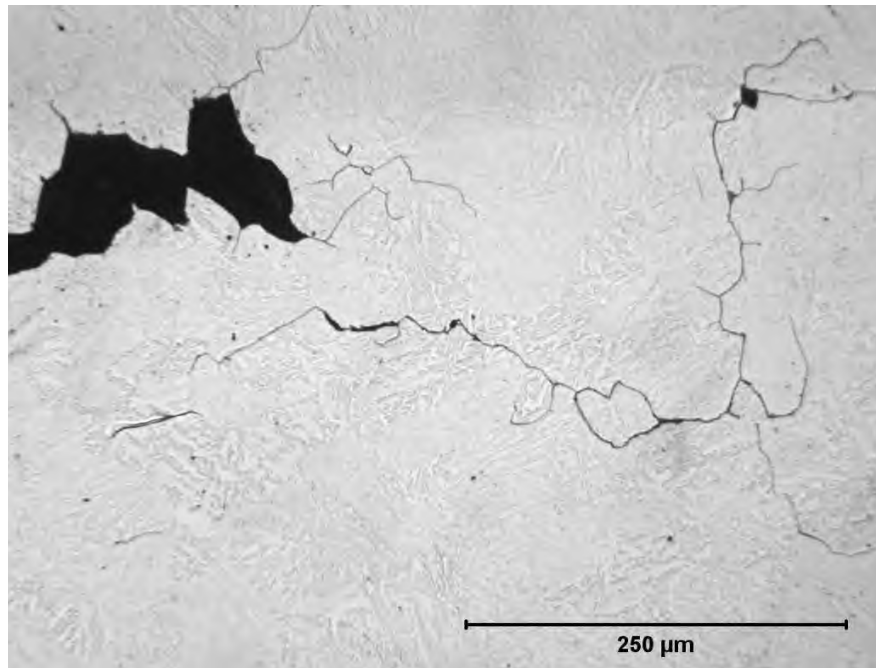


Fig. 453. Photomicrograph of transverse section L349153 at location shown in Fig. 451.

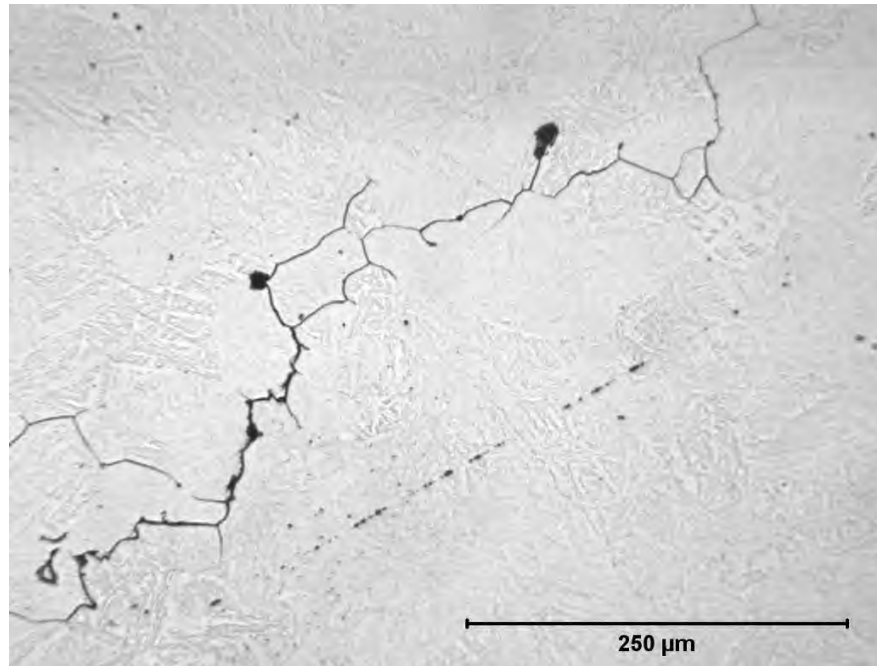


Fig. 454. Photomicrograph of transverse section L349153 at location shown in Fig. 451.

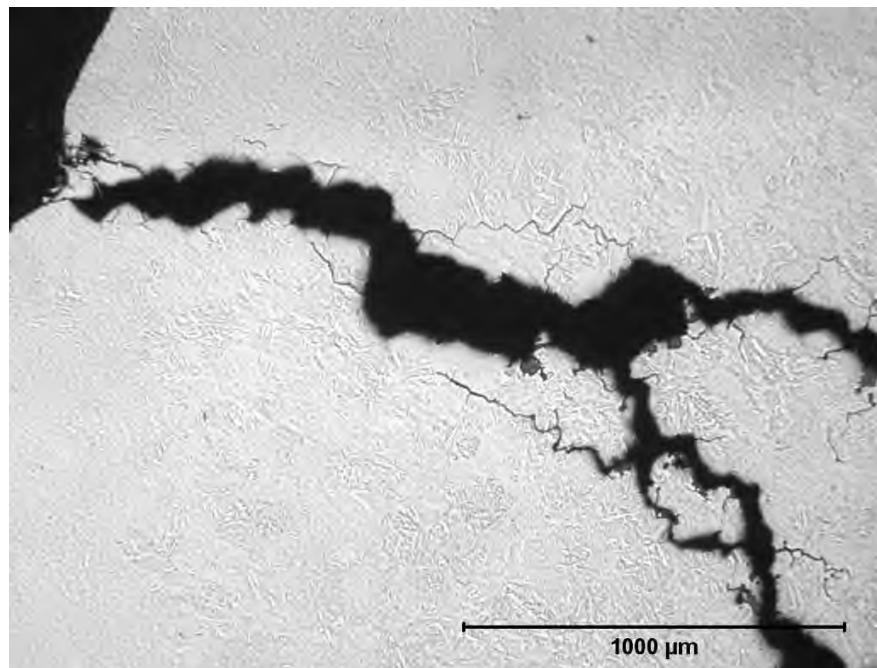


Fig. 455. Photomicrograph of planar section L349154 at location shown in Fig. 451.

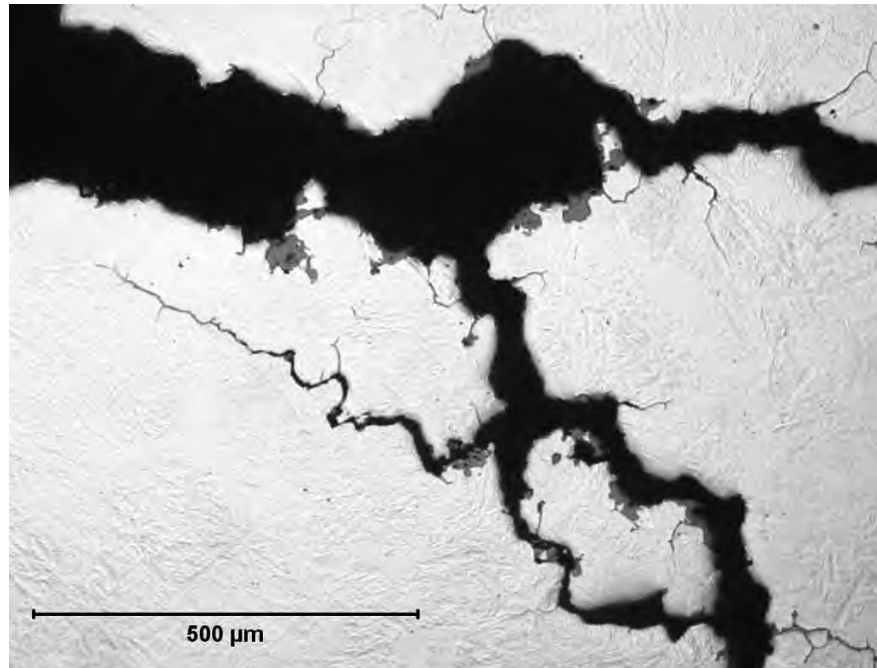


Fig. 456. Photomicrograph of planar section L349154 at location shown in Fig. 451.

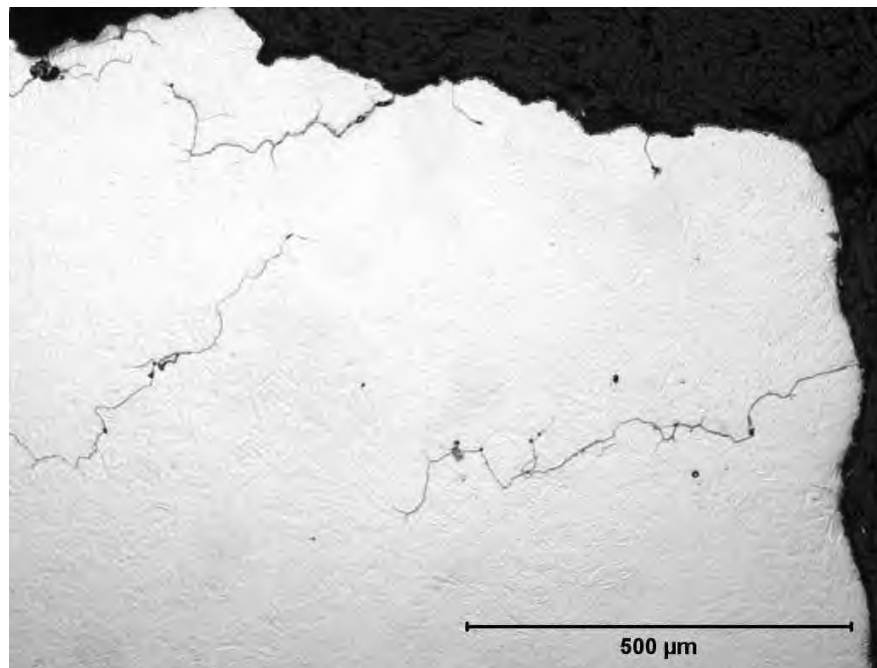


Fig. 457. Photomicrograph of transverse section L349155 at location shown in Fig. 451.

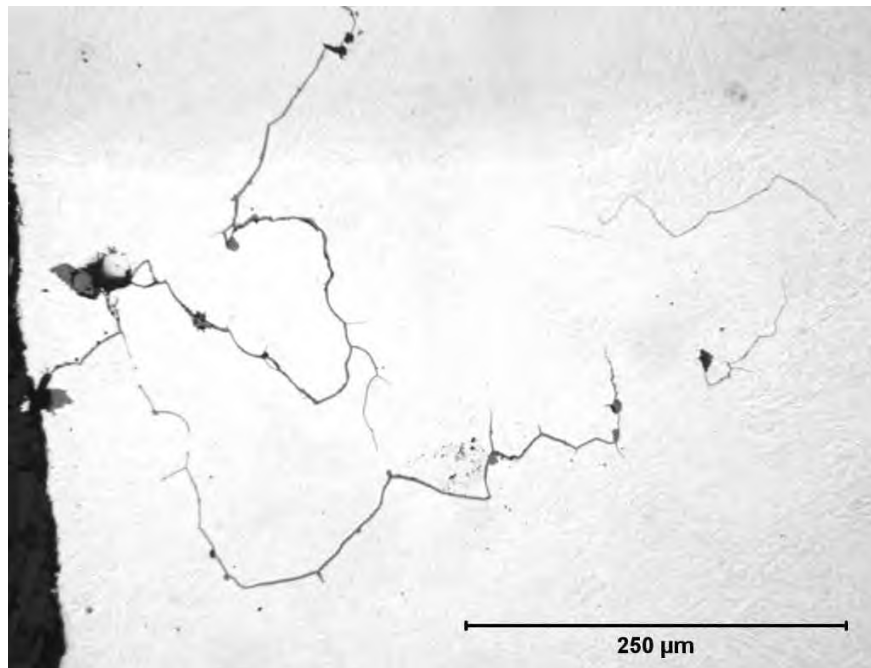


Fig. 458. Photomicrograph of transverse section L349155 at location shown in Fig. 451.

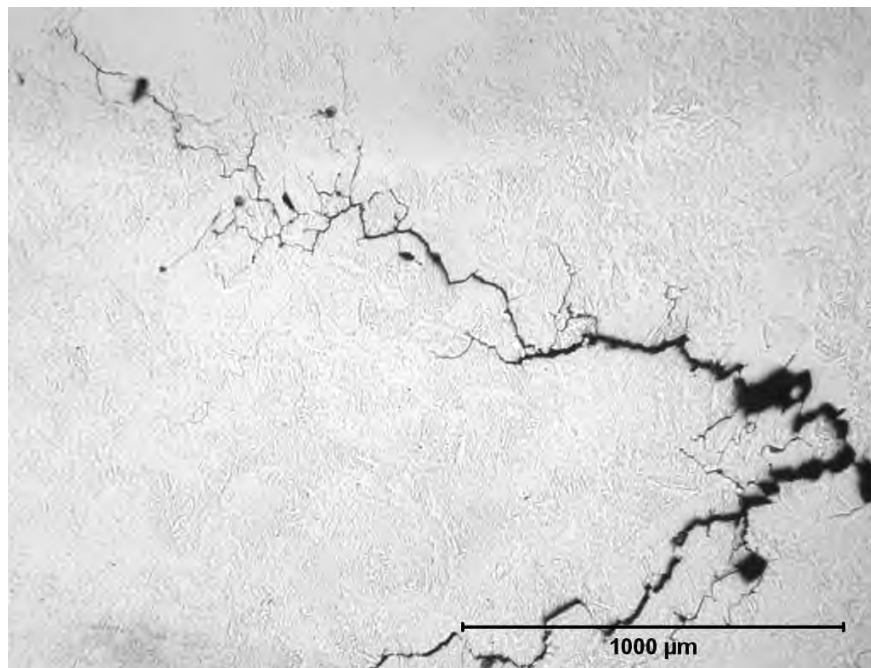


Fig. 459. Photomicrograph of planar section L349156 at location shown in Fig. 451.

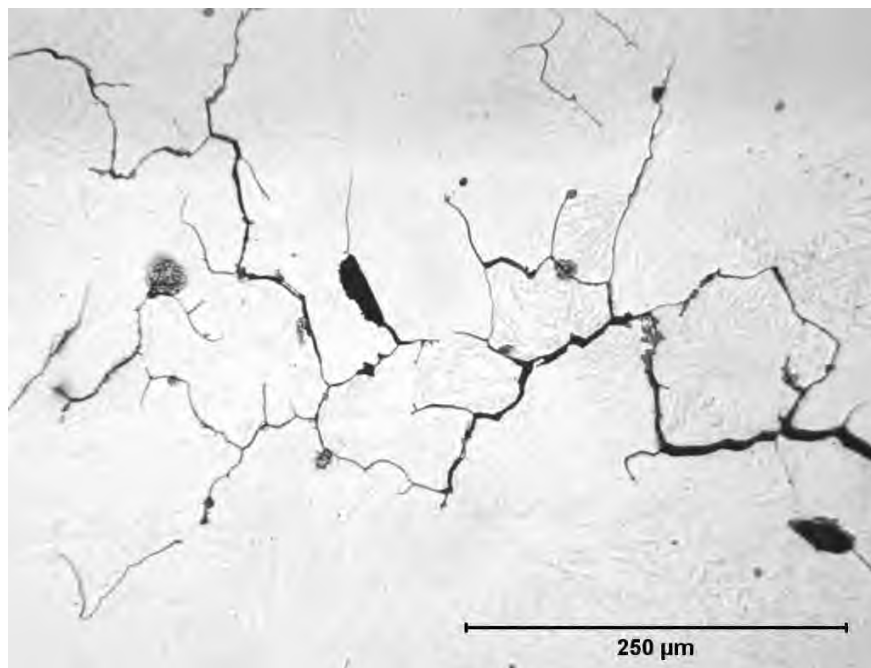


Fig. 460. Photomicrograph of planar section L349156 at location shown in Fig. 451.

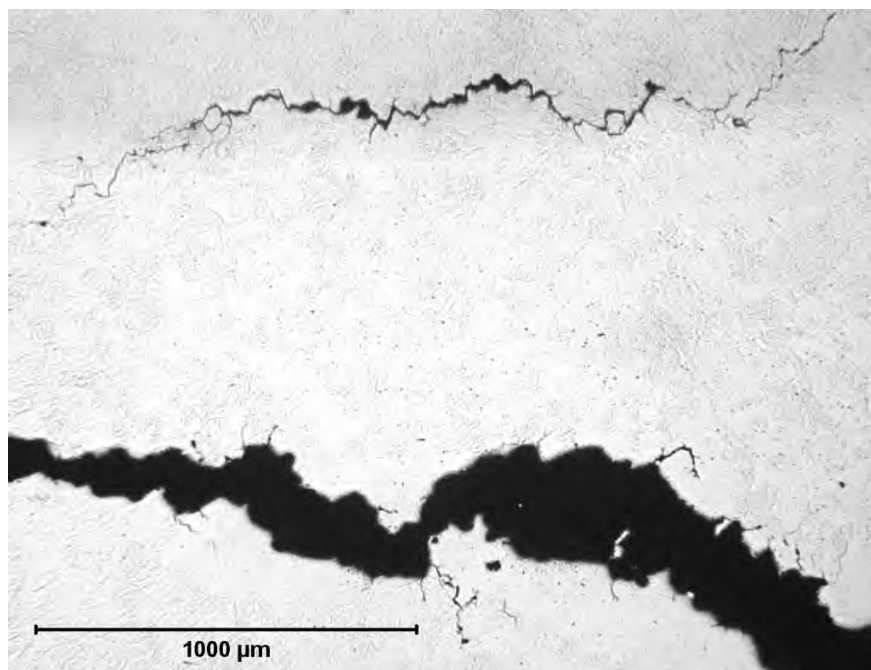


Fig. 461. Photomicrograph of transverse section L349157 at location shown in Fig. 451.

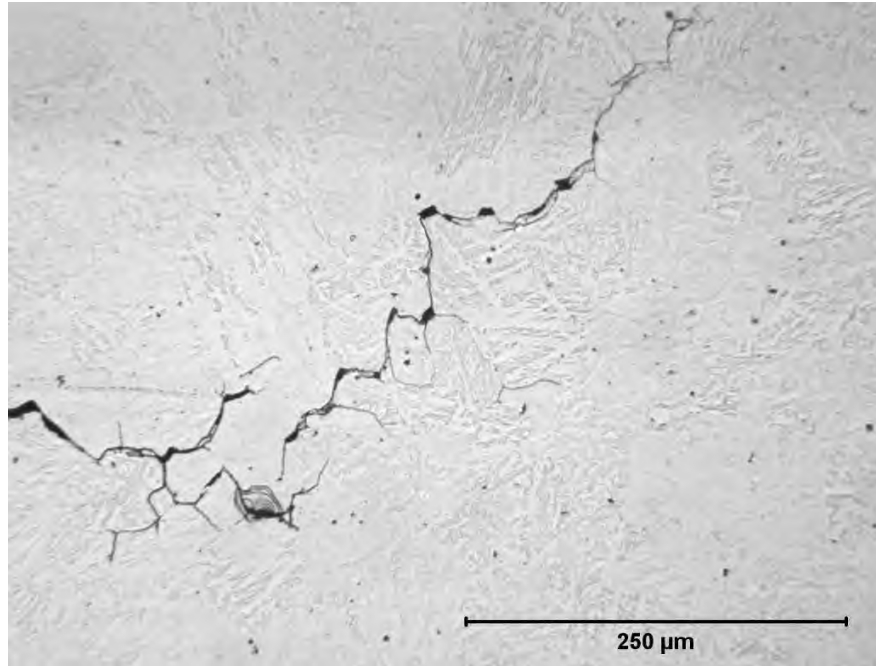


Fig. 462. Photomicrograph of transverse section L349157 at location shown in Fig. 451.

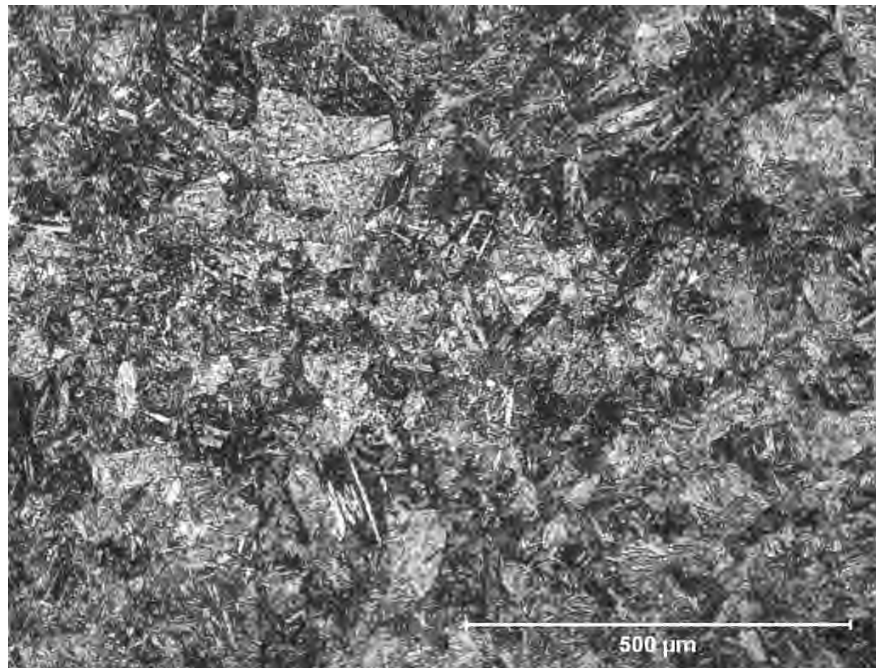


Fig. 463. Photomicrograph of transverse section L349157 at location shown in Fig. 451.

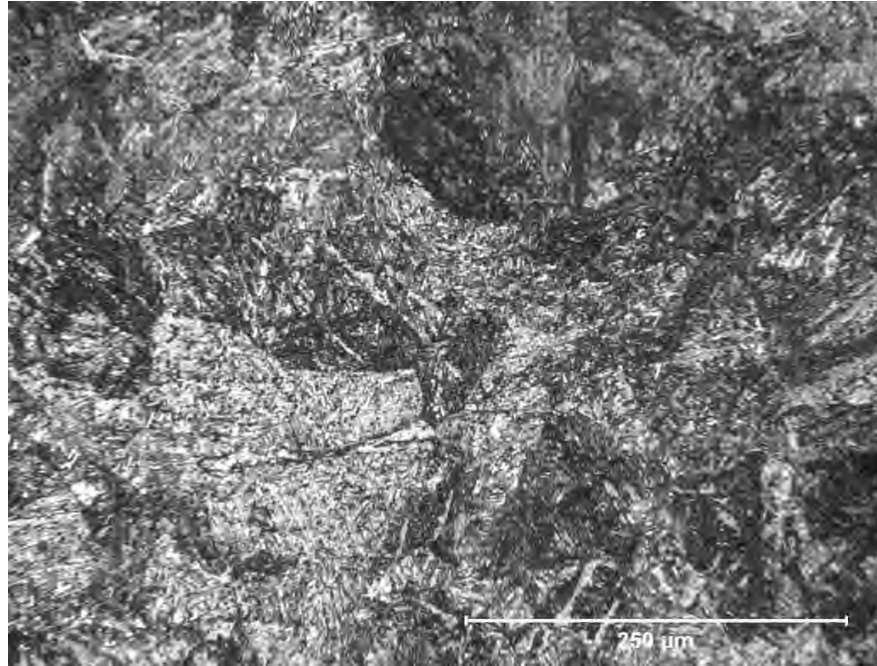


Fig. 464. Photomicrograph of transverse section L349157 at location shown in Fig. 451.

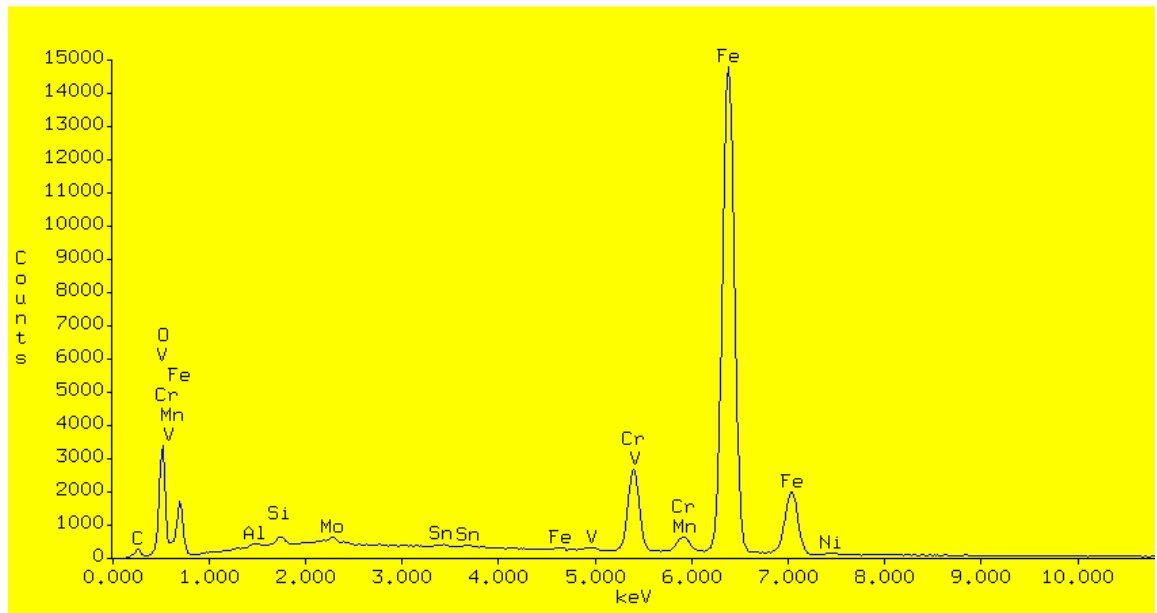


Fig. 465. Energy Dispersive Spectrograph of deposit sample L349136, location A.

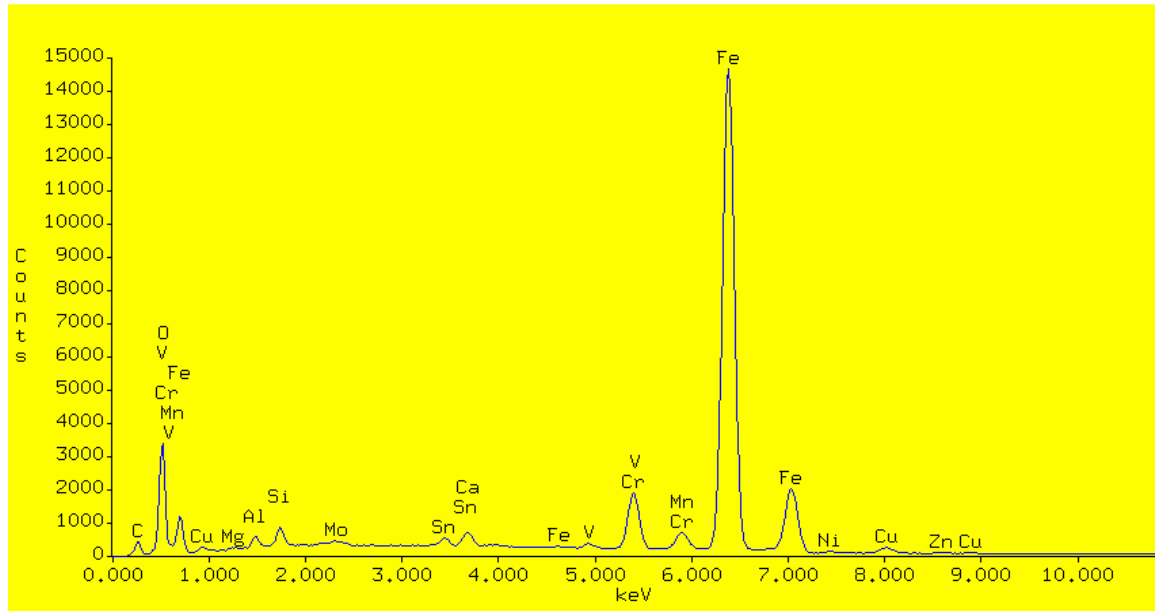


Fig. 466. Energy Dispersive Spectrograph of deposit sample L349136, location B.

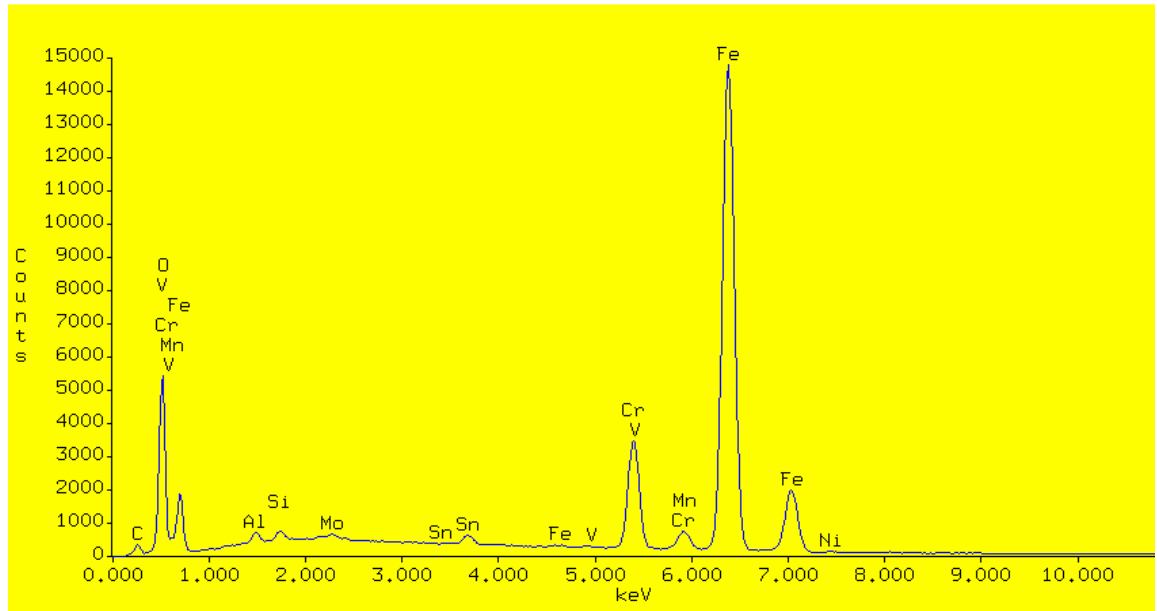


Fig. 467. Energy Dispersive Spectrograph of deposit sample L349137.

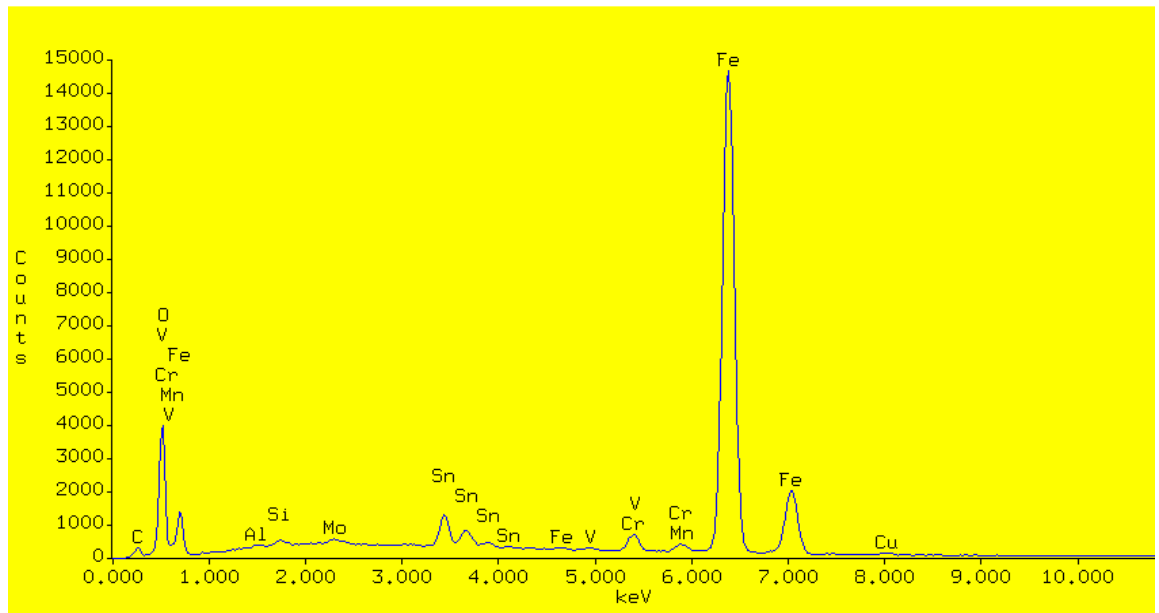


Fig. 468. Energy Dispersive Spectrograph of deposit sample L349138.

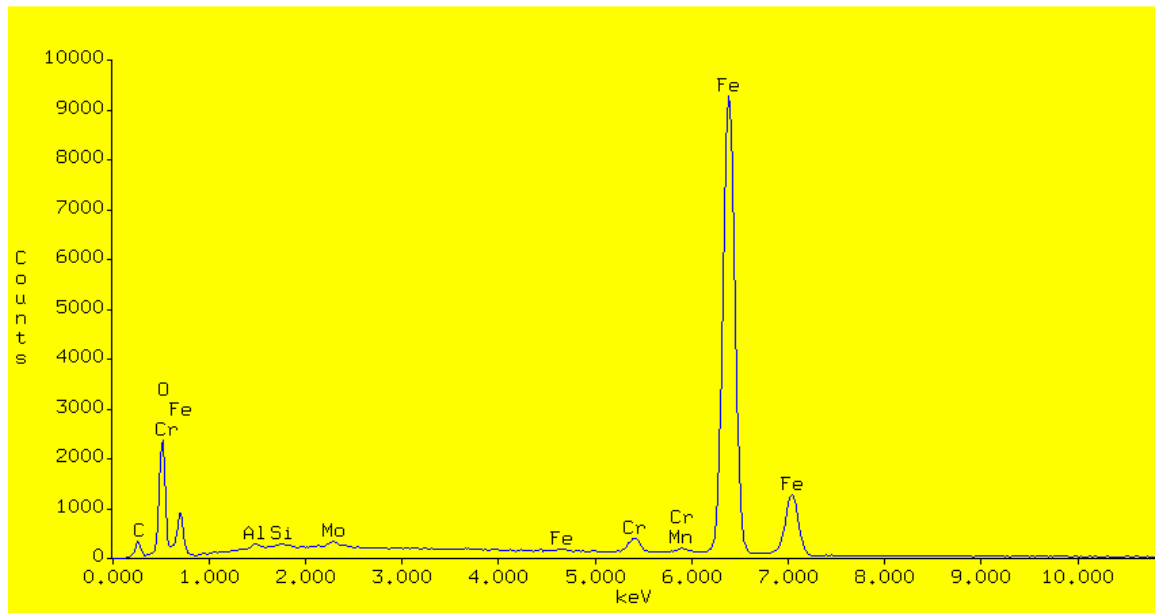


Fig. 469. Energy Dispersive Spectrograph of deposit sample L349141.

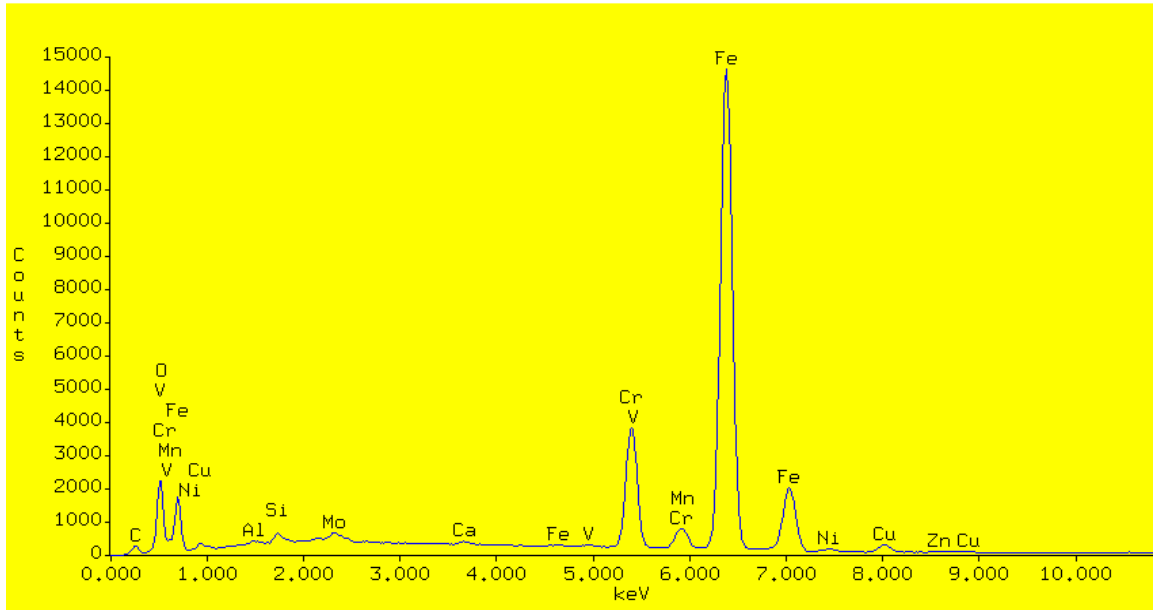


Fig. 470. Energy Dispersive Spectrograph of deposit sample L349143

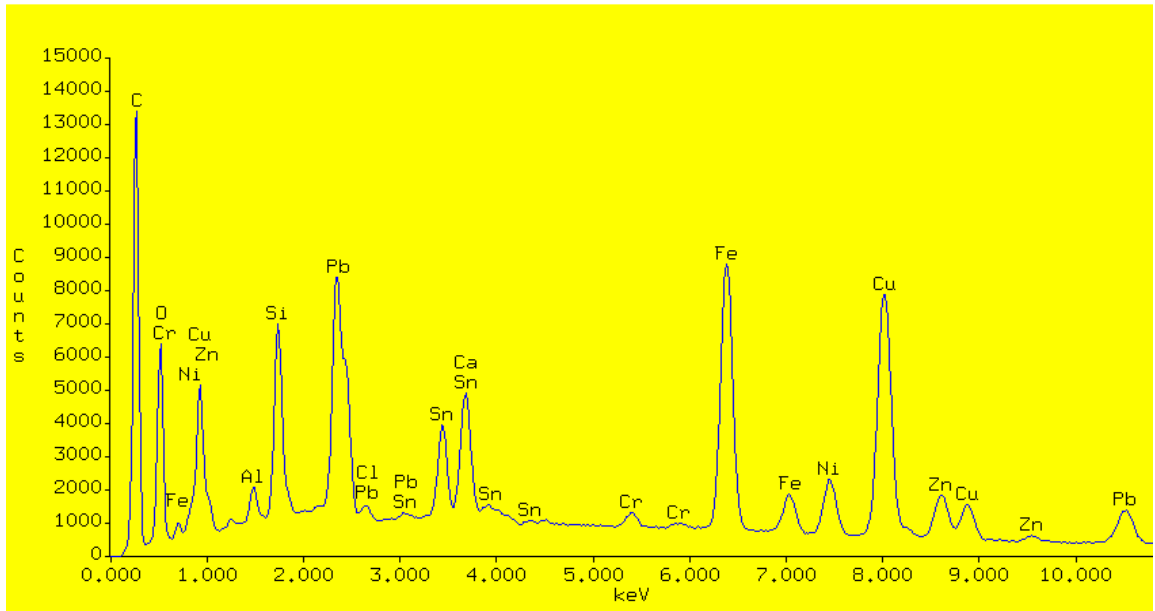


Fig. 471. Energy Dispersive Spectrograph of deposit sample SID 14837.

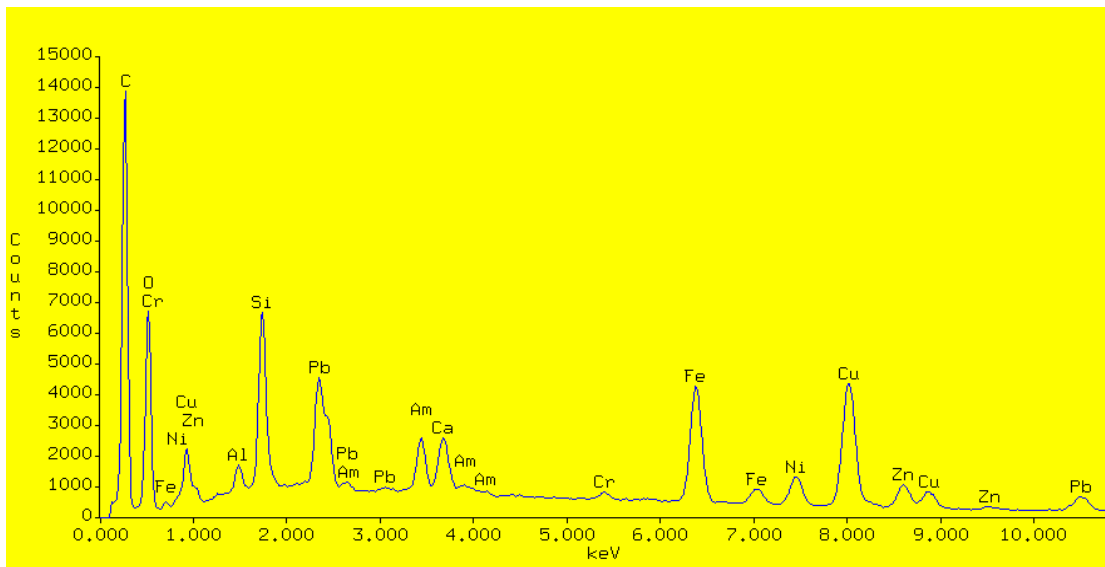


Fig. 472. Energy Dispersive Spectrograph of deposit sample SID 14839.

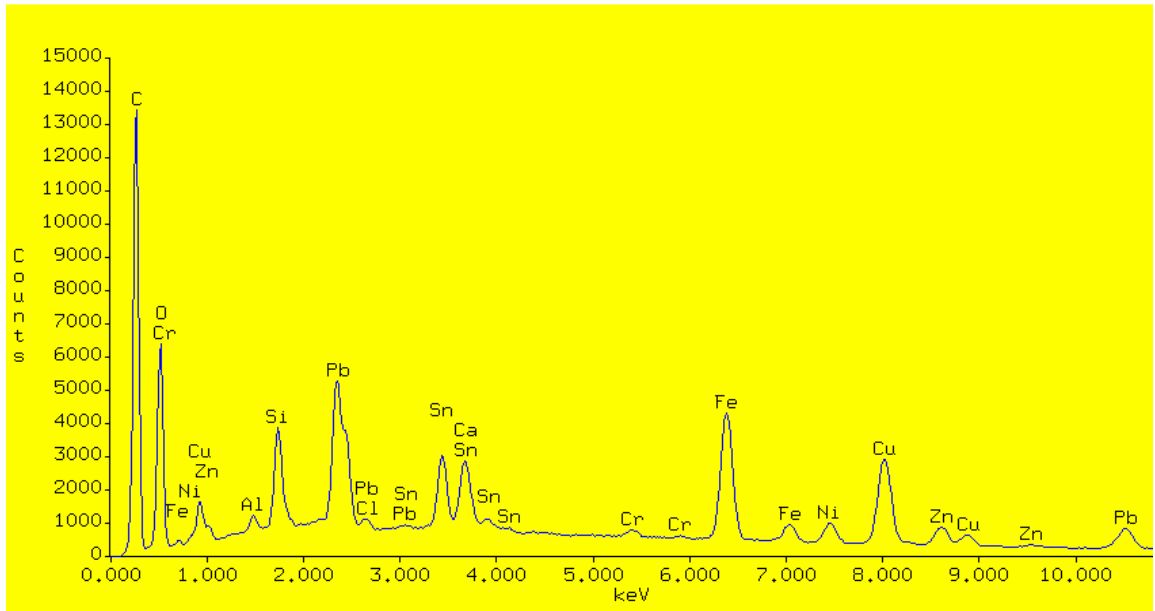


Fig. 473. Energy Dispersive Spectrograph of deposit sample SID 15034.

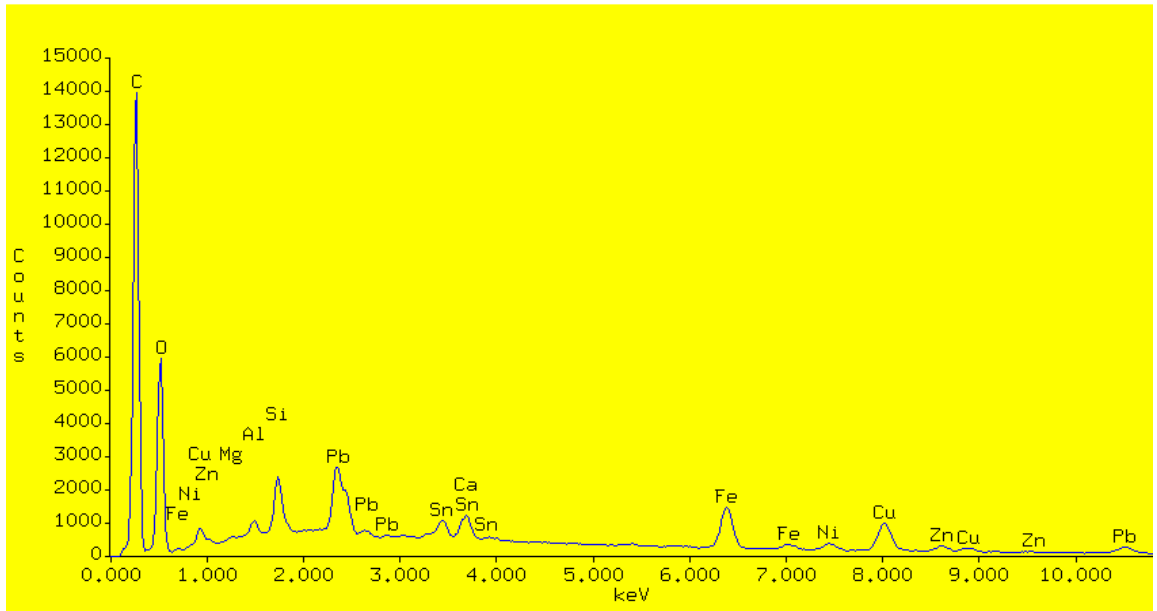


Fig. 474. Energy Dispersive Spectrograph of deposit sample SID 14937.

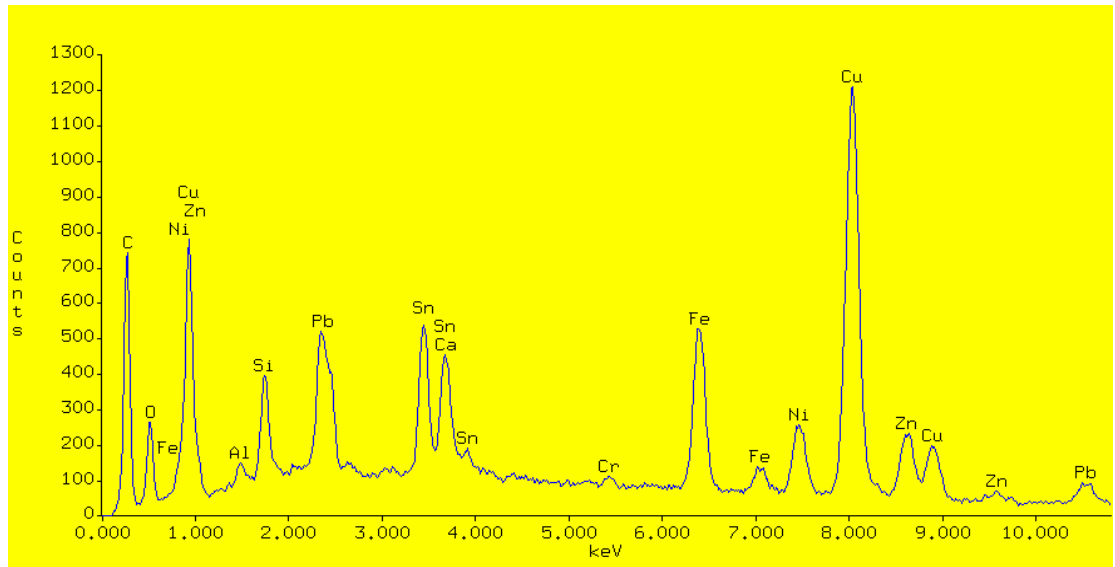


Fig. 475 Energy Dispersive Spectrograph of deposit sample SID 14938.

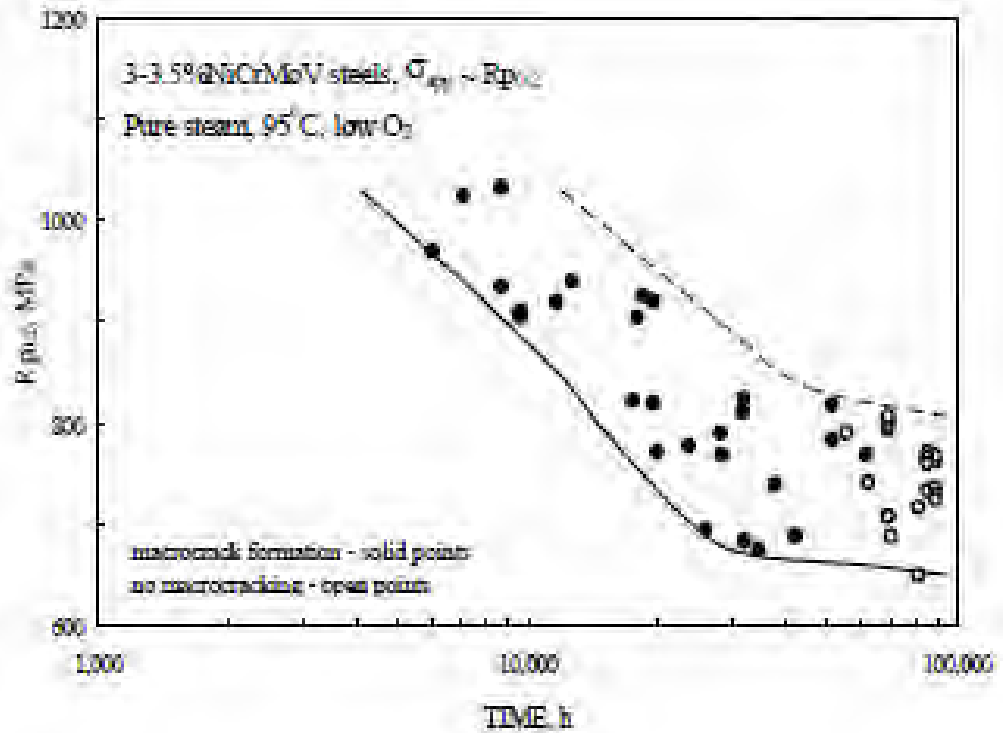


Fig. 476. The effect of strength on the stress corrosion crack initiation properties for 3-3.5%NiCrMoV steels in pure low oxygen condensing steam at 95°C (Ref 5).

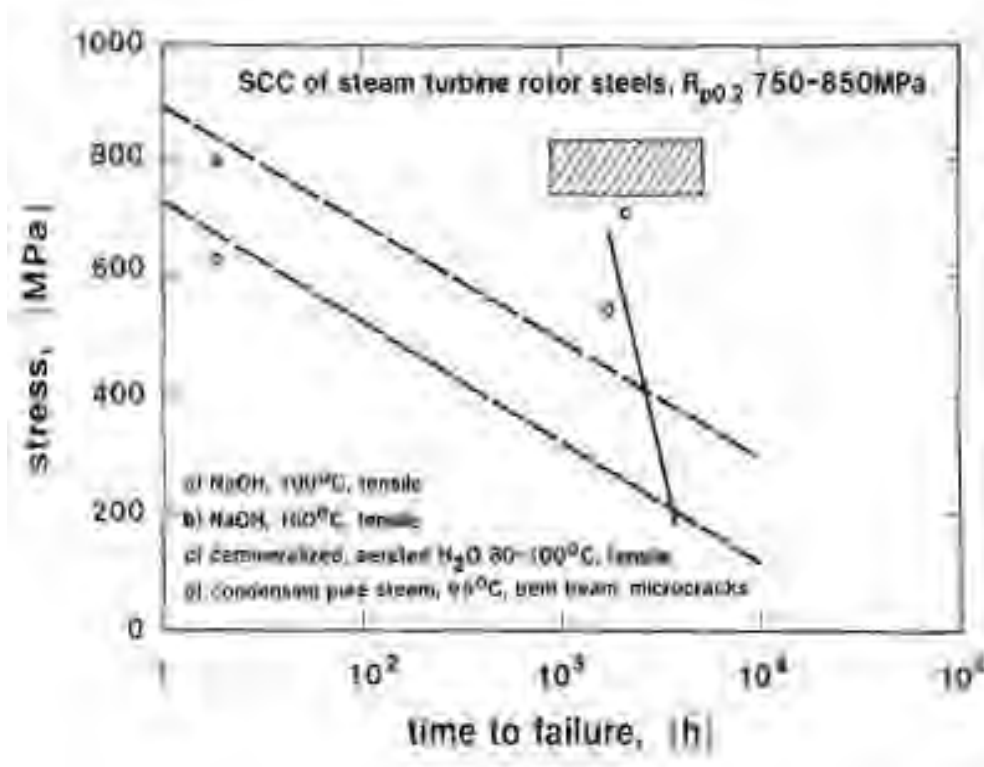


Fig. 477. Effect of stress and environment on time for stress corrosion crack initiation (Ref 6).

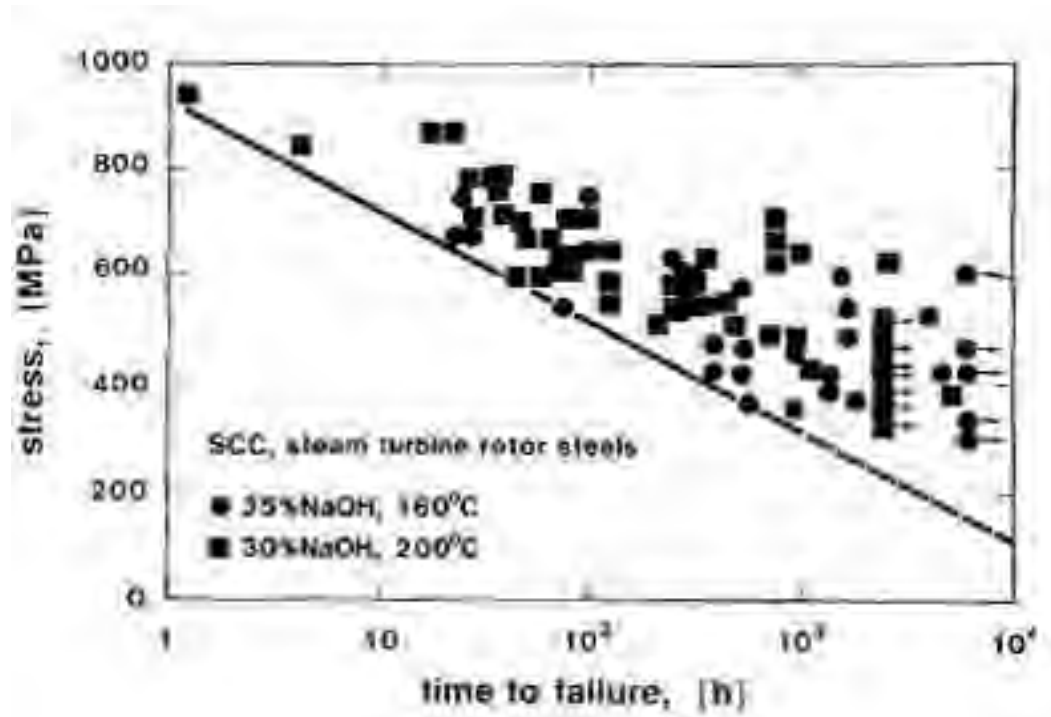


Fig. 478.. Stress corrosion cracking of steam turbine rotor steels in concentrated aqueous NaOH solutions (Ref 6).

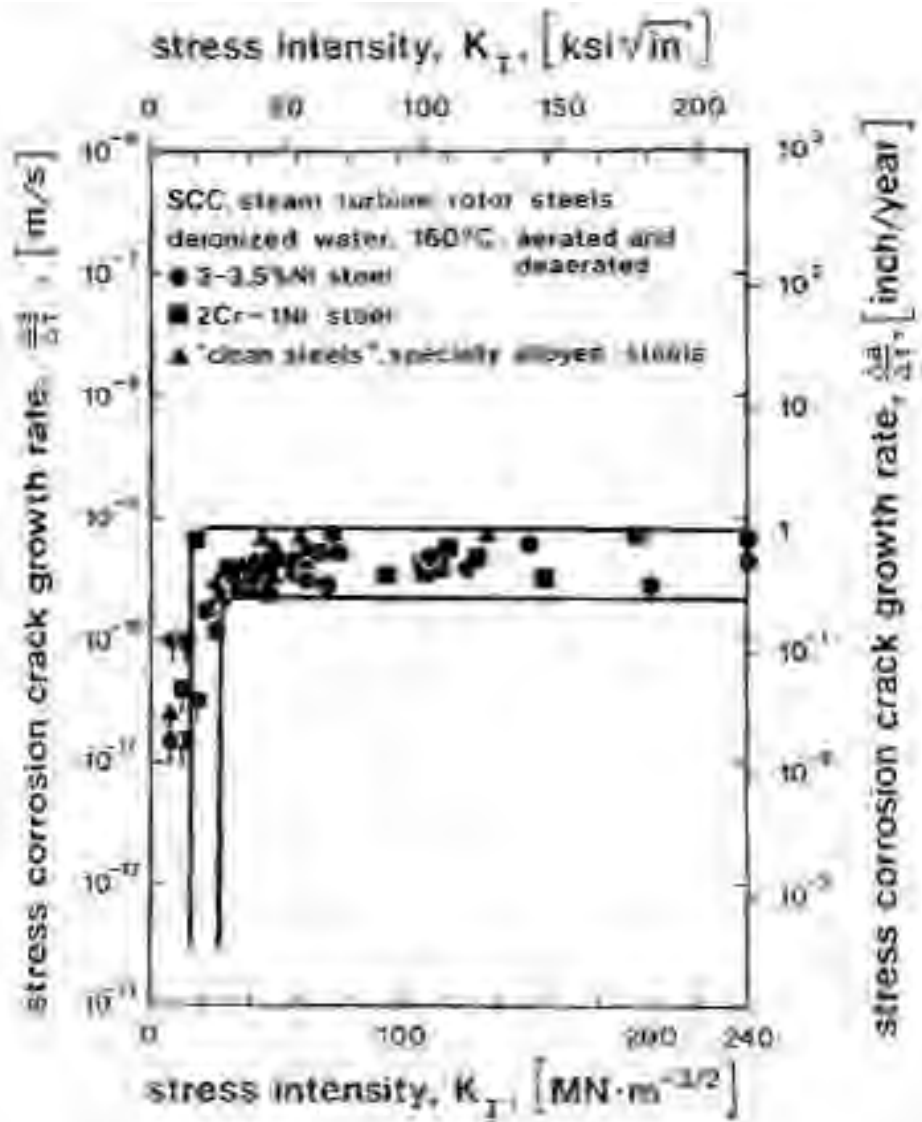


Fig. 479. Effect of stress intensity on the growth rate of stress corrosion cracks in various steam turbine rotor steels, exposed to water at 160°C (Ref. 7).

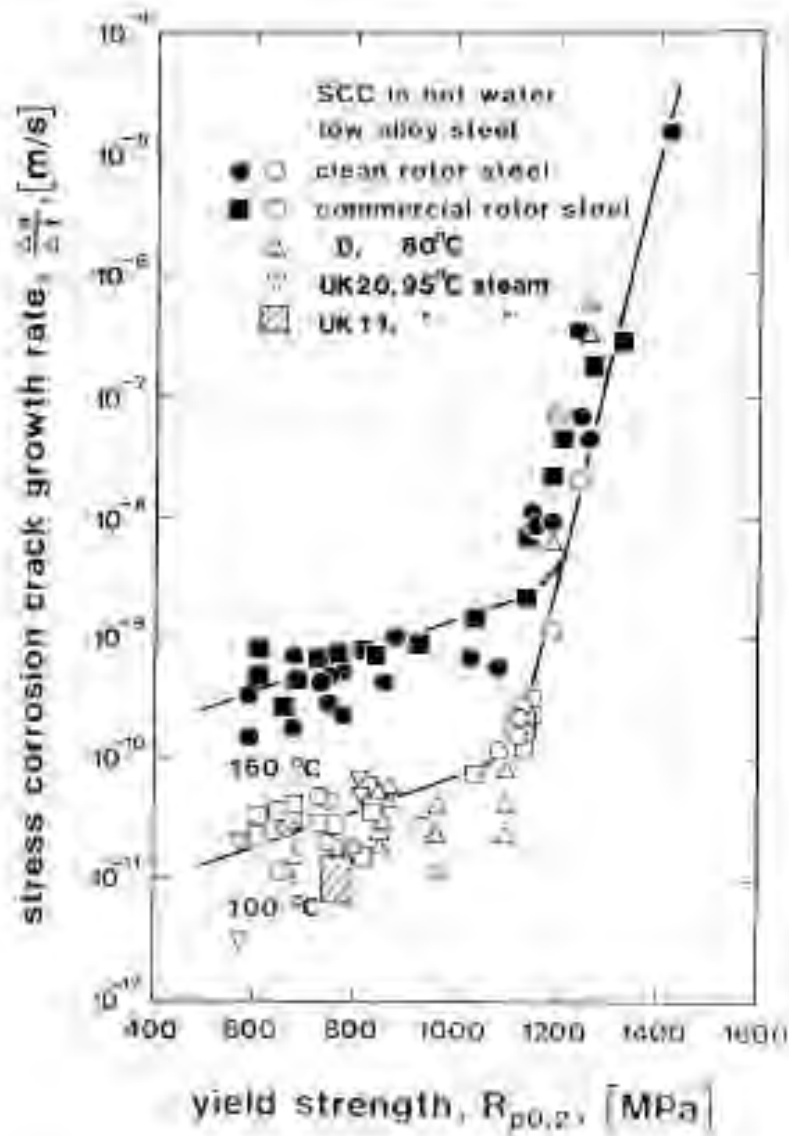


Fig. 480. The effect of yield strength on the growth rates of stress corrosion cracks in steam turbine rotor steels exposed to water (Ref. 7).

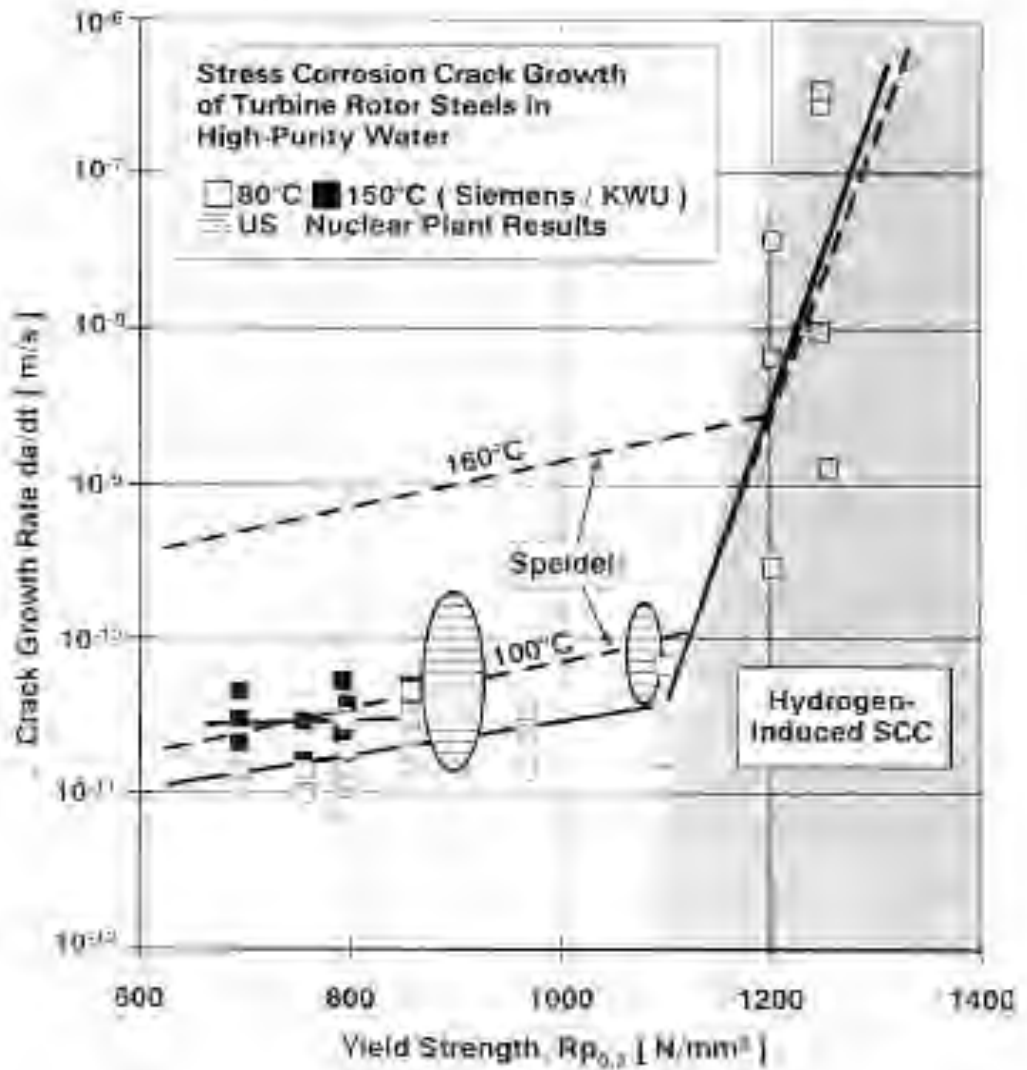


Fig 481. Yield strength dependence of stress corrosion crack growth in NiCrMoVsteels at different temperatures (Ref. 6).

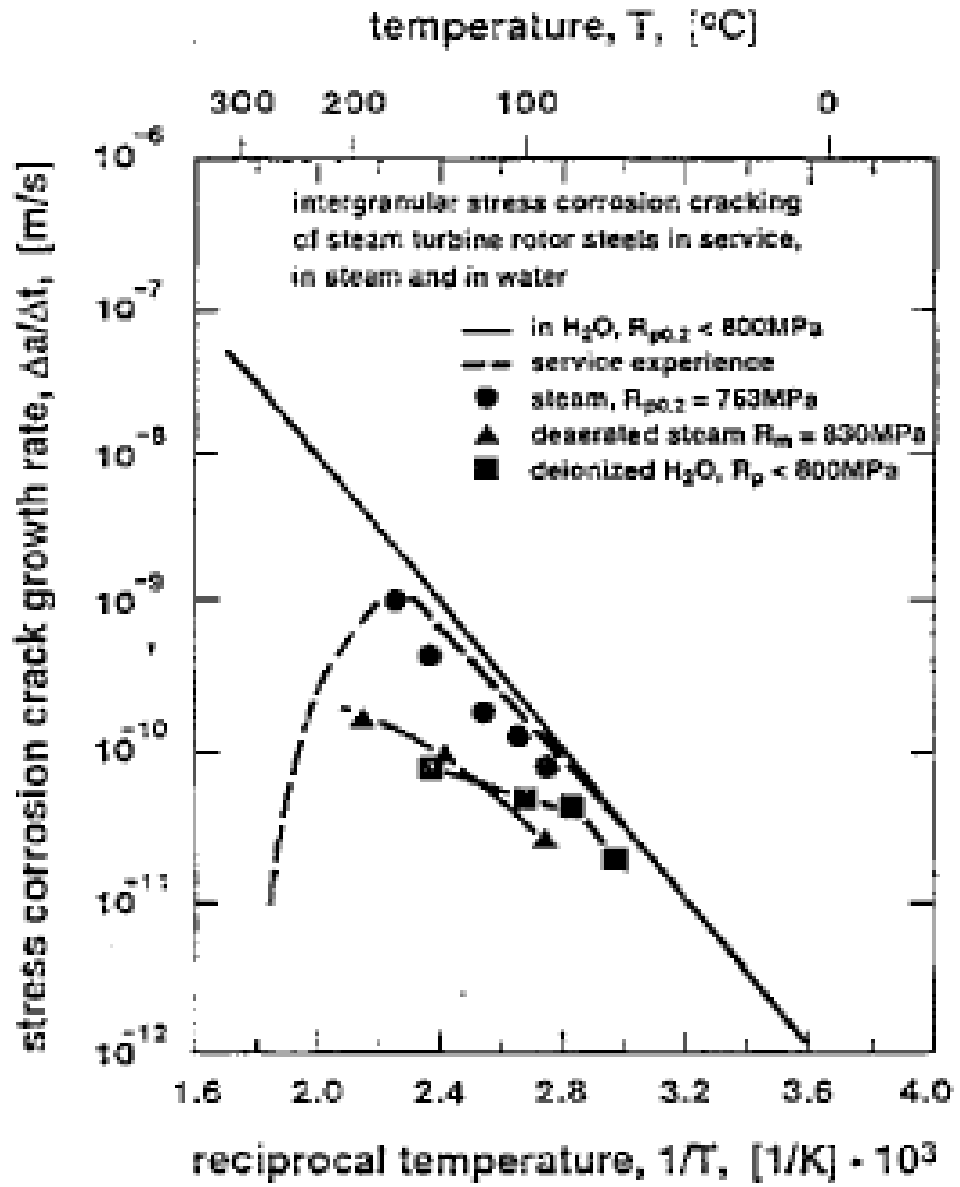


Fig. 482. Effect of temperature on stress corrosion crack growth rate (Ref 8).

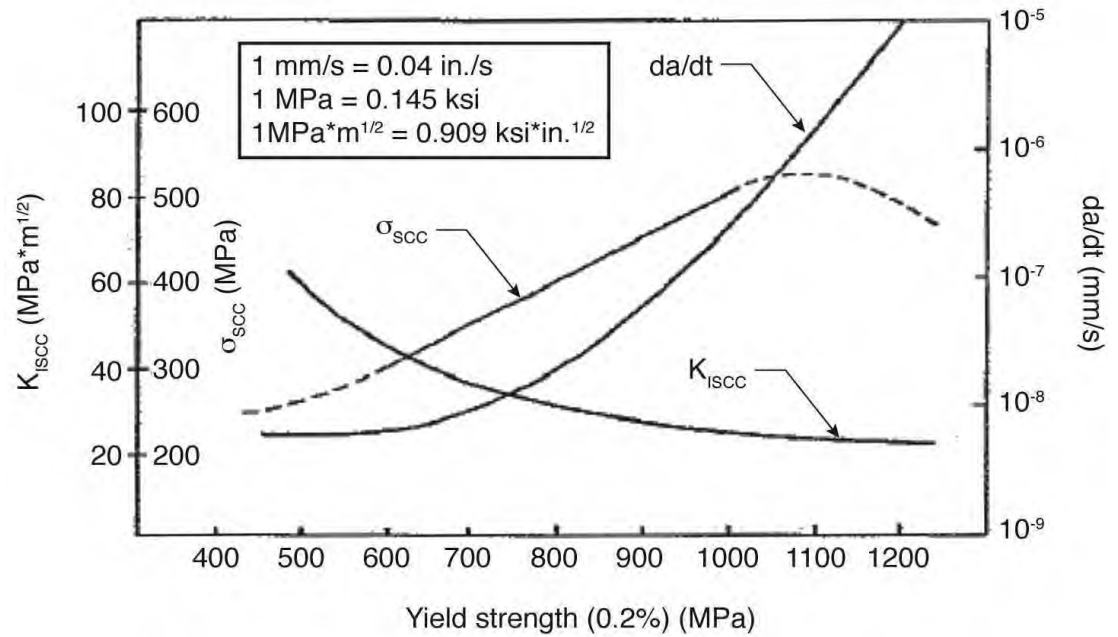


Fig. 483. Stress corrosion behavior of NiCrMoV disk steel vs. yield strength for "good"water and steam (Compiled from published data. Where K_{ISCC} = threshold stress intensity, σ_{SCC} = threshold stress, and da/dt = Stage 2 CGR.) (Ref. 9)

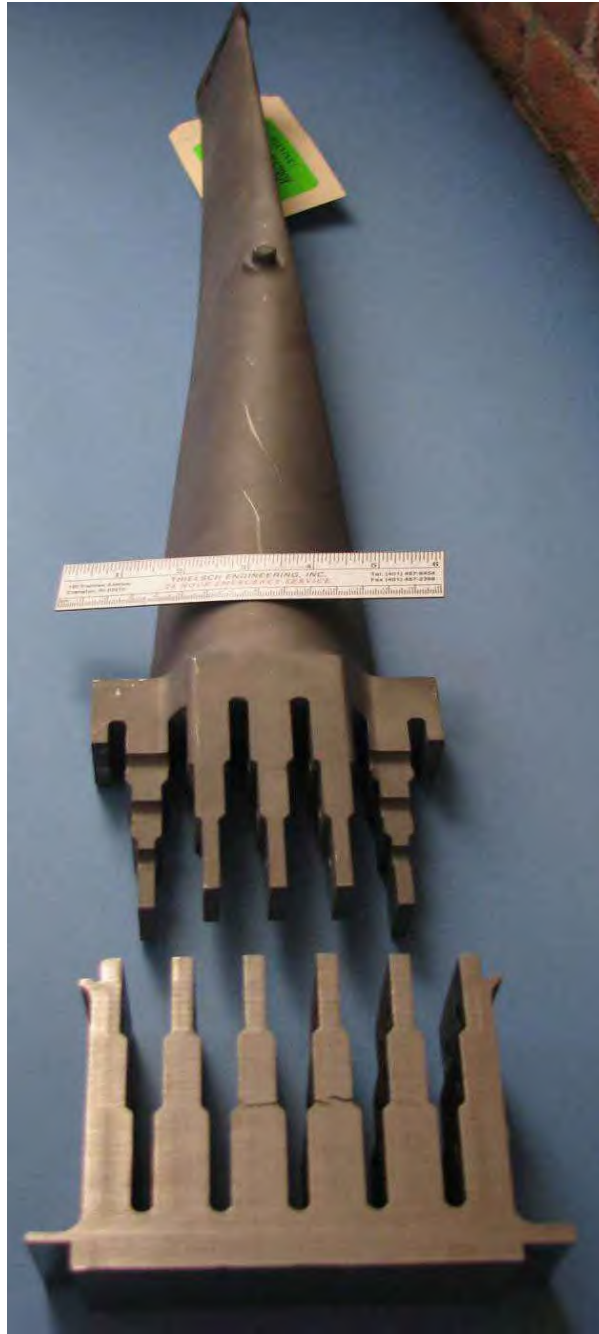


Fig. 484. Transverse section of turbine end L-1 disk rim containing the finger pinned blade attachments from low pressure turbine "B" L-1 and a L-1 blade from the low pressure turbine "A" supplied to facilitate construction of the FEA solid model.

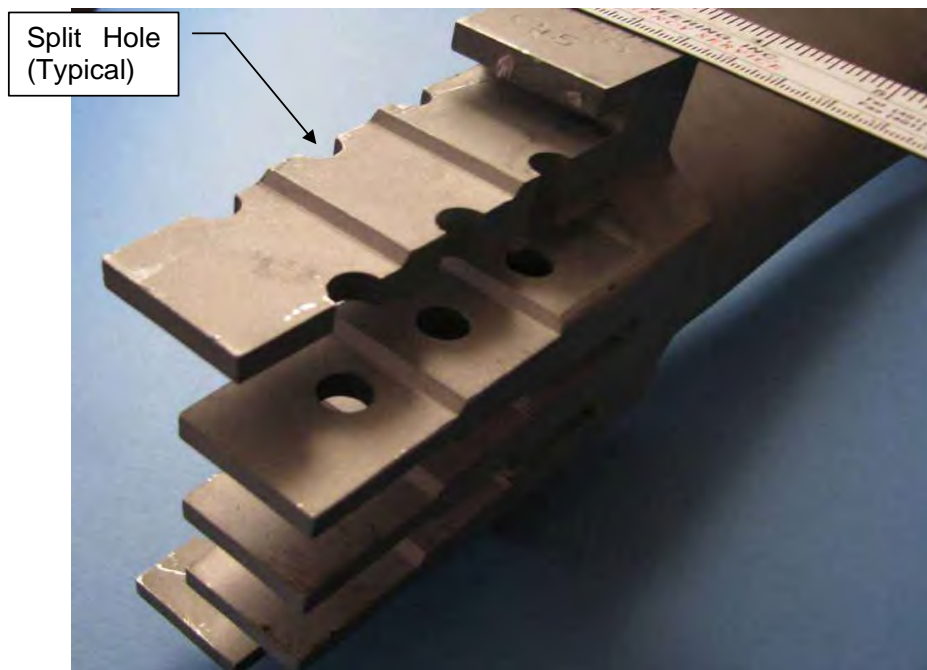


Fig. 485. Close-up photograph of low pressure turbine L-1 blade finger attachment area.

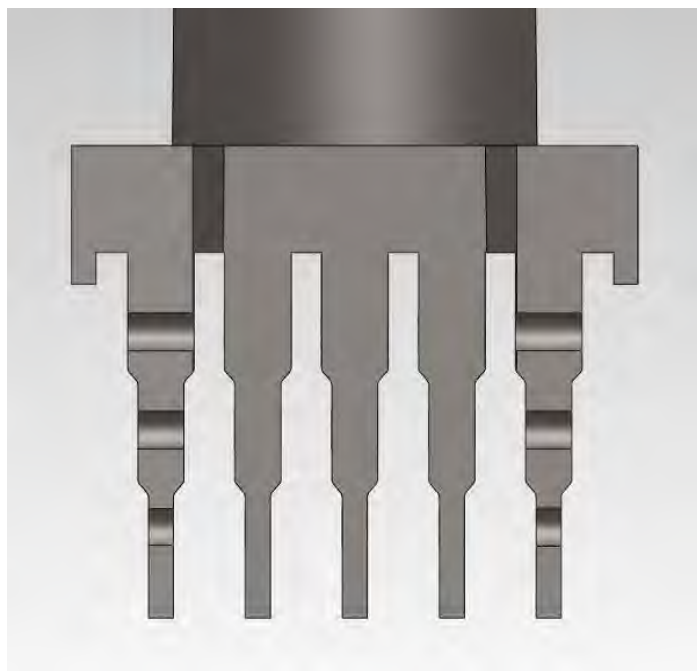
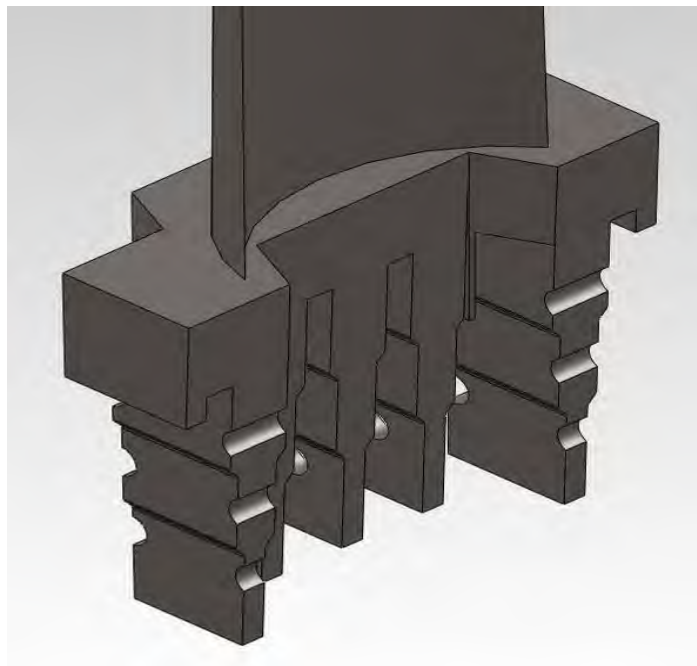


Fig. 486. Close-ups of solid model of low pressure turbine L-1 blade finger region.

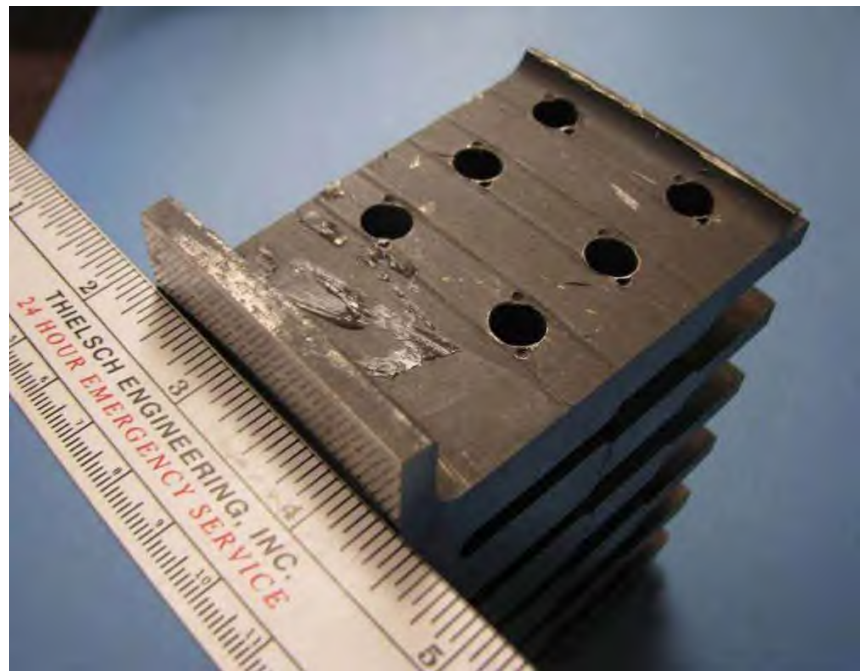


Fig. 487. Close-up photographs of low pressure turbine L-1 disk rim finger pinned blade attachment area.

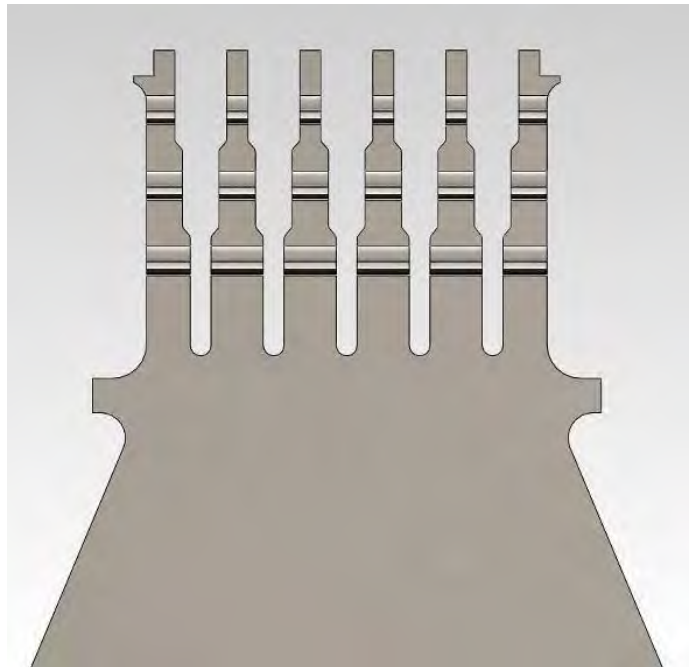


Fig. 488. Close-ups of solid model of low pressure turbine L-1 disk rim finger pinned blade attachment region.

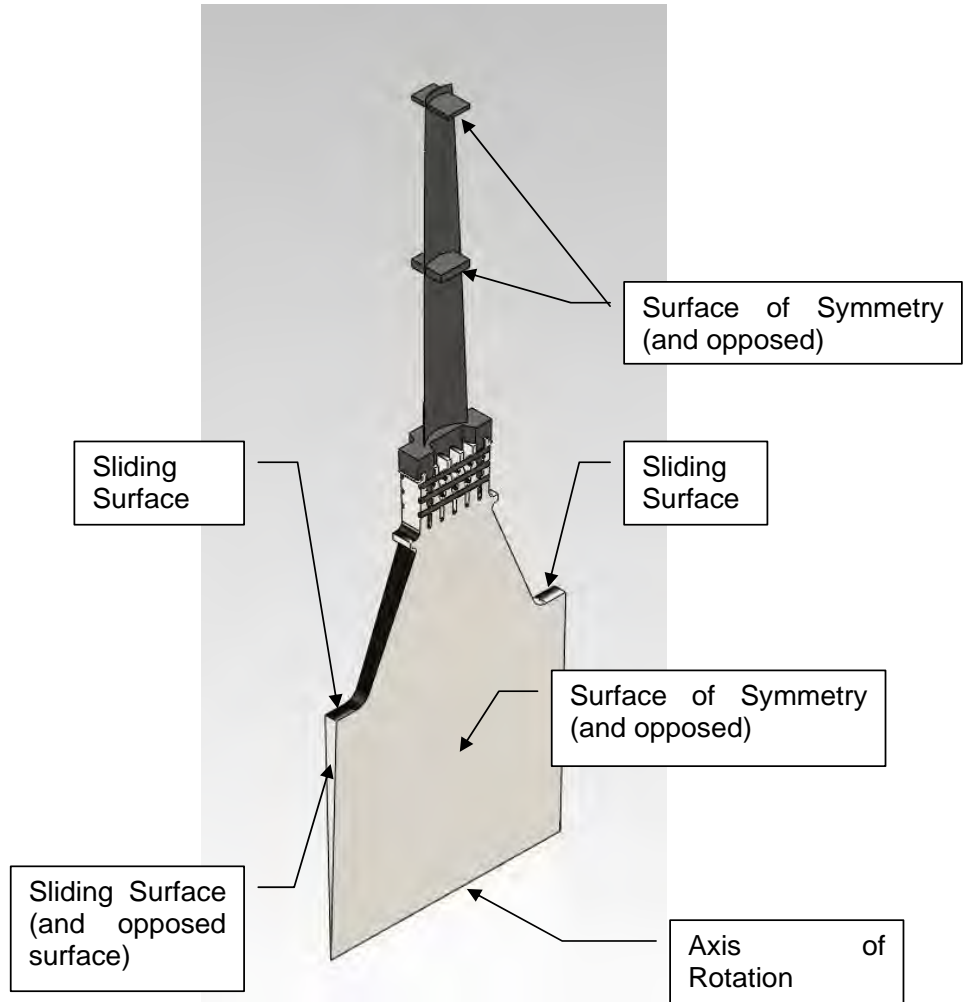


Fig. 490. Assembled solid model.

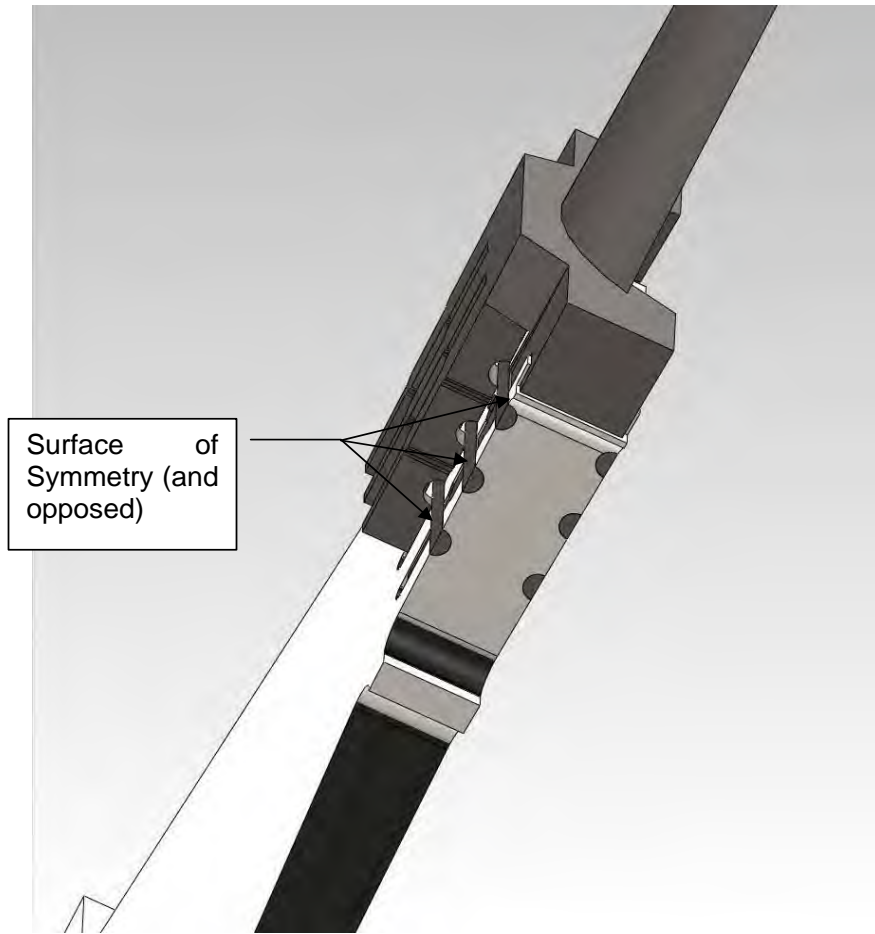


Fig. 491. Close-up of solid model at blade-disk connections.

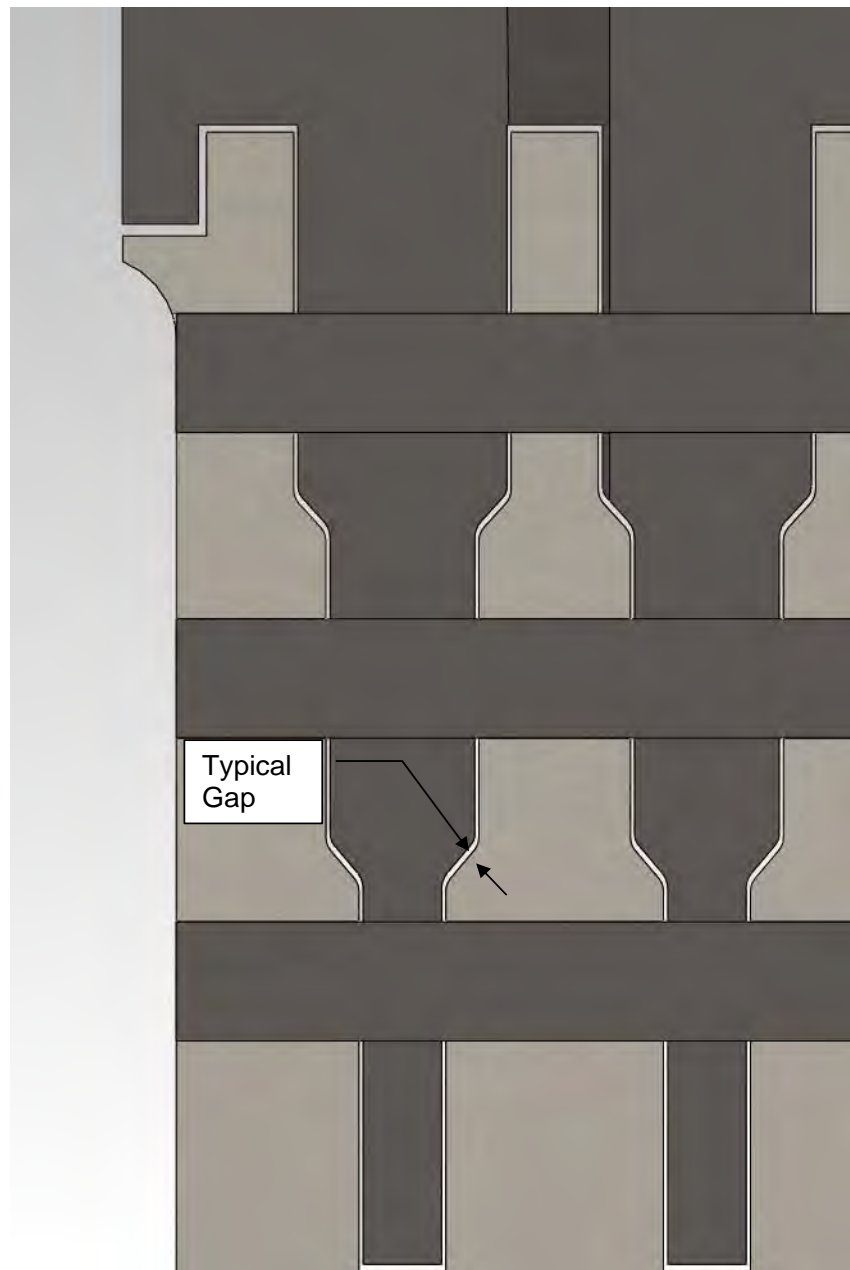


Fig. 492. No-contact condition between blade and disk fingers.

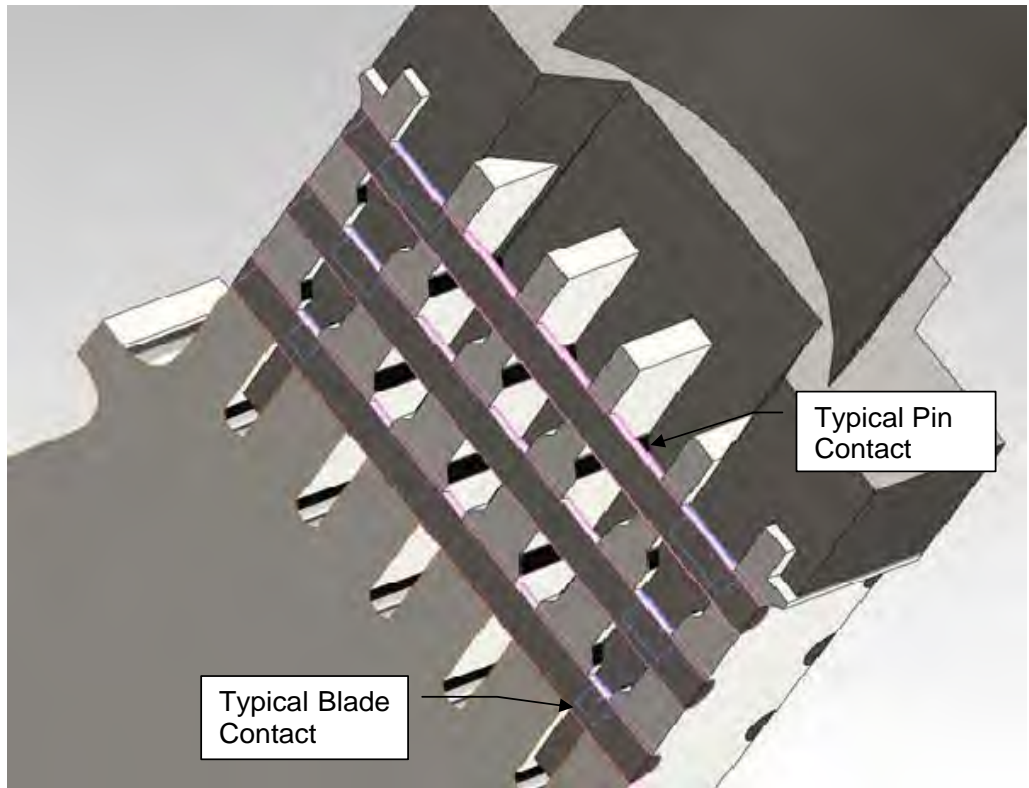


Fig. 493. No penetration contact condition between pins and half-holes of outer fingers of the blade.

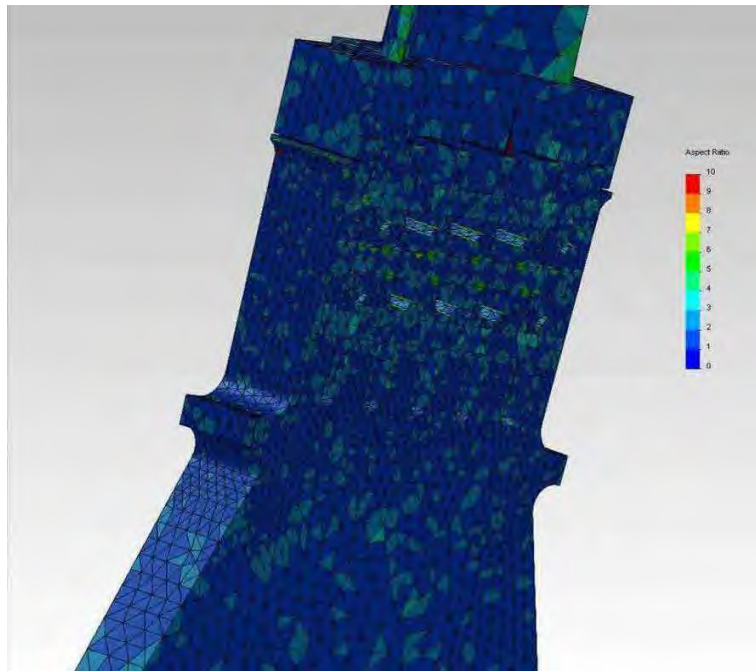


Fig. 494. Mesh aspect ratio in disk-blade sections.

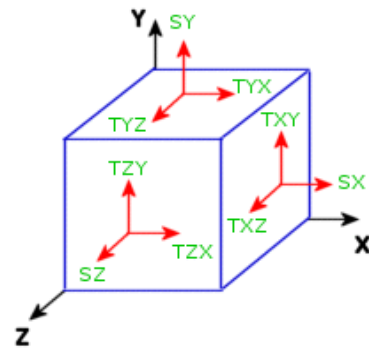


Figure (1)

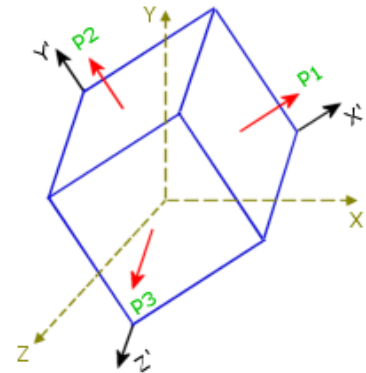


Figure (2)

At certain orientation of the material element shown in Figure (1), the shear stress components vanish and stresses reduce to pure normal stresses as shown in Figure (2).

Fig. 495. 3-D state of stress.

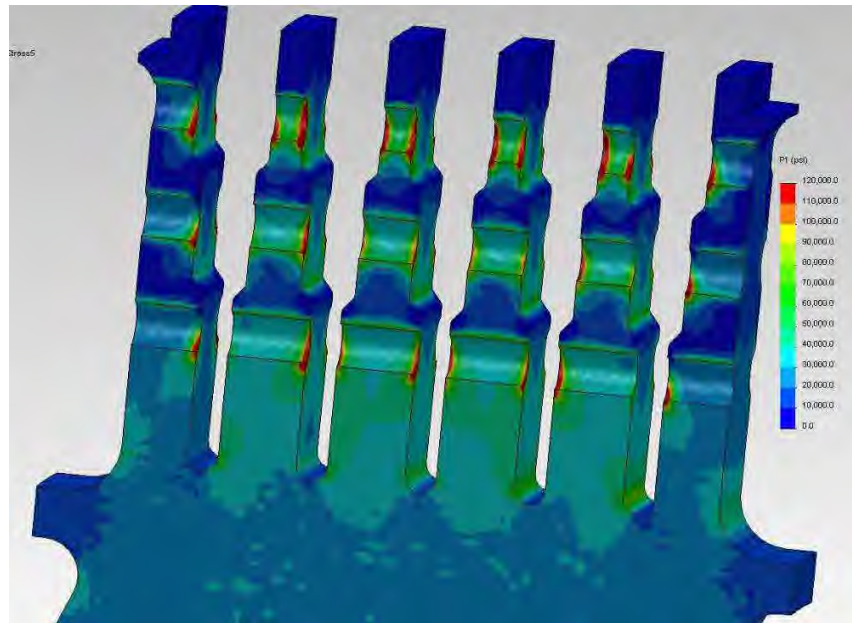


Fig. 496. 1st Principal Stress – General Results

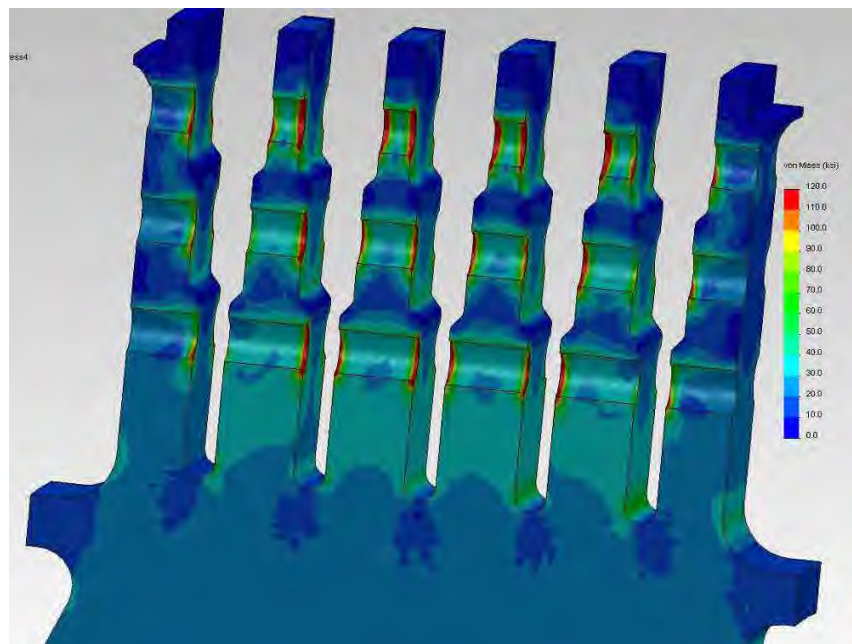


Fig. 497. Von Mises Stress – General Results

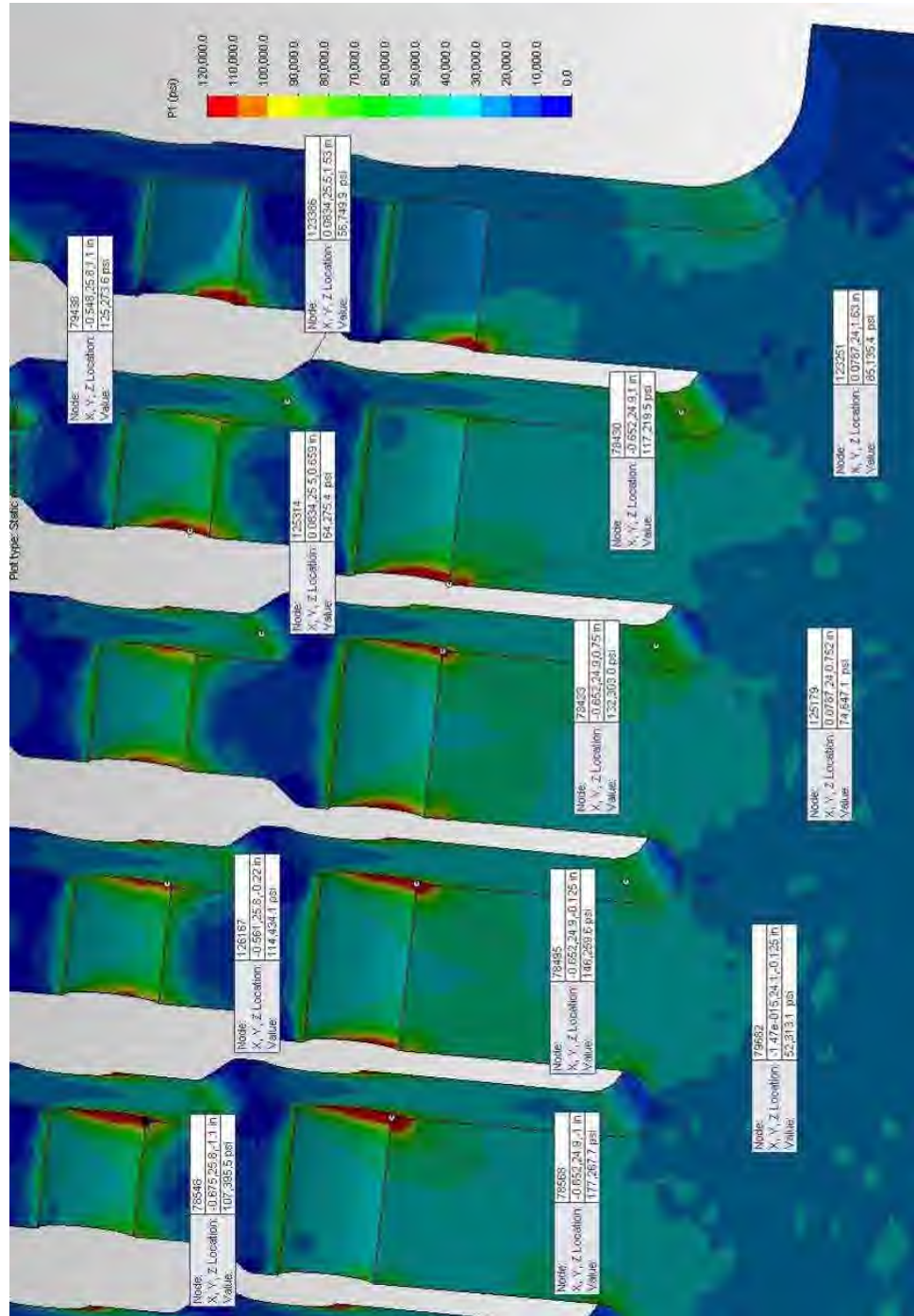


Fig. 498. 1st Principal Stress probed using uniform ledge radii of 0.060"

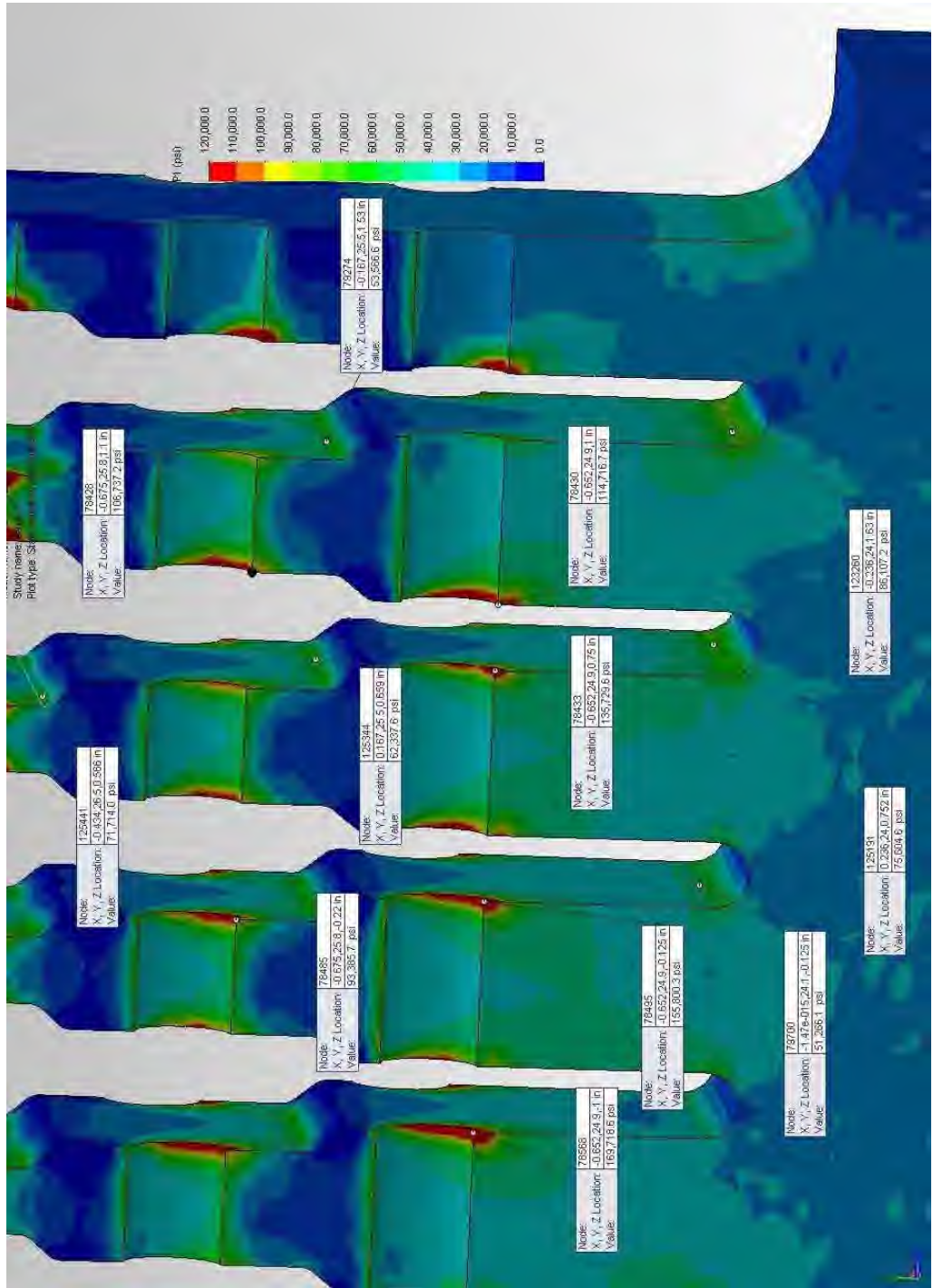


Fig. 499. 1st Principal Stress probed using ledge radii of 0.020" and 0.033"

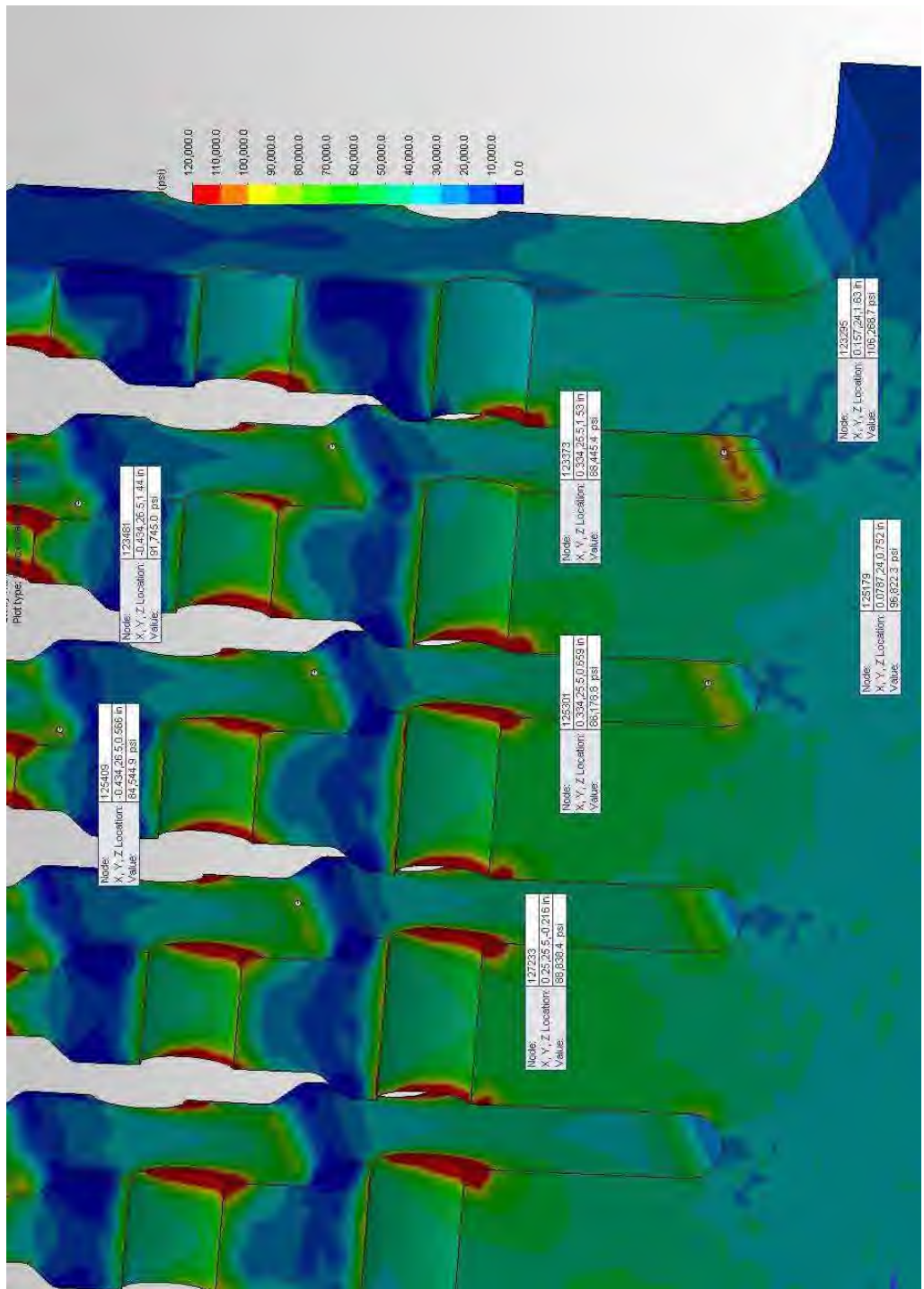


Fig. 500. 1st Principal Stress probed, uniform radii of 0.060" operating at 4100 rpm.

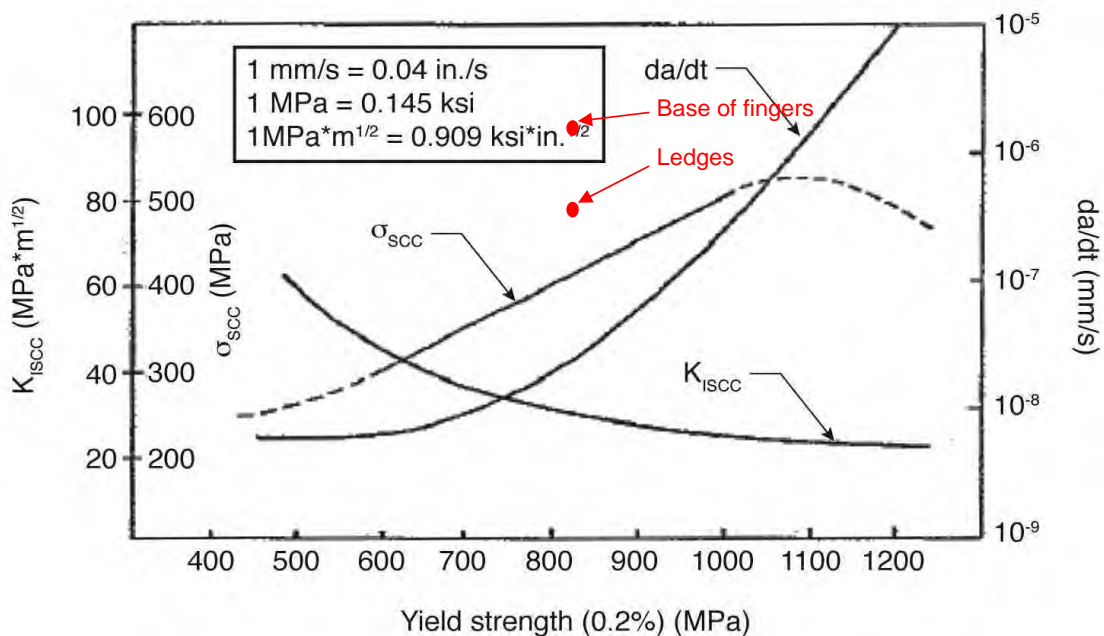


Fig. 501. Stress corrosion behavior of NiCrMoV disk steel vs. yield strength for "good" water and steam showing calculated tensile stress (red points) at ledges and base of fingers of the LP L-1 disk finger pinned blade attachments. No data point for the calculated tensile stress at the pin holes is shown because the value is outside the maximum graph parameters. (Where K_{ISCC} = threshold stress intensity, σ_{SCC} = threshold stress, and da/dt = Stage 2 CGR.)

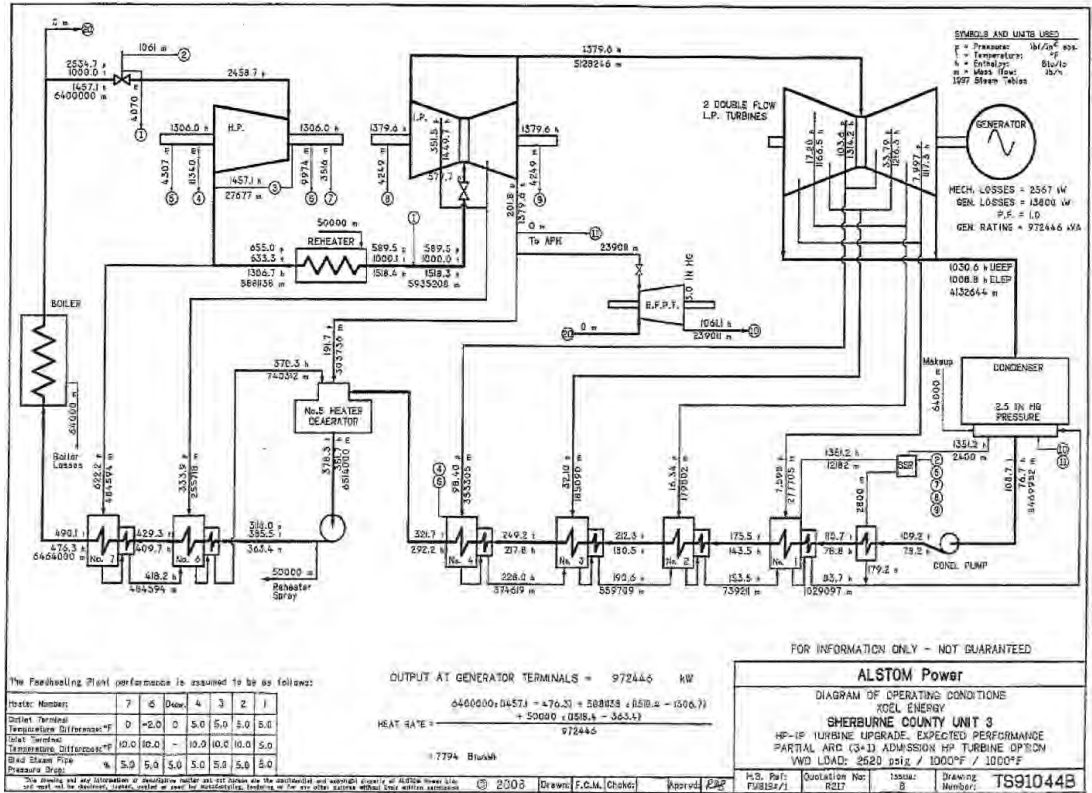


Fig. 502. Heat Balance Diagram for Unit No. 3

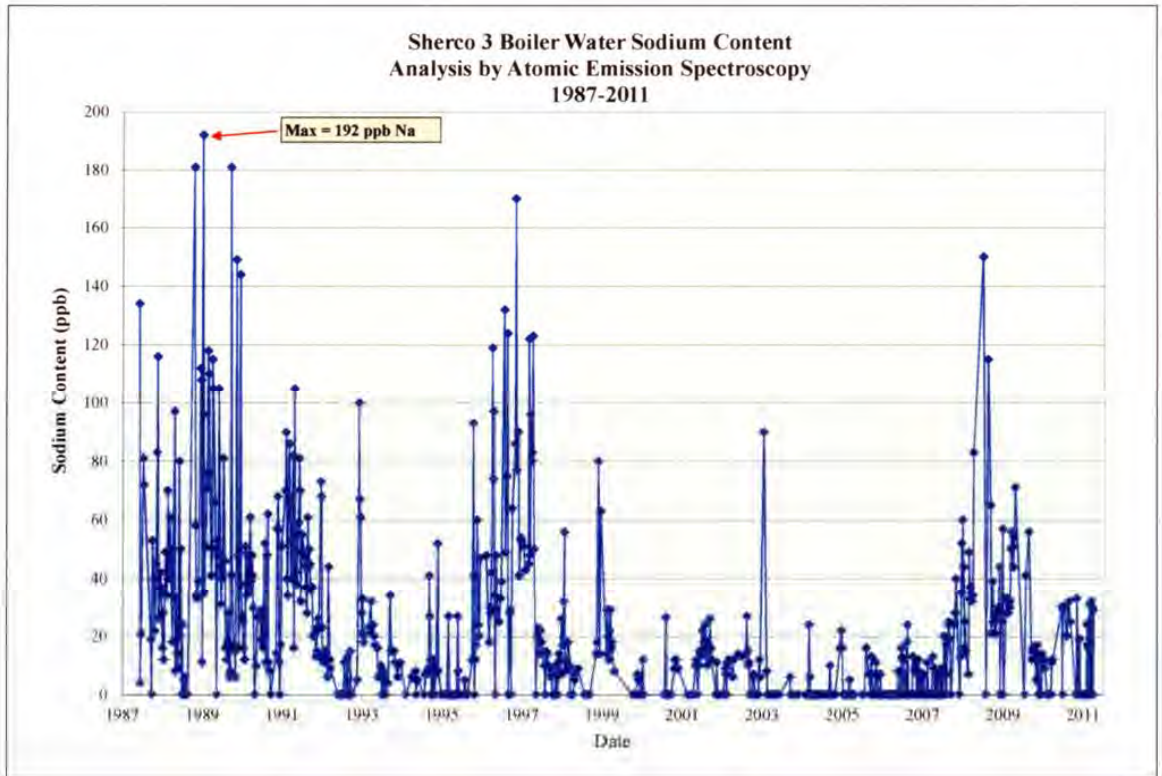


Fig. 503. Boiler Water Sodium Content Analysis of Grab Samples from Sherco No. 3 from 1987 through November 2011. Analysis by Atomic Emission Spectroscopy.

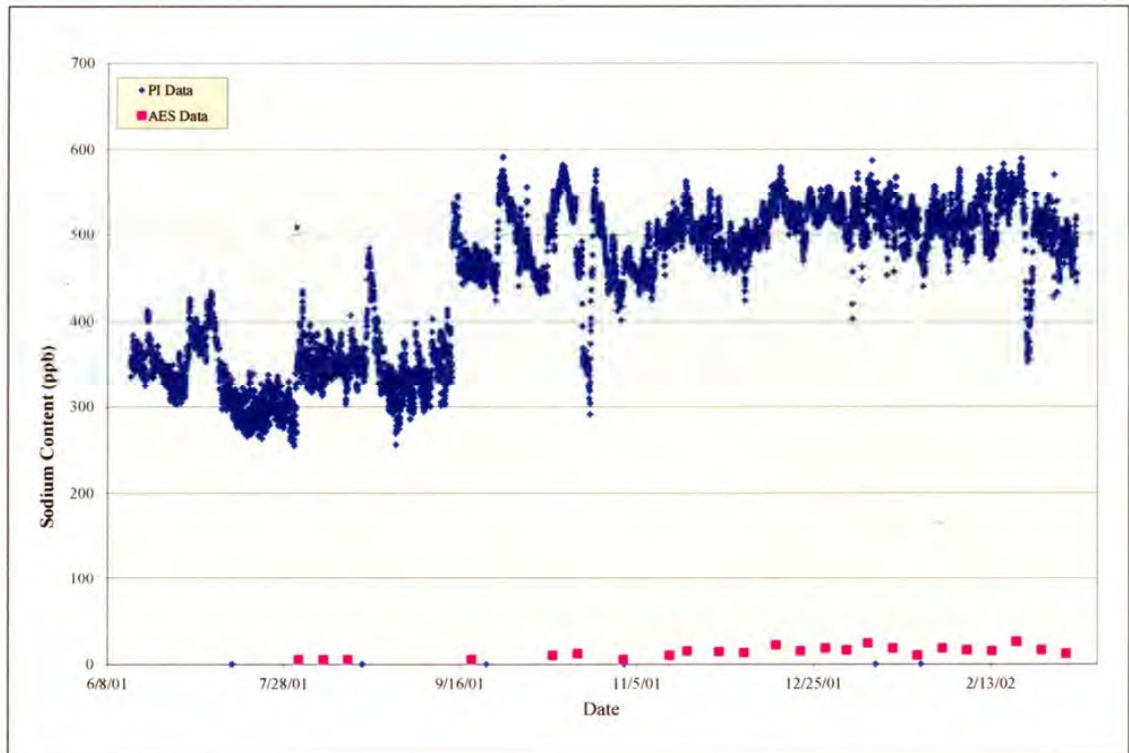


Fig. 504. Boiler Water sodium content as determined by online monitoring instrumentation (PI) and from Atomic Emission Spectroscopy of grab samples during 2001 and 2002.

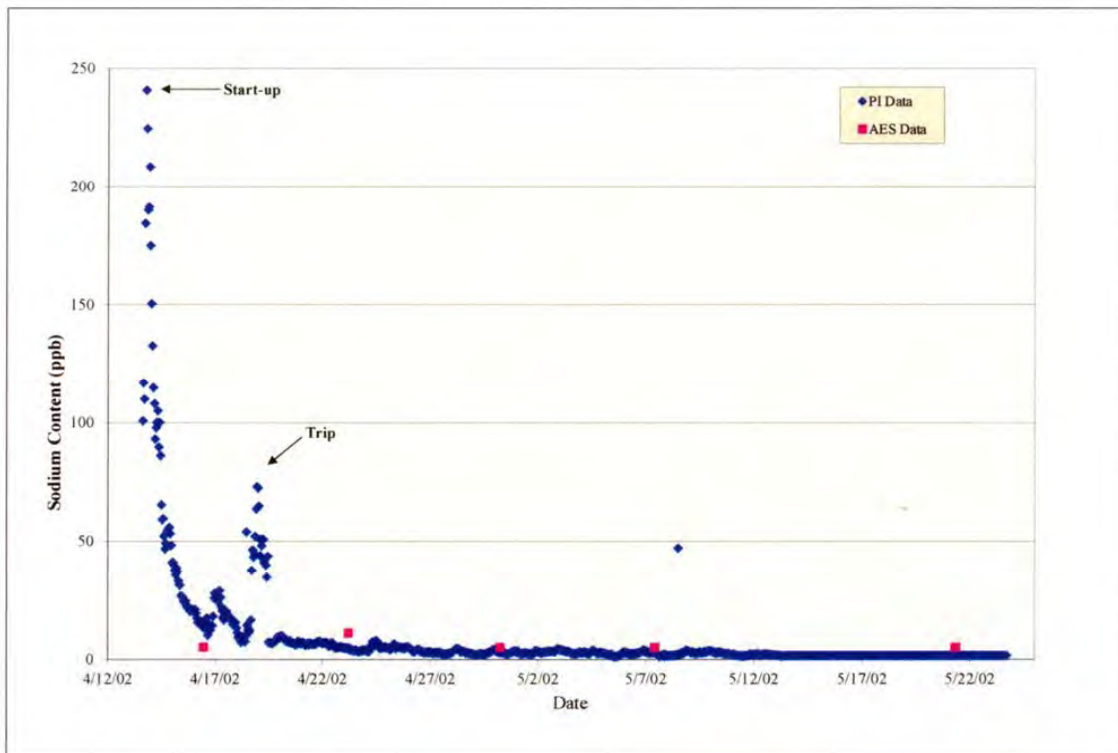


Fig. 505. Boiler water sodium content measured by Atomic Emission Spectroscopy of grab samples and online monitoring instrumentation (PI) after "synchronization" of the online monitoring instrumentation.

Current Owner	Original Owner	Plant/Station Name	Status Sep-12	STATE	Unit	Turbine OEM	Nameplate (in kw)	Turbine Frame Designation	Turbine Type	Steam Conditions	LSB Length	In-Service Date
Southern Company - ALAP	Alabama Power	Barry 4	In Service	AL	4	General Electric	403,800	D8	TC2F33.5	2400-1000-1000	33.5"	May-69
Entergy - PG/Ark	Arkansas Power & Light	Independence 1	In Service	AR	1	General Electric	850,000	G3	TC4F33.5	2400-1000-1000	33.5"	Sep-83
Entergy - PG/Ark	Arkansas Power & Light	Independence 2	In Service	AR	2	General Electric	850,000	G3	TC4F33.5	2400-1000-1000	33.5"	Jul-84
Entergy - PG/Ark	Arkansas Power & Light	White Bluff 1	In Service	AR	1	General Electric	850,000	G3	TC4F33.5	2400-1000-1000	33.5"	Jun-80
Entergy - PG/Ark	Arkansas Power & Light	White Bluff 2	In Service	AR	2	General Electric	850,000	G3	TC4F33.5	2400-1000-1000	33.5"	May-81
Pinacle West Capital Corp	Arizona Public Service	Cholla 4	In Service	AZ	4	General Electric	414,000	D8	TC2F33.5	1800-1000-1000	33.5"	Mar-81
Tri-State G & T Association Inc	Tri-State G & T Association	Craig 1	In Service	CO	1	General Electric	446,400	D8	TC2F33.5	2400-1000-1000	33.5"	Jun-80
Tri-State G & T Association Inc	Tri-State G & T Association	Craig 2	In Service	CO	2	General Electric	446,400	D8	TC2F33.5	2400-1000-1000	33.5"	Jan-80
Tri-State G & T Association Inc	Tri-State G & T Association	Craig 3	In Service	CO	3	General Electric	446,400	D8	TC2F33.5	2400-1000-1000	33.5"	Aug-84
Xcel Energy - NCE	Public Service Co. of Colorado	Fort St. Vrain 1	In Service	CO	1	General Electric	336,044	D8D	TC2F33.5	2400-1000-1000	33.5"	Dec-76
Wisconsin Energy Corp - Wisvest	United Illuminating	New Haven Harbor 1	In Service	CT	1	General Electric	460,300	D8	TC2F33.5	2400-1000-1000	33.5"	Jul-75
Xcel Energy - NRG	NU - Connecticut Light & Power	Middletown 4	In Service	CT	4	General Electric	414,900	D9	TC2F33.5	1800-950-950	33.5"	Jun-73
Xcel Energy - NRG	NU - Connecticut Light & Power	Montville 6	In Service	CT	6	General Electric	414,900	D9	TC2F33.5	1800-950-950	33.5"	Jul-71
CP&L Energy, Incorporated	Florida Power Corporation	Crystal River 4	In Service	FL	4	General Electric	739,300	G3	TC4F33.5	2400-1000-1000	33.5"	Nov-82
CP&L Energy, Incorporated	Florida Power Corporation	Crystal River 5	In Service	FL	5	General Electric	739,300	G3	TC4F33.5	2400-1000-1000	33.5"	Sep-84
TECO Energy	Tampa Electric	Big Bend 3	In Service	FL	3	General Electric	445,500	D8	TC2F33.5	2400-1000-1000	33.5"	Feb-76
Southern Company - GAP	Georgia Power	Scherer 1	In Service	GE	1	General Electric	891,000	G3	TC4F33.5	2400-1000-1000	33.5"	Nov-82
Southern Company - GAP	Georgia Power	Scherer 2	In Service	GE	2	General Electric	832,500	G3	TC4F33.5	2400-1000-1000	33.5"	Nov-84
Southern Company - GAP	Georgia Power	Scherer 3	In Service	GE	3	General Electric	891,000	G3	TC4F33.5	2400-1000-1000	33.5"	Jan-87
Southern Company - GAP	Georgia Power	Scherer 4	In Service	GE	4	General Electric	891,000	G3	TC4F33.5	2400-1000-1000	33.5"	Jan-89
Southern Company - GAP	Georgia Power	Yates 6	In Service	GE	6	General Electric	403,800	D8	TC2F33.5	2400-1000-1000	33.5"	Jun-74
Southern Company - GAP	Georgia Power	Yates 7	In Service	GE	7	General Electric	403,800	D8	TC2F33.5	2400-1000-1000	33.5"	Jan-74
AES Corporation - G Plains	Central Illinois Lighting	Edwards, E.D. 2	In Service	IL	2	General Electric	280,500	D6	TC2F33.5	2400-1000-1000	33.5"	May-68
Edison International - EME	Commonwealth Edison	Powerton 5	In Service	IL	5	General Electric	892,800	G3	TC4F33.5	2400-1000-1000	33.5"	May-72
Edison International - EME	Commonwealth Edison	Powerton 6	In Service	IL	6	General Electric	892,800	G3	TC4F33.5	2400-1000-1000	33.5"	Nov-75
Sunflower Electric Power Corp - TE	Sunflower Electric Power Corp	Holcomb 1	In Service	KS	1	General Electric	349,000	D8	TC2F33.5	2000-1000-1000	33.5"	May-83
LG&E Energy Corp	Louisville Gas & Electric Co.	Mill Creek 3	In Service	KY	3	General Electric	462,600	D8	TC2F33.5	2400-1000-1000	33.5"	Jun-78
Cleco Corporation	Central Louisiana Electric	Rodemacher 1	In Service - Brame Energy Center	LA	1	General Electric	445,500	D8	TC2F33.5	2400-1000-1000	33.5"	Jun-75
DTE Energy Company	Detroit Edison	Greenwood 1	In Service	MI	1	General Electric	815,400	G3	TC4F33.5	2400-1000-1000	33.5"	Apr-79
DTE Energy Company	Detroit Edison	Trenton Channel 9	In Service	MI	9	General Electric	535,500	G3D	TC4F33.5	2400-1000-1000	33.5"	Jan-68
Xcel Energy - NSP	Northern States Power	Sherburne County 3	In Service	MN	3	General Electric	809,643	G3	TC4F33.5	2400-1005-1005	33.5"	Jan-87
PNM	PSC of New Mexico	San Juan 1	In Service	NM	1	General Electric	361,000	D8	TC2F33.5	1800-1000-1000	33.5"	Dec-76
Xcel Energy - NRG	Consolidated Edison of NY	Arthur Kill 3	In Service	NY	3	General Electric	535,500	G3D	TC4F33.5	2400-1000-1000	33.5"	May-69
Reliant Energy - ED	Houston Lighting & Power	Limestone 1	In Service	TX	1	General Electric	813,400	G3	TC4F33.5	2400-1000-1000	33.5"	Jan-85
Reliant Energy - ED	Houston Lighting & Power	Limestone 2	In Service	TX	2	General Electric	813,400	G3	TC4F33.5	2400-1000-1000	33.5"	Jan-86
San Antonio, City PSB	San Antonio, City PSB	Braunig, V.H. 3	In Service	TX	3	General Electric	417,000	D8	TC2F33.5	2400-1000-1000	33.5"	May-70
San Antonio, City PSB	San Antonio, City PSB	Sommers, O.W. 1	In Service	TX	1	General Electric	446,000	D8	TC2F33.5	2400-1000-1000	33.5"	Apr-72
Texas Municipal Power Agency	Texas Municipal Power Agency	Gibbons Creek 1	In Service	TX	1	General Electric	444,000	D8	TC2F33.5	2000-1000-1000	33.5"	Jan-83
TXU	Texas Utilities Electric	Eagle Mountain 3	Retired	TX	3	General Electric	396,200	D9	TC2F33.5	1800-950-950	33.5"	Jun-71
TXU	Texas Utilities Electric	Valley 3	Mothballed	TX	3	General Electric	396,000	D9	TC2F33.5	2000-1000-1000	33.5"	May-71
ScottishPower [UK] - PacifiCorp	PacifiCorp -Utah Power & Light	Hunter 3	In Service	UT	3	General Electric	446,400	D8	TC2F33.5	2400-1000-1000	33.5"	Mar-83
ScottishPower [UK] - PacifiCorp	PacifiCorp -Utah Power & Light	Huntington 1	In Service	UT	1	General Electric	446,400	D8	TC2F33.5	2400-1000-1000	33.5"	Mar-77
ScottishPower [UK] - PacifiCorp	PacifiCorp -Utah Power & Light	Huntington 2	In Service	UT	2	General Electric	446,400	D8	TC2F33.5	2400-1000-1000	33.5"	Jan-74
Dominion	Virginia Power	Chesterfield 6	In Service	VA	6	General Electric	693,900	G3	TC4F33.5	2401-1000-1000	33.5"	May-69
Dominion	Virginia Power	Possum Point 5	In Service	VA	5	General Electric	882,000	S2	TC6F33.5	2400-1000-1000	33.5"	May-75
Dominion	Virginia Power	Yorktown 3	In Service	VA	3	General Electric	882,000	S2	TC6F33.5	2400-1000-1000	33.5"	Jun-74
Alliant Energy - WPL	Wisconsin Power & Light	Edgewater 4	In Service	WI	4	General Electric	330,000	D8	TC2F33.5	2000-1000-1000	33.5"	Nov-69
Alliant Energy - WPL	Wisconsin Power & Light	Edgewater 5	In Service	WI	5	General Electric	380,000	D8	TC2F33.5	2400-1000-1000	33.5"	Dec-84
Wisconsin Energy Corp - WEPCo	Wisconsin Electric Power	South Oak Creek 8	In Service	WI	8	General Electric	324,000	G4	TC4F33.5	2400-1050-1000	33.5"	Oct-67
ScottishPower [UK] - PacifiCorp	PacifiCorp -Pacific Power & Light	Johnston, D. 4	In Service	WY	4	General Electric	360,000	D8	TC2F33.5	1800-1000-1000	33.5"	Mar-72

Fig 506. Installation List of General Electric Manufactured Steam Turbines That May Have Finger Pinned Blade Attachment Design in the Low Pressure Turbine L-1 Stage Disk Similar to Sherco Unit 3.

APPENDIX A

**SHERCO UNIT NO. 3
PROTOCOLS**

Appendix A1

List of Protocols
Sherco Unit No. 3 Root Cause Analysis

Protocol No.	Purpose
1	Removal of low pressure turbine "B" L-1 turbine end fractured disk rim at GE Service Center.
1 Modified	Removal of low pressure turbine "B" L-1 generator end cracked disk rim and low pressure turbine "A" L-1 turbine and generator end cracked disk rims at GE Service Center.
2	Forensic examination of low pressure turbine "B" turbine end L-1 fractured disk rim.
3	Forensic examination of low pressure turbine "B" turbine end L-1 blade pins from fractured disk rim.
4	Forensic examination of low pressure turbine "B" turbine end L-1 blades from fractured disk rim.
5	Forensic examination of generator shaft fracture.
6	Forensic examination of exciter shaft fractures.
7	Forensic examination of low pressure turbine "B" L-1 generator end cracked disk rim and low pressure turbine "A" L-1 turbine and generator end cracked disk rims.
8	Not Used
9	Not Used
10	Forensic examination of deposit samples removed from various locations of high pressure, intermediate pressure and low pressure turbines "A" and "B".

Appendix A2

Protocol No. 1



February 14, 2012

**Protocol for the Removal of the Damaged Rim (L-1) from the LP-B Rotor:
Sherburne County Generating Plant Unit 3 failure November 19, 2011
Becker, MN**

This protocol is an update for the removal of the LP-B turbine rotor rim (L-1). The generator rotor and both LP turbines have been removed from the turbine/generator train, secured, protected, shrink-wrapped, and shipped to the General Electric facility in Chicago (General Electric Service Center 6045 S. Nottingham Ave. Chicago, IL 60638). The generator rotor fracture surface has been cut from the shaft with a band saw and is being shipped to Engel Metallurgical.

It is expected that the LP-B rotor rim at the turbine end (L-1) will be removed Wednesday, February 15, 2012 or Thursday February 16, 2012 as provided in the protocol noted below. The attached drawings and MSDS provide additional information related to this protocol.

Representatives of Interested Parties who are present at the repair facility will be consulted as the fracture surface is being removed. Each party agreeing to this protocol understands that the preservation of evidence is a priority, and should deviations from this protocol become necessary, the present representatives will participate in any discussions to ensure any evidence deemed relevant by any Interested Party is preserved. The parties also understand that rebuilding the rotors is a priority and that any deviations from this protocol cannot unreasonably delay the rebuilding of the rotors. Interested Parties who are not represented at the repair facility have no say about the process.

Appendix A3

The rim from the LP-B rotor will be treated as evidence and transported to Engel Metallurgical where other evidence is stored.

Interested Party representatives must sign in at the repair facility to observe fracture surface removal. By signing the sheet, Interested Party representatives confirm that they and their principals have read and will abide by this protocol.

The following rules govern the evidence preservation process:

PROTOCOL FOR FAILED LP-B TURBINE END ROTOR RIM (L-1)

(see attached drawings)

1. The subject rotor has been protected on the outer rim and has been shipped to the GE facility in Chicago.
2. The individual blade slot locations in the failed disk will be numbered using a vibrapeen marker to reference the blades and rim sections starting at -0- point on the flange of the rotor. The blades that are still remaining in the failed disk will be removed if the locking pins can be readily removed. If not, the blade airfoils will be sectioned from the roots at the platform.
3. Samples will be collected of the deposits on the rotor using cotton swabs.
4. The exposed fracture surfaces on the failed wheel will be protected with bubble wrap in the grooves. This wrap will be covered with shrink wrap. The outer surfaces of wheel at the pin holes will be cleaned of the present residues by wiping the area with acetone or alcohol. These solvents are not to be put on the interior portions of the wheel groove. The purpose of the solvent wipe is to permit the tape to adhere to the wheel. Special aluminum tape will be applied over the shrink wrap and around the sides of the wheel to cover the locking pin holes. The tape will be overlapped 50%. The edges of the tape will then be sealed with silicone sealant. This protection system will be tested on the generator end

Appendix A4

mating wheel groove in LP-B and water tested to assure that the tape and silicone will seal the wheel cavity. Extreme care should be exercised to assure no mechanical or chemical damage to the entire rim of the failed disk.

5. Circumferential cuts will be made using a 0.315 inch wide parting tool at a location 0.700 inches below the root groove. The cuts will be made in both the front and rear sides of the subject disk. The cuts shall be made using a water soluble oil coolant (MSDS attached). No contamination of the outer rim of the disk is allowed.
6. The outer portion of the failed wheel will be parted from the rotor as a complete ring. This ring will then be sectioned radially at the 60 degree and 240 degree locations. These cuts will remain dry and free from contaminants. The cuts can be made using an abrasive wheel, saw, or plasma torch.
7. The two removed sections will be further protected with bubble wrap to assure no mechanical damage. The sections will then be shrink wrapped to protect the sections from chemical contamination. The blades removed from the failed row will also be wrapped with bubble wrap to assure no further mechanical damage and also shipped.
8. The sections along with blades removed from the failed row will be placed in wooden crates and shipped to Engel Metallurgical at 925 Industrial Drive S., Sauk Rapids, MN 56379

THE GENERATOR ROTOR SHAFT FRACTURE SURFACE HAS BEEN REMOVED AND PREPARED FOR SHIPMENT TO ENGEL METALURGICAL.

Appendix A5

Modified Protocol No. 1



March 6, 2012

**Protocol for the Removal of the Three Remaining L-1 Rims
from the LP Turbine Rotors:
Sherburne County Generating Plant Unit 3 Failure November 19, 2011
Becker, MN**

This protocol is an update for the removal of the LP-B turbine rotor rims to include the generator end L-1 wheel of the LP-B turbine and the two L-1 wheels of the LP-A turbine. The LP rotors have been shipped to the General Electric facility in Chicago (General Electric Service Center 6045 S. Nottingham Ave. Chicago, IL 60638). The rims will be removed from the rotors in a manner similar to that of the LP-B L-1 turbine end rim outlined in the protocol dated February 14, 2012 with the major exception of protecting the finger dovetails from cutting fluid. The removal of the rims is expected to start on March 8.

Representatives of Interested Parties who are present at the repair facility will be consulted as the rims are being removed. Each party agreeing to this protocol understands that the preservation of evidence is a priority, and should deviations from this protocol become necessary, the present representatives will participate in any discussions to ensure any evidence deemed relevant by any Interested Party is preserved. The parties also understand that rebuilding the rotors is a priority and that any deviations from this protocol cannot unreasonably delay the rebuilding of the rotors. Interested Parties who are not represented at the repair facility have no say about the process.

Appendix A6

The rims from the LP-B rotor will be treated as evidence and transported to Engel Metallurgical where other evidence is stored.

Interested Party representatives must sign in at the repair facility to observe fracture surface removal. By signing the sheet, Interested Party representatives confirm that they and their principals have read and will abide by this protocol.

The following rules govern the evidence preservation process:

PROTOCOL FOR THE THREE INTACT LP TURBINE ROTOR L-1 WHEELS

1. The subject rotors have been has been shipped to the GE facility in Chicago.
2. The individual blade slot locations in the disk will be numbered using a Vibro Peen marker to reference the blades and rim sections starting at -0- point on the flange of the rotor. The blades in the disk will be removed if the locking pins can be readily removed. If not, the blade airfoils will be sectioned from the roots at the platform.
3. Circumferential cuts will be made using a 0.315 inch wide parting tool at a location 0.700 inches below the root groove. The cuts will be made in both the front and rear sides of the subject each disk. The cuts shall be made using a water soluble oil coolant (MSDS attached).
4. The outer portion of the wheel will be parted from the rotor as a complete ring. This ring will then be sectioned radially at the 60 degree and 240 degree locations. These cuts will remain dry and free from contaminants. The cuts can be made using an abrasive wheel, saw, or cutting torch.
5. The two removed sections of each rim will be protected with bubble wrap to assure no mechanical damage. The sections will then be shrink-wrapped to protect the sections from chemical contamination. The removed blades will also be wrapped with bubble wrap to assure no further mechanical damage and also shipped.

Appendix A7

6. The sections along with blades removed from the row will be placed in wooden crates and shipped to Engel Metallurgical at 925 Industrial Drive S., Sauk Rapids, MN 56379

Appendix A8

TEST PROTOCOL NO. 2**FOR SHERCO NO. 3 LP ROTOR-B FAILED L-1 RIM
ENGEL METALLURGICAL PROJECT 954-001**

Date: March 29, 2012

This protocol will be executed at Engel Metallurgical Ltd. As per previous protocols, all of the components selected for metallurgical evaluation relative to the Sherco No. 3 failure were protected, crated and shipped to Engel Metallurgical Ltd. for storage. These components were unpacked per the protocol dated March 12, 2012. Laboratory testing is expected to commence at 9:00 AM on April 3, 2012.

The following metallurgical examination and testing protocol is proposed for the evaluation of the Sherco No. 3 LP Rotor-B failed L-1 wheel rim that was removed from LP rotor-B. All cutting will be performed without any coolant (that is, "dry cut") unless otherwise agreed by the parties present during the metallurgical testing. Photographs will be taken to document the location of each section removed from the rim. Prior to the commencement of this protocol, the parts will have been photographed at Engel Metallurgical and will be made available to all parties attending.

All data generated during the execution of this protocol will be shared amongst all parties present. To ensure that time is used efficiently, a single person designated by Les Engel shall take all photographs of the rim during the examination and testing. All parties present will have an opportunity to identify regions of interest and ensure that the appropriate photographs have been taken by the designated photographer. Should any party determine that the photography process described herein is inefficient or ineffective, the parties present may agree on a different process for photographing the evidence.

1. Perform visual examination of rim as-received. Images will be taken of areas of interest.
2. Remove selected surface deposit samples from wheel rim for subsequent energy dispersive spectroscopy (EDS). Samples will be removed using cotton swabs and/or adhesive carbon tabs.
3. Perform EDS on the samples collected in Task 2, as well as samples removed at Xcel prior to shipment and at the GE Chicago repair shop during the removal of the rim.
4. Select and remove area(s) from the wheel rim for further evaluation.
5. Perform visual examinations of existing as-received fracture surfaces at magnifications of 1X to 30X with the aid of a stereomicroscope. Images may be taken of areas of interest.
6. Open selected cracks to expose the fracture surfaces, as needed.
7. Perform visual examinations of exposed crack, fracture surfaces in as-received condition at magnifications of 1X to 30X with the aid of a stereomicroscope. Images may be taken of areas of interest.

Appendix A9

8. Using a scanning electron microscope (SEM) with EDS capabilities, examine select fracture surface(s).
9. If necessary, determine if and what further analytic method may be required for the surface analysis of the fracture surfaces. Any further chemical analysis beyond EDS would likely need to be completed at a facility outside of Engel Metallurgical.
10. Clean fracture surface(s) examined during Task 8 ultrasonically in 1% Alconox solution, rinse with hot water and ethyl alcohol followed by drying in hot air. If this methodology is insufficient to clean the fracture surface(s), other cleaning methods may be necessary. Any further surface cleaning will be performed by agreement of parties present.
11. Perform visual examinations of the cleaned fracture surfaces at magnifications of 1X to 30X with the aid of a stereomicroscope. Images will be taken of areas of interest.
12. Perform SEM/EDS on the cleaned fracture surfaces. Images will be taken of areas of interest.
13. Remove a radial section of the rim exhibiting an intact dovetail (finger portion to which the blades are attached) for subsequent dimensional evaluation. The dimensions, measurement techniques and locations of the dimensional evaluation will be agreed upon by all parties present prior to commencement. A single record of all dimensions will be collected.
14. Select and remove metallographic cross section(s) from the rim.
15. Metallographic cross section(s) will be prepared in accordance with standard metallographic practice.
16. Examine the metallographic cross section(s) using a metallograph and/or SEM/EDS. Images will be taken at areas of interest.
17. Perform microhardness testing on selected metallographic cross section(s).
18. Perform hardness testing on selected radial section(s) from the rim.
19. If needed and with the agreement of parties present, perform high sensitivity fluorescent penetrant inspection of the remaining portions of the rim.
20. Perform radial room temperature tensile tests on samples from fingers of the dovetail region of the rim.
21. Perform quantitative chemical analysis of wheel rim material.

The evaluation of these components will continue on a weekly basis until completed. It is estimated that the above protocol will require at least five days to complete, but may take significantly longer. This proposed test protocol may be altered during the examination depending upon the results of the testing. Each party understands that should deviations from this protocol become necessary, the representatives present at the examination may participate in

Appendix A10

any discussions regarding these deviations. Interested Parties who are not represented at the repair facility have no say about the process.

Interested Parties may be present during this evaluation of evidence. The Interested Parties must notify Daniel Berglund (612-564-4885) if they plan to attend. Parties will follow the Revised Memorandum of Understanding. The data and photographs generated during the execution of this protocol will be made available upon request to all Interested Parties

Appendix A11

TEST PROTOCOL NO. 3**FOR SHERCO No. 3 LP ROTOR-B LOCKING PINS FROM FAILED L-1 WHEEL
ENGEL METALLURGICAL PROJECT 954-001**

Date: April 4, 2012

This proposal will be conducted at Engel Metallurgical Ltd. to initiate the following tasks. As per previous protocols, all of the components selected for more detailed metallurgical evaluation relative to the Sherco No. 3 failure analysis were protected, crated, and shipped to Engel Metallurgical Ltd. for storage. These components have been unpacked per the protocol dated March 12, 2012. The following tasks are proposed to be conducted. It is expected that these activities will commence at 9:00 a.m on April 17, 2012.

The following metallurgical examination and testing protocol is proposed for the evaluation of locking pins from the Sherco No. 3 LP Rotor-B failed L-1 rim. All cutting will be performed without any coolant (that is, "dry cut") unless otherwise agreed by the parties present during the metallurgical testing. Photographs will be taken to document the location of each section removed from the rim. Prior to the commencement of this protocol, the parts will have been photographed at Engel Metallurgical and will be made available to all parties attending.

Data generated during the execution of this protocol will be shared amongst all parties present. To ensure that time is used efficiently, a single person designated by Les Engel shall take all photographs of the pins during the examination and testing. All parties present will have an opportunity to identify regions of interest and ensure that the appropriate photographs have been taken by the designated photographer. Should any party determine that the photography process described herein is inefficient or ineffective, the parties present may agree on a different process for photographing the evidence.

1. Perform visual examination of as-received pins. Images will be taken of areas of interest. Subsequent evaluation tasks will also be documented photographically.
2. Energy dispersive spectroscopy (EDS) will be performed on surface deposits. Samples can be directly analyzed or deposits can be removed using cotton swabs and/or adhesive carbon tabs.
3. Clean selected pins with detergent.
4. Perform visual examination of cleaned pins at magnifications of 1X to 30X. Images will be taken of areas of interest.
5. Obtain weights of select pins with minimal damage.
6. If needed, select pins may be subject to fluorescent penetrant inspection.
7. A section will be removed from selected pins for chemical analysis.
8. Perform hardness testing on selected pins.